SELECTIVE FLUORESCENCE SENSING OF BIOLOGICAL THIOLS USING A BODIPY BASED BIFUNCTIONAL PROBE AND THE CATALYTIC ACTIVITY OF SHORT PEPTIDE AMPHIPHILE NANOSTRUCTURES: IMPLICATIONS ON THE ORIGIN OF LIFE

A THESIS
SUBMITTED TO THE DEPARTMENT OF CHEMISTRY
AND THE GRADUATE SCHOOL OF ENGINEERING AND SCIENCE
OF BİLKENT UNIVERSITY
IN PARTIAL FULFILLMENT OF THE REQUIREMENTS
FOR THE DEGREE OF
MASTER OF SCIENCE

By
YİĞİT ALTAY
July, 2013

I certify that I have read this thesis and that in my opinion it is fully adequate, in scope and in quality, as a thesis for the degree of Master of Science.

…….

Prof. Dr. Engin U. Akkaya (Advisor)

I certify that I have read this thesis and that in my opinion it is fully adequate, in scope and in quality, as a thesis for the degree of Master of Science.

…….

Assoc. Prof. Dr. Dönüş Tuncel

I certify that I have read this thesis and that in my opinion it is fully adequate, in scope and in quality, as a thesis for the degree of Master of Science.

…….

Asst. Prof. Dr. Salih Özçubukçu

Approved for the Graduate School of Engineering and Science:

…….

Prof. Dr. Levent Onural

Director of the Graduate School

ABSTRACT

SELECTIVE FLUORESCENCE SENSING OF BIOLOGICAL THIOLS USING A BODIPY BASED BIFUNCTIONAL PROBE AND THE CATALYTIC ACTIVITY OF SHORT PEPTIDE AMPHIPHILE NANOSTRUCTURES: IMPLICATIONS ON THE ORIGIN OF LIFE

Yiğit Altay

M.S. in Department of Chemistry

Supervisor: Prof. Dr. Engin U. Akkaya

July, 2013

Chemosensor development is an attractive field of modern chemistry and there exist large amount of contribution from all over the world. The biological importance of thiols triggered the development of sensors to differentiate especially cysteine (Cys), homocysteine (Hcy) and glutathione (GSH) which play key roles in biological systems. Concentration of those thiols results in number of diseases and their structural similarity complicates the differentiation. Optical probes especially fluorescent ones are widely employed for that purpose since it offers simplicity, sensitivity and low detection limits as well as real time analysis. BODIPY core is decorated with a Michael acceptor nitro-styrene group to covalent incorporation of thiols and with an aza-crown moiety to recognition of N-terminus of them. The work in this thesis is the first example in which one of them is separated from others or three of them separated from each other's by chain length difference using fluorescence spectrometry.

Formation of short peptides (2-4 aa residues) is considered to be likely under primordial conditions, following a number of scenarios. In this work, it is constructed a short peptide library limiting our choice of amino acids to those believed to be available at larger concentrations such as Gly, Ala, Asp and Cys. It is demonstrated that when acylated at the N-terminus, nanostructures of varying size and shapes were formed. Investigations on the catalytic activity of these nanostructures under different conditions are presented. The findings on the correlation of peptide structure and nanostructure formation and/or catalytic activity are presented.

Keywords: Bodipy, molecular sensor, gluthathion, fluorescence,amino acid, peptide, catalytic activity.

ÖZET

BODIPY TABANLI BİFONKSİYONEL SENSOR İLE BİYOLOJİK TİYOLLERİN FLORESANS SEÇİCİ TAYİNİ VE YAŞAMIN KAYNAĞI ARAYIŞINDA KISA PEPTİT AMFİFİL NANOYAPILARIN KATALİTİK AKTİVİTELERİNİN İNCELENMESİ

Yiğit Altay

Kimya, Yüksek Lisans

Tez Yöneticisi: Prof. Dr. Engin U. Akkaya

Temmuz, 2013

Kemosensör geliştirme çalışmaları modern kimyanın ilgi çeken alanlarından birisidir ve bu alana tüm dünyadan büyük katkılar bulunmaktadır. Tiyollerin biyolojik sistemlerdeki önemi büyüktür. Biyolojik öneme sahip tiyollerden sistin (Cys), homosistin (Hcy) ve glutatiyon (GSH) kilit rol oynamaktadır. Benzer yapılara sahip bu tiyolerin hücre içi değerlerinin değişmesi durumunda sedef hastalığı, karaciğer yetmezliği, kanser, lökosit kaybı gibi birçok hastalık meydana gelmektedir. Bu sebeplerden ötürü, tiyol tayini çalışmaları büyük öneme sahiptir. Optik problar ve özellikle floresans olan optik problar kolay, hassas ve düşük algılama limitleri ve gerçek zamanlı analiz imkânları nedeniyle sıklıkla bu amaca yönelik kullanılmaktadır. Bu çalışmada BODIPY tiyollerin kovalent bağlanması için Michael alıcısı nitro-stiren grubu ile ve tiyollerin N-uçlarının tanınmasını sağlayan aza-taç eter grubu ile modifiye edilmiştir. İlk defa bu çalışma ile bu üç önemli tiyol, zincir uzunlukları arasındaki farklardan yararlanarak floresans spektroskopisi ile birbirinden ayırt edilmiştir.

Birçok senaryoya göre ilksel koşullar altında kısa peptitlerin (2-4 aminoasit) oluşabildiği bilinmektedir. Bu çalışmada, ilkel koşullarda daha yüksek derişimlerde bulunduğu bilinen Gly, Ala, Asp ve Cys aminoasitleri ile kısıtlanarak kısa peptit kütüphanesi oluşturulmuştur. Asetillenmiş N-ucuna sahip peptitlerin, değişik boyut ve şekillerde nanoyapılar oluşturduğu gözlenmiş ve bu yapıların değişik koşullar altındaki katalitik etkinlikleri incelenmiştir. Bu çalışmada peptit yapıları ve oluşan nanoyapılar ve/veya katalitik etkinlik ilişkileri üzerindeki bulgular sunulmuştur.

*Anahtar Kelimeler:*Bodipy,moleküler sensör, glutatiyon,floresans, amino asit, peptit, katalitik aktivite.

Dedicated to my beloved

mother and father

ACKNOWLEDGEMENTS

I would like to express my sincere appreciation to my research supervisor Prof. Engin Umut Akkaya. It would have been impossible for me to accomplish the work without his guidance, support and encouragement. I consider being his student as a great privilege and I would like to take this opportunity to offer my deepest gratitude for everything he has done for me. It has been an honor being a member of his research group.

I would like to thank Salih Özçubukçu whom I have learnt what I know about peptide chemistry. The days spent in his lab were not only contributed to my scientific knowledge but the discussions with him provided me a better understanding of science and its philosophy.

I also would like to express my appreciation to all of those with whom I have had the pleasure to work within the past four years. I am sincerely grateful to my colleagues Safacan Kölemen, Ruslan Guliyev, Tuğba Özdemir, Sündüs Erbaş, Onur Büyükçakır for their support and helpful discussions during the course of this research project. It has been a pleasure working with group members of Akkaya Lab. I thank them all for helpful discussions and collaborations as well as for their friendship.

I have received great support, encouragement and companionship from Can Aykanat, Pınar Kınay, Tuğçe Durgut and Tuba Yaşar during the past few years. I thank them all from the bottom of my heart for their valuable friendship.

I am grateful for the privilege of meeting Meniz Tezcan who has significantly important contributions on the work presented in this thesis. Other than being an outstanding collaborator, she is one of the brightest minds that I have ever met.

Last but not the least; I would like to thank my family for their unconditional love, continuous support and understanding for what I am doing and what I want to do. I owe them a lot for their support throughout my life.

LIST OF ABBREVIATIONS

BODIPY :Boradiazaindacene

CD : Circular Dichroism

Cys : Cystein

DIEA : Diisopropylethyl amine

DMF : Dimetylformamide

EtOH : Ethanol

FL : Fluorophore

FMOC : Fluorenylmethyloxycarbonyl

FTIR : Fourier Transform Infra-Red

GSH : Glutathione

HBTU : O-(Benzotriazol-1-yl)-N,N,N′,N′tetramethyluronium hexafluorophosphate

Hcy : Homocystein

HRMS : High Resolution Mass Spectroscopy

ICT : Internal Charge Transfer

MeOH : Methanol

NMR : Nuclear Magnetic Resonance

PeT : Photoinduced Electron Transfer

pNPA : p-nitrophenylacetate

PS : Photosensitizer

SEM : Scanning Electron Microscopy

TFA : Trifluoroacetic acid

TLC : Thin Layer Chromatography

TABLE OF CONTENTS

LIST OF FIGURES

LIST OF TABLES

CHAPTER 1
INTRODUCTION

Thiols have a great importance in biological systems. Among possible biologically relevant thiols three of them play key roles; namely, cysteine (Cys), homocysteine (Hcy) and glutathione (GSH) (Figure 1). Those thiols have similar structures and generally results in number of diseases such as psoriasis, liver damage, cancer, and leucocyte loss if levels of cellular thiols have altered. In more detail, Cys deficiency causes slow growth of children, liver damage, loss of muscle, and hair depigmentation. Elevated level of Hcy in plasma triggers Alzheimer diseases. On the other hand, GSH which is a non-protein-thiol takes place in cellular functions such as intracellular signal transduction, gene regulation, and intracellular redox activities. Apart from above three, thiophenols are known to be a highly toxic and environmentally unfriendly. Thus, the detection of thiols has become a very important task. Optical probes especially fluorescent ones are widely employed for that purpose. This is apparent because fluorescence detection offers simplicity, sensitivity and low detection limits as well as real time analysis.

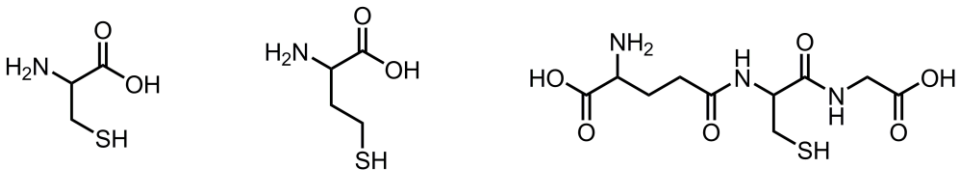

Cysteine (Cys) Homocysteine (Hcy) Gluthathione (GSH)

Figure 1. Structures of Cys, Hcy and GSH.

Probe design for thiol sensing mostly utilizes thiols strong nucleophilicity and high binding affinity towards metal ions. Based on these features, fluorescence sensing of thiols involves characteristics reactions between probe and thiol such as Michael addition, cyclization, and cleavage of disulfide bond in the presence of thiols. One can find many literature examples with these approaches. In most of them Cys, Hcy and GSH were detected together or only two of those were separated from the other. There is no example in which one of them is separated from others or three of them separated from each other's by fluorescence spectra.

The molecular origin(s) of life is one of the most essential questions in modern biology and chemistry. The RNA world hypothesis could give satisfactory explanations for the evolvement of the biochemical networks but it cannot explain the connection between the primeval molecules and first RNA molecules. It is obvious and practically impossible that molecules with high complexity cannot be evolved spontaneously. Formation of tubular, vesicular and fibrilar structures via self-assembly of peptides as simple as dipeptides has been demonstrated recently. In addition to that, dipeptides can be used as template for synthesis of other peptides and can act as catalysts. In contrast to complex RNA molecules, it is very likely that functional short peptides can be synthesized under primordial earth conditions.

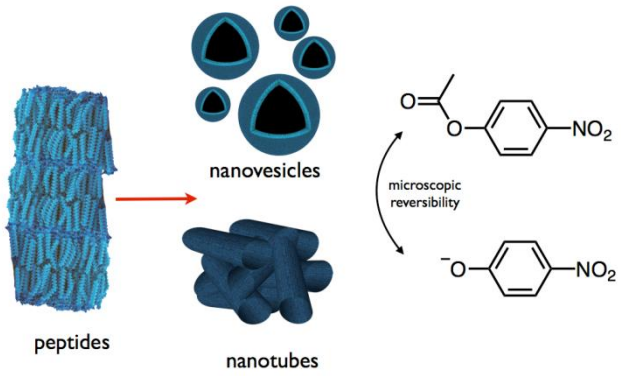

Figure 2. Schematic representation of hydrolysis reaction by peptide nanostructures.

In this thesis, a novel mechanism for the origin of life is proposed using the ability of short peptides to form well-ordered nanostructures and catalysis of chemical reactions. This model may help to explain early processes that led to the evolution of current biochemical systems that allow the functioning of living systems. For that purpose four natural amino acids (glycine, alanine, aspartic acid and cysteine) are selected because of their simplicity, primordial occurrence and known catalytic activity. A peptide library is constructed with alternating the sequence of amino acids. In each sequence, each amino acid used once and N-terminus of the peptides are acetylated with ten-carbon-long hydrocarbon chains to make peptides amphiphilic. Under same conditions, some of the peptides formed nanostructures adopting β-sheet conformation. Catalytic properties of these peptides are studied on the hydrolysis of p-nitrophenyl acetate benefiting from the fact of microscopic reversibility principle.[1]

CHAPTER 2
BACKGROUND

2.1 What is Supramolecular Chemistry?

Physics declared its reign with the beginning of everything, the Big Bang. Then chemistry came along as the temperature decrease; elementary particles formed small atoms, and they united to make more and more complex molecules. These molecules formed aggregates, aggregates formed membranes, defining the protocells of which eventually give rise to emergence of life. Life is the highest expression of chemistry.

Molecular chemistry focuses on the covalent bond. Starting from *Wöhler*'s[2] urea synthesis to the synthesis of Vitamin B_{12} by *Woodward*[3] and *Eschenmoser*,[4] molecular chemistry is strengthened more and more. But there was a gap for the non-covalent interactions waiting to be filled. And the supramolecular chemistry aimed to gain control over non-covalent intermolecular interactions.

Supramolecular chemistry is a highly interdisciplinary field of science focusing on the chemical, physical and biological characteristics of molecular systems that are held together by the non-covalent intermolecular interactions rather than the molecule itself. Intermolecular forces are weaker with respect to covalent bonds. This is the reason why supramolecular species are thermodynamically less stable, kinetically more labile and dynamically more flexible.

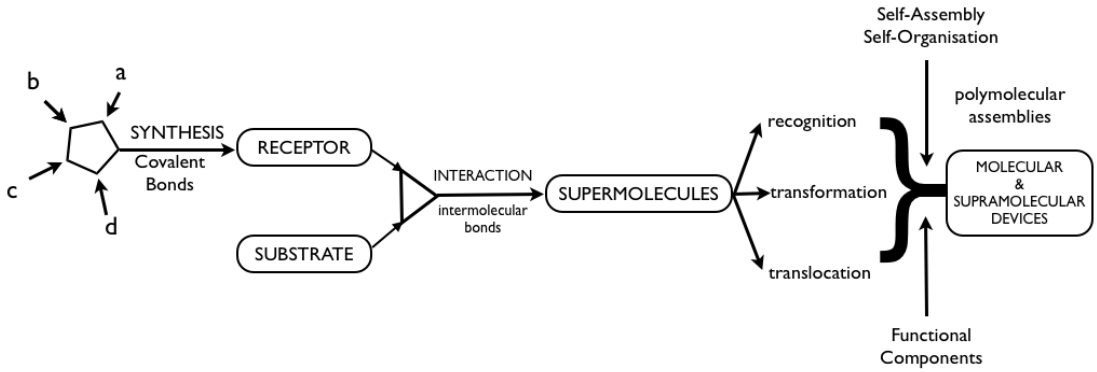

Figure 3. From molecular to supramolecular chemistry; molecules, supermolecules, molecular and supramolecular devices.

2.2 Molecular Recognition

Molecular recognition can be defined by the information and the energy carried by the selection of substrate by a certain receptor molecule. It may also involve a specific function.[5] Recognition can be considered as binding with a purpose. Receptors are such an example. Structurally well-defined set of intermolecular interactions undergoes through recognition processes. Complex or the supermolecule is formed upon binding of guest (analyte) to the host (receptor). Characterization can be done by its thermodynamic and kinetic stability and selectivity. It means that the amount of energy and information brought into operation are characteristic for such processes.

2.2.1 Recognition, Information and Complementarity

Molecular information can be stored molecularly and can be read out supramolecularly through molecular recognition. At the beginning of 1970's, studies on selective complexation of metal ions facilitated the use of notions of recognition and information which were used in relation with biological systems.[6] Since then molecular recognition has become a very frequently used term and a major field of research in chemistry.

Architecture of the receptor is capable of storing information in its binding sites; and the rate of formation and dissociation of the supermolecule provides a read out. Conformation, chirality and dynamics also come into play during the receptor characterization in addition to its size and the shape. In addition to eventual reactivity that may allow the coupling of complexation with other processes (protonation, deprotonation, oxidation and reduction); features such as size, shape, charge, polarity, polarisability, van der Waals interactions, number and the arrangement on the receptor architecture carries information for the characterization of binding sites. Thickness, hydrophilicity or hydrophobicity and overall polarity plays important role in the action of ligand layer. In addition, the mutual balance between solvation of guest by host and the complexation affects the stability and selectivity.

The most fundamental and the general notion of supramolecular chemistry is the information. In this respect, supramolecular chemistry could be considered as molecular informatics that concerns molecular storage and read out and processing the information via molecules or supermolecules.[7,8]

Interactional and geometrical complementarity between associating species is implied by recognition. So that the double complementarity principle extend over energetics in addition to geometrical ones such as the lock and key and steric fit concepts introduced by Emil Fischer.[9]

In order to get high recognition by a receptor molecule ρ, there should be a large difference between the binding free energies of a given substrate σ and the other substrates. Deviation from the statistical distribution is the ultimate result. There are several factors that should be taken into consideration to achieve large differences in affinity:

1) Complementarity between ρ and σ in terms of size and shape
2) Interactional complementarity.
3) Large contact areas between ρ and σ.
4) Multiple interaction sites to compensate the relative weakness of non-covalent interaction.
5) Strong overall binding.

In addition, two partners (ρ and σ) should have overlapping hydrophobic/hydrophobic or hydrophilic/hydrophilic domains to overcome the medium effects that play an important role in interaction of solvent molecules with ρ and σ.

Biological molecular recognition represents the most complex expression of molecular recognition leading to highly selective binding, reaction, transport, regulation etc. It provides study cases, illustration and inspiration for the unraveling of basic principles and for the design of model systems as well as abiotic receptors.

2.2.2 Design Principles of Molecular Receptors

Molecular receptors are defined by their characteristic property of binding selectively to ionic or molecular substrates (or both) by means of various intermolecular interactions, leading to an assembly o two or more species, a supermolecule. The principles of molecular recognition should be expressed in the design of a molecular receptor. Receptor chemistry represents a generalized version of coordination chemistry. But it is not limited to transition-metal ions and extending to all type of substrates: cationic, anionic, or neutral specie of organic, inorganic or biological nature. [10]

In order to achieve high recognition, every factor should be taken into account in the design of the receptor. In particular, complementarity depends on a well-defined three dimensional architecture with the correct arrangement of binding sites. Furthermore, ρ and σ will be in contact over a large area, if ρ is able to wrap around its guest so as to establish numerous non-covalent binding interactions and sense its molecular size, shape, and architecture. These are important especially in design of receptor molecules containing intramolecular cavities, clefts or pockets into which the substrate may fit.

Macrocyclic structures are of special interest for designing artificial receptors. They are large and may therefore contain cavities of appropriate size and shape. They possess numerous branches, bridges, and connections that allow the construction of a given architecture having specific dynamic features. Binding of a substrate into the cavity will yield an inclusion complex, a *cryptate*. [11] In addition to maximizing the contact area, inclusion also leads to almost complete solvent exclusion from the receptor site. Thus the displacement of solvent molecules by the substrate on binding is minimized.

The balance between rigidity and flexibility is important especially for binding and the dynamic properties of ρ and σ. On one hand, rigid receptors are expected to have highly efficient recognition since they are highly stabile and highly selective. On the other hand, substrates bind to flexible receptors by an induced fit.[12] This may present high selectivity but lower stability since a part of the binding energy is used

in the conformational change. The designed dynamics are more difficult to control than rigidity. So receptor design covers both static and dynamic aspects of macrocyclic structures.

Chelating and macrocyclic ligands are frequently employed due to high thermodynamic stability of their complexes. The chelate effects refers to the enhanced stability of complex containing chelate rings as compared to a similar system containing fewer or no rings. Starting from the five membered chelate rings, chelate effect decreases with increasing ring size. Longer chains have higher configurational entropy and thus ring formation becomes increasingly improbable.

The macrocyclic effect is related to the chelate effect and refers to the increased thermodynamic stability of macrocyclic systems compared to their acyclic analogues. Macrocyclic hosts are less heavily solvated than their acyclic analogues and therefore less energy is required for desolvation (coordination is more enthalpically favorable). Macrocyclic ligands are less flexible and consequently have less disorder to lose on complexation than their acyclic analogues (in other words, coordination is more entropically favorable because of the relative rigidity of the receptor).

The enhanced binding of guest species provided by chelating or macrocyclic hosts has been employed in the design of many receptors operating through a variety of intermolecular forces.

2.2.3 Anion Recognition

Anionic species play crucial roles in chemistry and in biology; however their binding characteristics have not extensively studied. The coordination chemistry of anions is expected to have significant outcomes in novel structures and chemical and biological properties. In the recent years, research in this field is increasingly active and slowly builds its path in the area of coordination chemistry. [13,14,15]

Anionic substrates possess a wide range of geometries: spherical (F^-, Cl^-, Br^-, I^-), linear (N_3^-, OCN^-), planar (NO_3^-, $R\text{-}CO_2^-$), tetrahedral (SO_4^-, ClO_4^-) and octahedral ($M(CN)_6^{n-}$).

Polyammonium macrocycles and macropolycycles have been studied most extensively as anion receptor molecules. They bind to inorganic anions, carboxylates and phosphates selectively with electrostatic and structural effects.

2.2.4 Cation Recognition

Cation detection is of great interest to many scientists from different fields including chemists, biologists, geologists and environmentalists. In many biological activities cations plays an important role such as enzyme activation (Zn^{2+}, Mg^{2+}, Mn^{2+}) , transmission of nerve impulses (Na^+, Mg^{2+} and Ca^{2+}), regulation of cell activity (Zn^{2+}, Mg^{2+} and Ca^{2+}) and muscle contraction (Na^+, K^+ and Ca^{2+}). Moreover, some metal ions are key component of metalloenzymes. In the treatment of high blood pressure and manic depression potassium and lithium are important serum parameters, respectively. Additionally, early detection of environmentally important toxic heavy metals such as mercury, cadmium and lead has great importance. For the cation detection, several methods are available: flame photometry, atomic absorption spectrometry, ion sensitive electrodes, electron microprobe analysis, neutron activation analysis, etc. These techniques are rather expensive and requires large amount of sample and continuous monitoring cannot be carried out.

Fluorescent sensors on the other hand provide real time analysis opportunities with high accuracy and selectivity. The design consists of a fluorophore connected to an ionophore. High stability and selectivity, metallic affinity, kinetically rapid sensitization and ease of target delivery are some of the criteria for good chemosensors. In such designs, signaling moiety converts the recognition into optical signal in the form of emission or shift in the absorption spectrum. These photophysical changes are due to perturbation of photoinduced processes.

Cyclic polyethers are one of the commonly used in recognition processes of positively charged metal ions (alkali, alkaline-earth and lanthanide cations). Three main classes may be distinguished:

1) natural macrocycles having antibiotic properties such as valinomycin or the enniatins;[16,17]

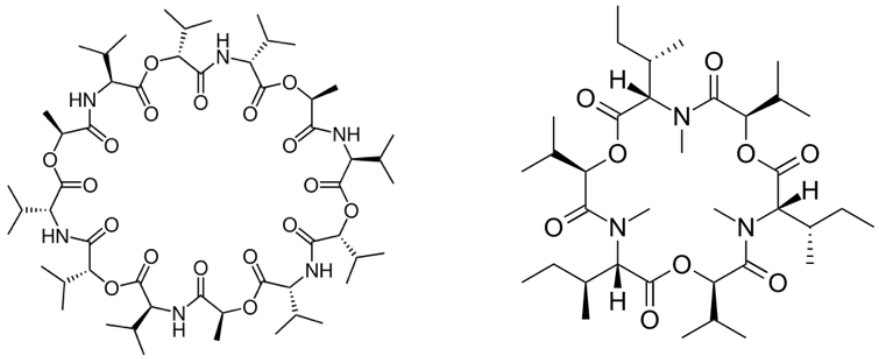

1 **2**

Figure 4. Valinomycin (*1*) and enniatin (*2*).

2) synthetic macrocyclic polyethers, the crown ethers,[18] their derivatives[19] and spherands.[20]

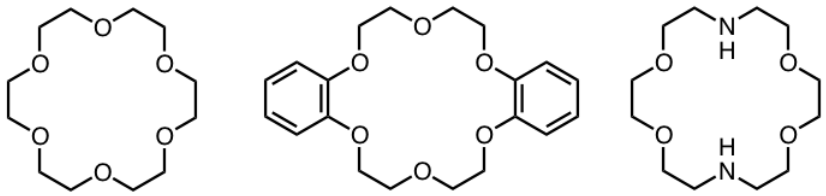

3 **4** **5**

Figure 5. Crown ether and its derivatives: 18-crown-6 (*3*), dibenzo-18-crown-6 (*4*), diaza-18-crown-6 (*5*),

3) synthetic macropolycyclic ligands, the cryptands[21,22] and cryptospherands.[23,24]

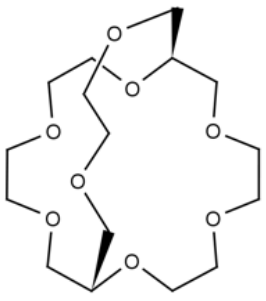

6

Figure 6. A cryptand.

There are numerous reports and studies on these supramolecules. For instance, valinomycin gives a strong and selective complex in which a K^+ ion is included in the macrocyclic cavity. Similar inclusion takes place in the complexes of crown ethers such as the complex of Rb^+ ion with dibenzo-18-crown-6.

2.3 Photophysics of Light Absorption and Emission

"Light plays an essential role in our lives: it is an integral part of the majority of our activities. The ancient Greeks, who for 'to die' said 'to lose the light', were already well aware of this" said Lois de Broglie in 1941. Light gives the color and brilliance to all works of art and nature. This brilliance is realized by absorption of light by the molecules.

An electronic transition occurs upon the absorption of an electron in which one electron from an orbital of a molecule in the ground state HOMO (or HOMO-1 etc.) to an unoccupied orbital LUMO (or LUMO+1 etc.). Photons being part of the UV-visible region have enough energy to induce such transitions. Photons being part of other regions may result in a wide variety of changes in the molecule upon excitation. These changes are summarized in Table 1.

Radiation	Wavelength	Photon Energy	Results of Absorption
Gamma-rays	< 0.01 nm	> 1 MeV	Nuclear reactions
X-rays	0.01-10 nm	124 eV-120 keV	Transitions of inner shell electrons
Ultra violet	10-400 nm	3.1-124 eV	Transitions of outer shell electrons
Visible	400-750 nm	1.7-3.1 eV	Transitions of outer shell electrons
Infrared	750nm-15 µm	80meV-1.7 eV	Molecular vibrations
Far IR	15µm-1 mm	1.2meV-80meV	Molecular rotations
Radar	1mm-1 m	1.2µeV-1.2meV	Oscillation of mobile electrons

Table 1. Impact of the electromagnetic radiations on molecular structures.

Fluorescence is defined as the emission of photons accompanying the S_1-S_0 relaxation. Since emission occurs from S, its characteristics do not depend on the excitation wavelength. Fluorescence and absorption have same 0-0 transitions however, fluorescence occurs at higher wavelengths (lower energy) than the

absorption since some of the excited state energy is lost due to vibrational relaxations.

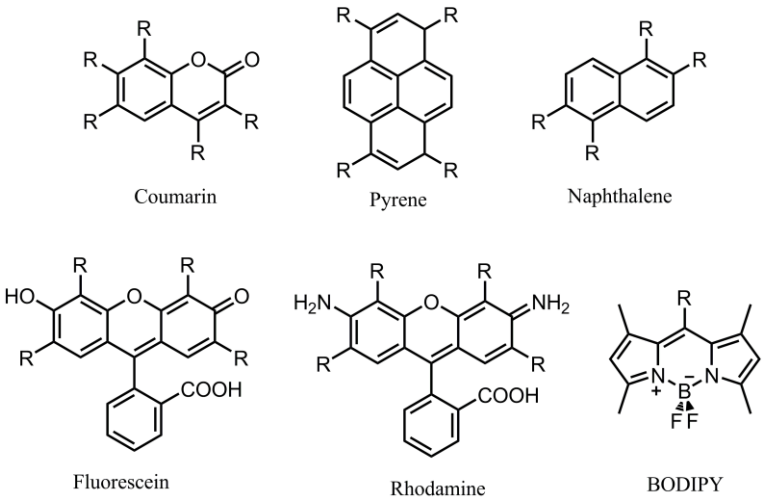

Figure 7. Structures of typical fluorescent substances.

In general, ground and excited states have similar vibrational level differences, so that the fluorescence spectrum often resemble the first absorption band and the gap between the maximum of the first absorption band and the maximum of fluorescence is called the *Stokes Shift*. So the main cause of Stokes shift is the rapid decay to the lowest vibrational level of S_1. In addition to this effect, fluorescent molecules can display further Stokes' shift due to solvent effects, excited-state reactions, complex formation and energy transfer.

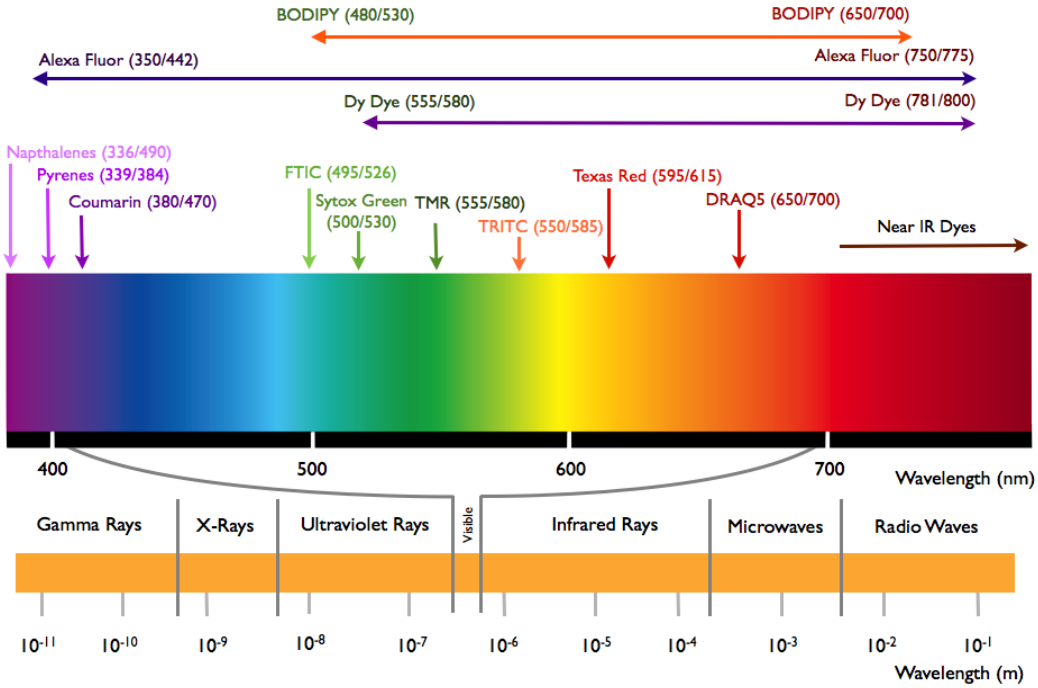

Figure 8. Distribution of dyes in the visible region.

2.3.1 Characteristics of Fluorescence Emission

There are several possible transitions between electronic states. Photon absorption, internal conversion, fluorescence, inter-system crossing, phosphorescence, delayed fluorescence and triplet-triplet transitions are the possible processes that are used to describe radiative and non-radiative transitions between electronic states. In the Perrin-Jablonski diagram (Figure 9) singlet electronic states are depicted as S_0, S_1, S_2,... and the triplet states T_1, T_2, T_3,... . Characteristic times of these processes can be found in the Table 2.

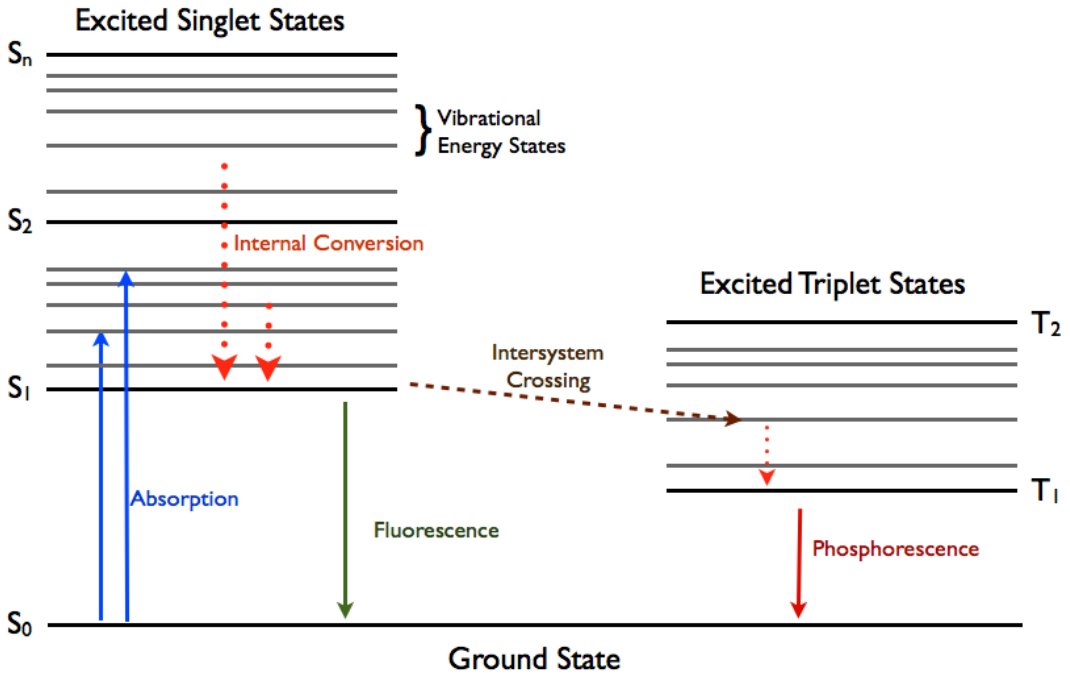

Figure 9. Perrin-Jablonski diagram and illustrations of the relative positions of absorption, fluorescence and phosphorescence processes.

Most elementary particles are in their ground state at room temperature. When these particles are irradiated by photons with proper energies, the electrons move to a higher energy state, which can also be termed as excited state. Once a molecule is excited by absorption of a photon, it can return to the ground state with emission of fluorescence, but many other pathways for de-excitation are also possible. These are internal conversion, intersystem crossing, intramolecular charge transfer and conformational change. Moreover, interactions in the excited state with other molecules such as electron transfer, proton transfer, energy transfer, excimer

formation, exciplex formation and photochemical transformations may compete with de-excitation.

Characteristic Times	
Absorption	10^{-15} s
Vibrational Relaxation	$10^{-12} – 10^{-10}$ s
Lifetime of the excited state S_1	$10^{-10} – 10^{-7}$ s (Fluorescence)
Intersystem Crossing	$10^{-10} – 10^{-8}$ s
Internal Conversion	$10^{-11} – 10^{-9}$ s
Lifetime of the excited state T_1	10^{-6} – 1 s (Phosphorescence)

Table 2. Characteristic times for transitions between electronic states.

2.4 Energy and Electron Transfer Processes

Light absorption significantly affects the electronic properties of molecules. It may induce intra- or intermolecular electron transfer processes leading to electron-hole separation.

2.4.1 Intramolecular Charge Transfer (ICT)

Intramolecular charge transfer (ICT) is a process that leads to blue or red shift in the emission spectrum of a fluorescent molecule and very common mechanism used in signaling. In the design of ICT-type chemosensors, fluorophore and the receptor units are directly bound to each other. The receptor is conjugated to the π-system of the fluorophore where it acts as an electron donor or electron acceptor according to the state of the fluorophore.

The electron density is redistributed when conjugated receptor-fluorophore system is excited by the absorption of a photon. This redistribution forms a dipole and internal charge transfer from donor to acceptor is thus triggered. When analyte bind to the system, it interacts with this excited state dipole. Interaction leads to significant changes in the both emission and absorption spectra.[25]

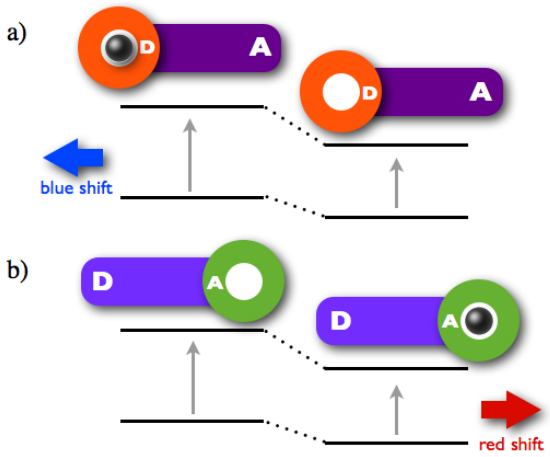

Figure 10. Spectral shifts of ICT type sensors: a) Interaction with the donor group, b) Interaction with the acceptor group.

If the receptor is electron rich, interaction with the cation leads to reduction of e-donation ability of that group which results in the weakening of conjugation. This interaction destabilizes the excited state more and results in the increase in the E gap between ground state and the excited state and thus a blue shift is observed in the absorption spectrum. In the reverse case scenario, if the receptor is electron poor, interaction with the cation leads to increase the electron withdrawing ability of that group. The interaction stabilizes the excited state more than ground state and so the E gap between ground state and excited state and thus red shift in the absorption spectrum is observed (Figure 10).

In literature, ICT is a frequently used mechanism in the design of fluorescent sensors. Compounds **1**[26] exhibit blue shift in both absorption and emission spectra upon cation binding and **2**[27] produce Ca^{2+}-induced red-shifts in the emission spectra. (Figure 11)

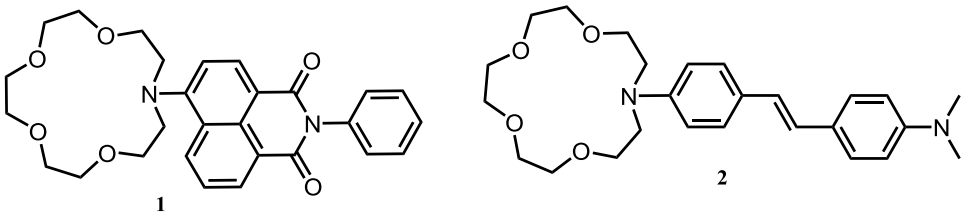

Figure 11. Crown containing ICT sensors.

In addition to chemosensing applications, ICT systems are also widely used in optoelectronics, such as organic light emitting devices,[28,29] nonlinear optical devices,[30] and solar cell materials.[31]

2.4.2 Photoinduced Electron Transfer (PeT)

The photogeneration of charge-seperated species by photoinduced electron transfer (PeT) is an important phenomenon for initiating photocatalytic reactions and for the transfer of photosignal.

Photoinduced electron transfer (PeT) corresponds to the primary photochemical processes of the excited-state species, R*→I, where R* can be an electron donor (therefore oxidised, $R^* + M \rightarrow R^{*+} + M^{*-}$) or electron acceptor (therefore reduced, $R^* + M \rightarrow R^{*-} + M^{*+}$) when reacting with another molecule, M. In, an electron is transfered between excited species and ground-state species. Since the electron transfers occur by electron-exchange interactions, orbital overlap is required.

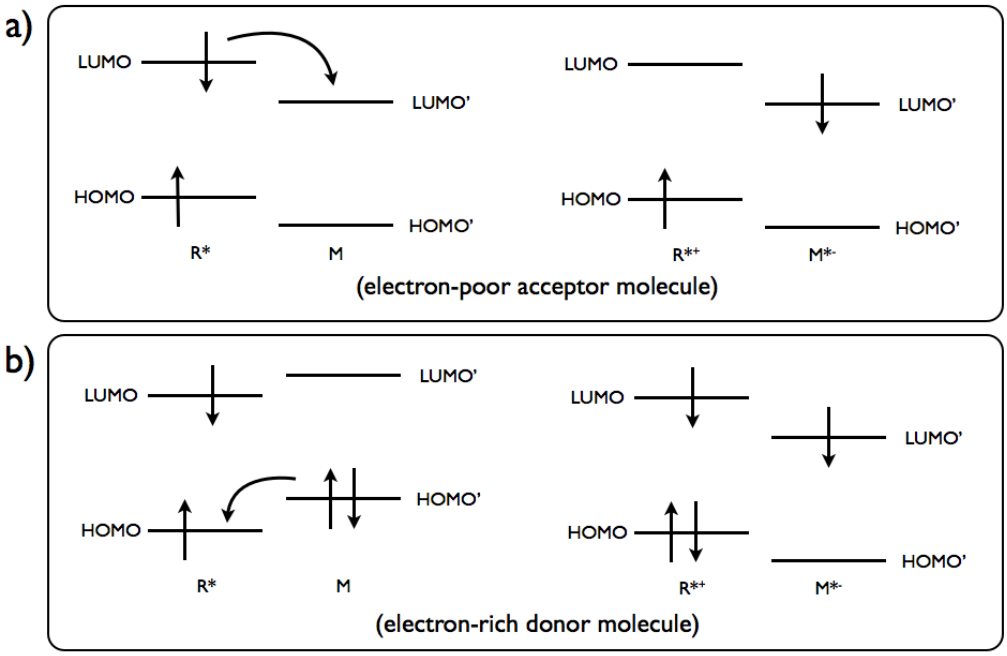

Figure 12. Molecular orbital representation of a) oxidative and b)reductive electron transfer.

Probe molecules used for PeT consist of three major components: fluorophore (fluorescent chromophore), spacer and receptor. Spacers, as small as methylene

bridges, are used to cut off the conjugation between fluorophore and the receptor to eliminate other possible pathways. Cation receptor group contains electron donating group and PeT occurs from the receptor to fluorophore and results in quenching of the latter. Upon binding of cation or H^+, fluorescence properties of the fluorophore restored as the electron transfer is inhibited. An electron is promoted from the HOMO to the LUMO when the fluorophore is excited. Thus PeT occurs from the HOMO of the receptor to that of the fluorophore. On binding, the redox potential of the electron-donating receptor is raised so that its HOMO becomes lower in energy than that of fluorophore. Thus, since PeT is not possible, fluorescence is observed.

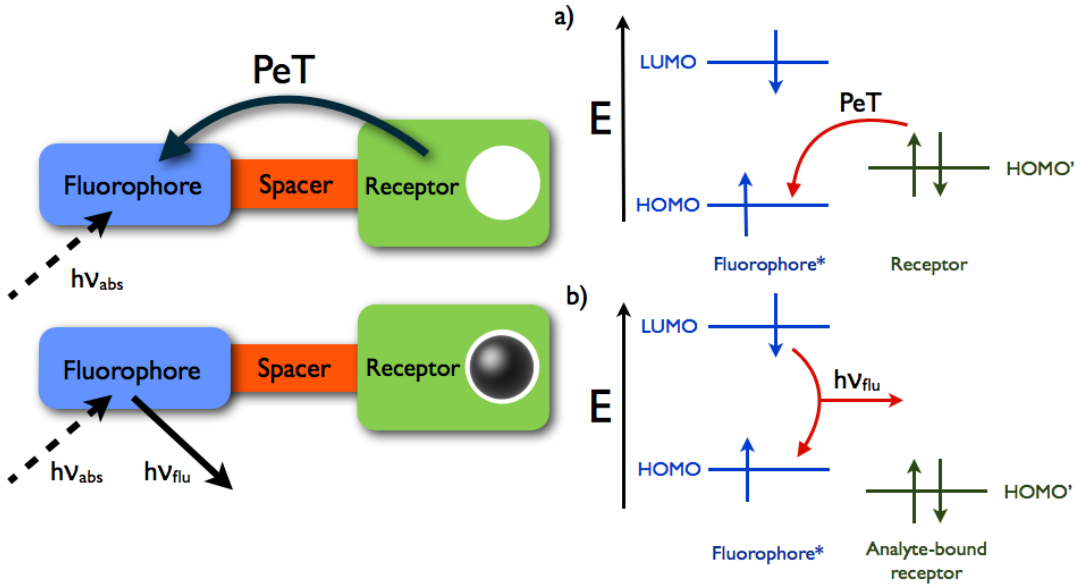

Figure 13. Molecular action of a fluorescent PeT potassium cation sensor as a molecular switch using a macrocyclic electron donor and anthracene fluorophore.

In literature, there are many examples of fluorescent probes for cations, including H^+, that are normally nonluminescent, but become fluorescent upon binding of cation.

Figure 14. Contributions to fluorescent PeT sensors from all over the world. [A. P. de Silva, T. S. Moody, G. D. Wright, Analyst, no. 134, pp. 2385–2393,2009. <http:// http://pubs.rsc.org/en/Content/ArticleLanding/2009/AN/b912527m>] - Reproduced by permission of The Royal Society of Chemistry.

PeT is the other widely used mechanism in the design of molecular probes. Molecule **3**[32] is the first molecule used in a molecular logic operation, namely used as a AND gate operator. There are two PeT pathways, one from electron rich tertiary amino and the other from crown ether group, blocking the fluorescence of anthracene moiety. Upon protonation of the amino group only does not recover the fluorescence since the PeT is still active through the crown ether moiety. Same thing is applicable for the binding of a Na^+ ion to the 18-crown-6 group. However, when both of the analytes, H^+ and Na^+, present PeT is blocked and the fluorescence emission of anthracene is recovered.

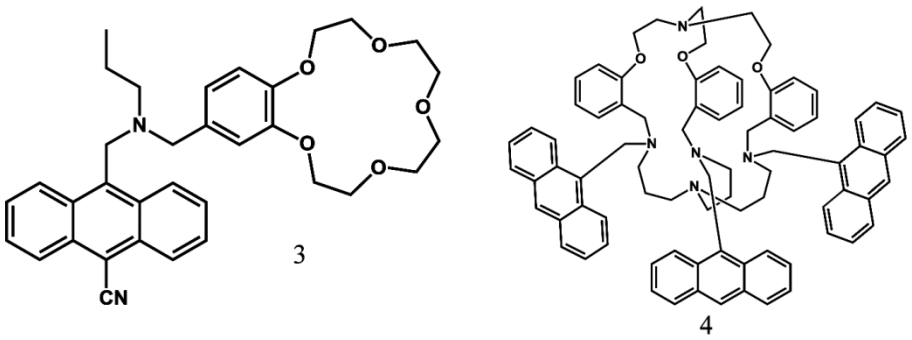

Figure 15. PeT based sensors.

Molecule **4**[33] is another molecular logic gate operator acting as an OR gate operator. It has poor chemoselectivity for transition metals, however shows significant emission enhancement upon addition of either Pb^{2+} or Eu^{3+} /Tb^{3+} ions or both of the ions.

2.5 Fluorescent Chemosensors and BODIPY Dyes

Fluorescent detection is a highly sensitive, easily processible, simple and cheap method to detect molecules or ions of interest. So that fluorescent chemosensors draw great attention. In the design of chemosensors, recognition and signaling processes have significant importance. In signaling, fluorescent core itself used as the signaling unit and a synthetic or biological receptor unit is incorporated to the system. Receptor set the limits of binding and selectivity. Because of that reason, a receptor should strongly and selectively bind to the target analyte. The fluorophore transforms information into optical signal as emitting light. As seen in the previous sections, binding of an analyte to the receptor may lead to significant changes in the photophysical properties of the fluorophore. With the help of these changes, presence and/or concentration of the analyte can be determined easily. What changes in the photophysical properties after the chemosensor undergoes complexation can be adjusted as desired in the design of the chemosensor. It can be in the form of enhancement or quenching of fluorescence signal via PeT mechanism, or shift in the emission wavelength via ICT mechanism.

There are several design models for fluorescent probes in accordance with the desired signaling process. Fluorophore-spacer-receptor or integrated systems are

examples of such designs (Figure 16). In fluorophore-spacer-receptor design, spacer cuts off the conjugation between receptor and the fluorophore whereas in the integrated systems receptor is a part of π-electron system of the fluorophore.

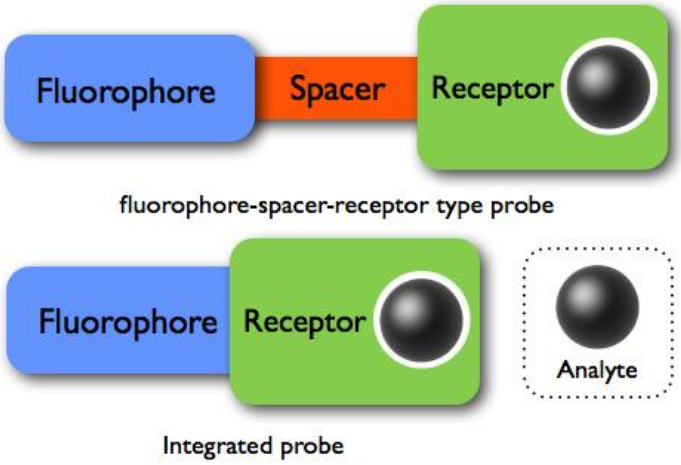

Figure 16. Schematic representations for the types of fluoroionophores.

Fluorescent dyes are used in a broad field in chemistry including supramolecular chemistry, photochemistry, biochemistry and physical chemistry. Among the large variety of fluorescent dyes known, boradiazaindacenes (BODIPY) have drawn increasing attention due to its high molar absorptivity, high fluorescence quantum yield, small Stoke's shift, high photostability and ease of synthesis.

Numbering of the BODIPY core skeleton shows differences with its precursor dipyrromethane. The central carbon is named as *meso* position which comes from the porphyrin nomenclature.

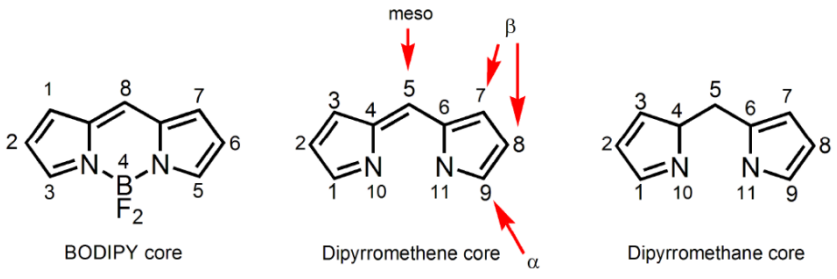

Figure 17. Structures and numbering of dipyrromethane, dipyrrin and Bodipy

BODIPYs are stable under a wide range of pH values but start to decompose in strongly acidic or basic conditions. Also solvent polarity does not have significant

role in their characteristics. In addition to these properties, one of the reasons that draw attention is the ease of functionalization and tunability. Today it is well known that all positions (1–8) on the BODIPY core are open to chemical modifications (Figure 18). Making structural modifications brings out new members of BODIPY family with some shifted photophysical properties.

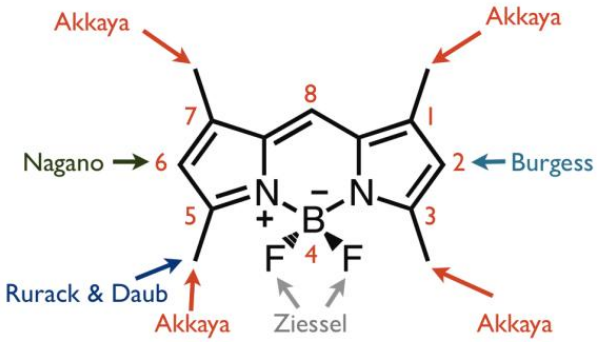

Figure 18. Important contributions to chemical modifications of the BODIPY core.

Akkaya *et al*. have important contributions to BODIPY chemistry especially in modification of the core in addition to their contributions to its applications in energy transfer cassettes, light harvesting systems, solar sensitizers, photodynamic therapy agents, fluorescent chemosensors and molecular logic gates. In the year 2009, they first reported the first member of the tetrasytryl-BODIPY dyes (molecule 10). Styryl groups are introduced to the BODIPY via Knoevenagel condensation on 1,3,5, and 7 position. Starting from unsubstituted core (abs. 500 nm/ ems. 525 nm); mono, di, tri and tetra substituted derivatives successfully managed to cover almost all the visible region extending to the near IR region with modifications on styryls.

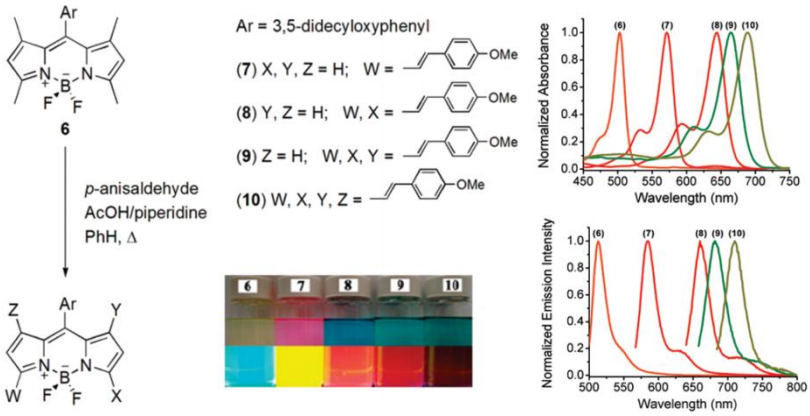

Figure 19. Mono-, di-, tri- and tetra-styryl BODIPY derivatives. Adapted with permission from (O. Buyukcakir, O. A. Bozdemir, S. Kolemen, S. Erbas, and E. U. Akkaya, "Tetrastyryl-Bodipy Dyes: Convenient Synthesis and Characterization of Elusive Near IR Fluorophores", Org. Lett., vol. 11 , no. 20, pp. 4644–4647, 2009.). Copyright 2013, American Chemical Society.

2.6 What is Life?

Is it possible to define "life"?

Obviously, one needs an operational definition to describe what life is and how can it be characterized and, at the same time, to have a historic description relating life as we know it to the history. Our inability to give a complete definition of life was discussed by Küppers.[34] However, in spite of this conclusion, as well as similar conclusions reached earlier by other researchers, the scientific literature is abundant with attempts to define life (see Appendix E).

Historically there always been huge division between what people define living and non-living systems. As a consequence, we consider beautiful and complex crystals as non-living systems and rather beautiful and more complex animals as living. Although in the last hundred and fifty years science blurred the sharp distinction between the two, now it is certain that there is a continuum between living and non-living systems. For instance, viruses are the natural systems that cannot actually satisfy all the properties of living systems such that it needs another host to reproduce and evolve.

The scientific approaches to the characterization of life may be divided according to two aspects of life: One view focuses on the molecular level, whereas the second is cell-centered view. Most of the characterizations and definitions in Appendix E can be attributed to the first point of view. The second view is presented by the notion of *autopoiesis* (Greek word for "self-producing"), according to which life cannot be characterized by means of just one component or attribute of its complex pattern.

Then what are the characteristics of life? First of all, life has a body. It differentiates the self from its surroundings. Second, life should have a metabolism. This is a process of life uses to convert resources into building blocks so that it can build and maintain itself. Third, life has a kind of inheritable information. Human beings reserve this information as DNA in their genome and inherit to its offspring. If the first two, body and metabolism, are coupled, moving and reproducing systems may

be obtained. With the addition of inheritable information, system would be more lifelike and would even capable of undergoing evolution.

2.7 History of the Search into the Origin of Life

A scheme of the major landmarks in the history of the search into the origin of life can be seen in Figure 20. Starting with Thales and ending with some of the names of the most recent theories.

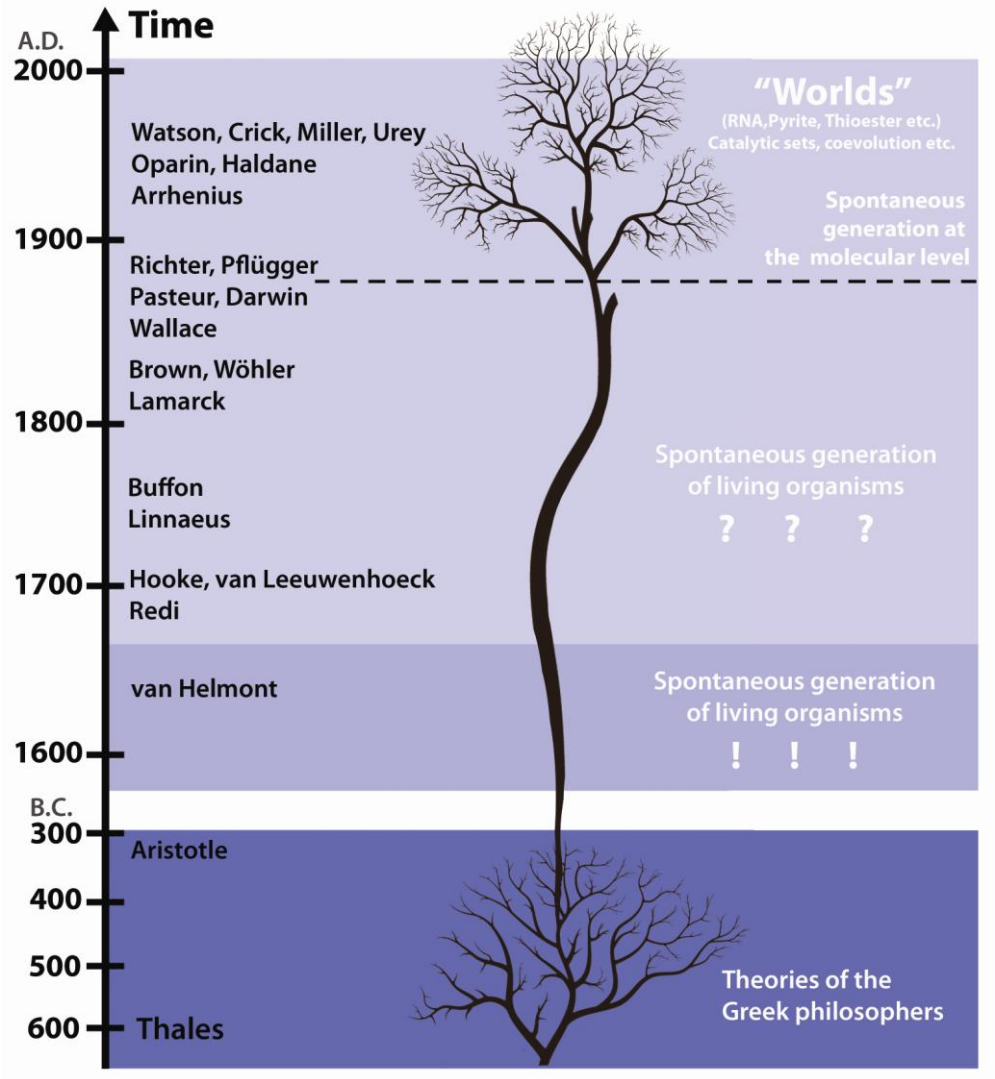

Figure 20. A scheme of the origin of life theories.

2.7.1 Historical Outlook

The scientific methodology was originated by the Greek philosophers, some 2.600 years ago. Curiosity was not forbidden by Greek traditions and beliefs. Moreover,

their philosophers explained the world in rational terms of mechanisms and natural processes and entities, not by divine actions. Two of the trivial questions they asked were what differentiates living from nonliving entities, and how plants and animals were formed. The Greek philosophers developed different ideas and proposals with regards to the problems they studied.

Thales, scholar from Miletus, is believed to have been the first Greek philosopher. He tried to discover the laws of nature by reasoning and understanding nature and observing the latter. According to him, magnet is a living entity since it causes iron bodies to move. Amber is also a living entity, since it can move other substances. Moreover, water is the substance of which the world is made; it is the ultimate substance out of which all things are generated and eventually perishes.[35]

A pupil of Thales, Anaximander first presented the elements of Darwinian evolution theory. He thought that adaptation to different conditions was needed in order to survive. According to him, life was formed spontaneously and abiogenetically, in the sea. Another supporter of abiogenesis was Xenophanes who was proposed that life is formed from nonliving substance.

The origin of life is explained by Empedocles as the association of soil and humidity under the influence of heat. Plants were the first formed out of these combinations. These were followed by the formation of limbs of animals which were seperated from each other but striving to combine with each other. Empedocles' proposition seems to contain elements of selection and struggle but not of evolution.

Leucippus is believed to have been the first philosopher who developed the concept of atoms. According to his school, there are four kinds of atoms: stone atoms, dry and heavy; water atoms, wet and heavy; air atoms, light and cold; fire atoms, light and hot. Combinations of these kinds of atoms make up all known and unknown materials. On the other hand Democritus, the pupil of Leucippus, argued that there is an infinite number of worlds like ours. Since there is infinite number of atoms, there should be an infinite number of worlds made up of these atoms. Epicurus was the most prominent follower of Democritus' atomic teaching. According to him, notion of motion of the atoms was a built-in feature, independent of any divine forces.

Aristotle was the most prominent opponent of the Democritus' atomic world. Randomness and lack of theology was not overlapping with the Aristotle's teachings. But he was apparently the first philosopher who described the graduality of living creatures and addressed the gradual transition between nonliving matter and plants and between plants and animals.

The Greek philosophers developed the school of thought that later became the mainstream of Western thinking regarding the origin of life, namely the spontaneous generation theory.

2.7.2 Spontaneous Generation

According to spontaneous generation theory, all living forms were formed by the generation power of the nature. Moreover, many of these living forms are still being formed today under certain favorable conditions, by spontaneous generation, not by means of seeds or parents.

The spontaneous generation theory was adopted and modified by the Stoic philosophers and accepted by the scholars of Rome and Alexandria. It was also adopted by the Christian church in both the East and West and become a dominant school in the Christian world for almost 2.000 years. It was considered almost natural in Europe because of the long tradition of belief. However, strictly religious arguments raised in time since God created all living creatures during the first days of creation.

Other and more rational doubts came from scientists. Ample observations supported the dictum of William Harvey, the discoverer of the mechanical principles governing the blood circulation: "Omne vivum ex ovo" (All living come from the egg). With regard to the spontaneous generation, Jan Baptistat van Helmont quoted if one puts a soiled shirt into the mouth of a jar containing grains of wheat, the ferment released from the soiled shirt, combining with the odor of the grain, transmutes the mixture into mice in about 21 days.[36] His ideas about the spontaneous generation were reflecting the contemporary thinking.

The initiation of critical experiments related to the spontaneous generation theory was carried out by Redi. Redi was interested in the problem of the deterioration of meat. Butchers of his time were covering fresh meat with a cloth or muslin to protect it from flies. He conducted experiments with meats and cloths and control experiments. And the observed the appearance of maggots in the meat. The presence of maggots in the uncovered meats only was connected to the source of maggots, namely flies. Thus it was the flies that caused the appearance of worms in the meat, not the spontaneous generation. Redi was also one of those experimentalists who thought that without experimental demonstration, belief is useless.

A technological breakthrough is happened in 1590 with the invention of optical microscope by Dutch brothers Francis and Zachary Janssen. It has magnification power of one order of magnitude larger than a magnifying lens had a decisive power on the assessment of the validity of spontaneous generation theory. This microscope developed by Antoni van Leeuwenhoek in 1676 had a magnification power of 275, just enough to discover microorganisms. Thus during the 17^{th} century, the spontaneous generation theory was re-examined more critically than in earlier generations.

2.7.3 Pasteur and Darwin

During the 200 years between the classical experiments of Redi and Pastuer, spontaneous generation theory was tested over and over again experimentally and gradually shifted its focus to smaller organisms. Pastuer designed an experimental system based on a glass flask of special design that a cotton plug prevents the entrance of bacteria into the bottle. The flask and the content is boiled for some time for sterilization and observed that no bacteria developed after sterilization. Thus he proved that bacteria are not formed by spontaneous generation.

Although Pasteur's work ended 200 year of controversy, it raised new questions without answers regarding the origin of life. Almost at the same time that Pasteur started his famous experiments regarding the spontaneous generation of bacteria, Darwin's book *On the Origin of Species* was published. Before Darwin, controversy

was on the origin of present day organisms; after Darwin, controversy also involved the origin of life.

Charles Darwin suggested that the original ignition of life may have begun in a pond of ammonia, phosphoric salts, electricity and heat. And the first compounds formed were chemically ready to undergo more complex changes. However, the sterile conditions of the to-day laboratories may affect the origin of life studies since at the present day such matter would be instantly absorbed which would not have been the case before living creatures were formed.

2.8 Primordial Soup Hypothesis

The biochemist Alexandre Ivanovitch Oparin adopted evolution as a central theme and integrated various scientific disciplines, mainly organic chemistry, biochemistry, geochemistry and astrophysics to develop a coherent and partially testable scenario in his first book entitled *Vozniknovenie Zhizny na Zemle* (The Origin of Life on Earth).

Based on available studies of his time, Oparin suggested that the prebiotic earth had a reducing atmosphere. He reasoned that the synthesis of certain organic compounds that are necessary building blocks for the evolution of life is possible only under an atmosphere containing no molecular or atomic oxygen. Organic compounds formed are thus gradually become more and more complex. And these complex molecules aggregated to form coacervates that are held together by hydrophobic forces from a surrounding liquid. Coacervates are capable of absorption and assimilation of other organic molecules from its environment. This can be speculated as mimicking of metabolism and coacervates served as the first chemical entities capable of undergoing evolutionary process, which eventually leads to the emergence of primitive living forms. These hypothetical creatures are named as *eubiont* and would probably be considered as an extreme anaerobic heterotrophic prokaryote.

2.9 Complex Biological Molecules and Protocells

Sidney W. Fox is experimented the primordial soup theory and the abiogenesis between 1964 and 1988. One of the most common sources for condensation reactions in the prebiotic environment is likely to have heat followed by dehydration. In one of the experiments, Fox heated mixture of amino acids with excess aspartic acid and glutamic acid at 150ºC to 180ºC for a few hours. And he observed formation of peptides having cross-linked, thread-like, submicroscopic architectures by dry heating. These peptides are called "proteinoids".

n amino acids(with excess asp and glu) $\rightarrow$ polypeptide(proteinoid) + n H_2O

The most successful attempts to synthesize polynucleic acids under plausible prebiotic conditions were carried out by Ferris and his coworkers. In of these studies, a montmorillonite clay mineral was used as an adsorbent and catalyst. The nucleotide monomers were activated by imidazole.

Polymerization reactions on the surface of iron(III) hydroxide oxide are another successful candidate for the protocell formation. A major problem in the polymerization reactions carried out in the presence of water, such as condensation of polynucleotides, is the destruction of the condensing agents and reactive intermediates by water, thus preventing the production of large polymers. Based on earlier works, Weber used iron(III) hydroxide oxide(Fe(OH)O) in the oxidative polymerization of 2,3-dimercapto-1-propanol. In addition to prebiotic plausibility of the reaction under study, it was noted by Weber that “redox reactions could have provided the energy for the earliest type of polymer synthesis involved in the origin of life.” Weber’s experiment plus theoretical considerations suggest that polysulfides could have had important functions in prebiotic reactions.

2.10 Early Conditions

The earth is about 4.57 billion years old. At the Hadean area (starting from the formation of planets till 3.8 billion years ago from now) its surface is was about 1500K according to the recent models and so surface was molten. In the process

known as “iron catastrophe”, melted iron-group elements (Fe, Ni and Co) passed through the lighter silicate molten rocks down to the core.[37] As the accretion input decreased, surface gradually cooled down and solid rocks started to emerge. A steam atmosphere began to condense and rain down to form primordial oceans. Surface temperatures below 100 ºC could have developed 4.4 billion years ago.[38] There is no geological evidence for prebiotic organic chemical processes prior to 3.8-3.9 billion years old terrestrial sediments.

Seawater composition during Hadean and Archean eras are not exactly known. Bu the most important feature of the early oceans were the oxidation-reduction reactions. In the circulating seawater, soluble Fe^{2+} was extracted from hot igneous rocks to serve as the major reductant of this water. Model calculations suggested that the redox capacity of the prebiotic oceans serve as the major source of reducing power needed for prebiotic synthesis.[28]

Banded iron formations (also known as banded ironstone formations or BIFs) are distinctive units of sedimentary rock that are almost always of Precambrian age. Banded iron formation is an important process in relation with the prebiotic atmosphere. The formation of these bands was a result of the photo-oxidation of soluble Fe^{2+} in the oceans, with the generation of ferric ions and molecular hydrogen.

$$Fe^{2+} + H^{+} + h\upsilon \rightarrow Fe^{3+} + \tfrac{1}{2} H_2$$

The importance of this reaction is that it could have supplied the reduced raw materials such as H_2, CH_4, and HCN to the primitive atmosphere. Banded iron formation also served as a sink for the oxygen produced by the photolysis of water vapor in the atmosphere.

The properties of early atmosphere provide deeper understanding of the origin of life processes, whether life originated near surface environments, in the hydro-thermal vents or somewhere else in space, then being brought to Earth by extraterrestrial bodies such as asteroids or comets.

According to Kasting [39] the early atmosphere was dominated by H_2O, CO_2, CO and N_2. Water was the most abundant volatile, followed by the carbon compounds. Based on the model calculations, Kasting suggests the possibility of a primitive atmosphere containing 10 bars of CO + CO_2, as well as approximately 1 bar of N_2, during the early history of Earth.

2.11 Origins of Homochirality

Why nature specifically selected only L-aminoacids? Is it determined by the laws of nature or by the chemical evolution? This question links the origin of life to the origin of molecular symmetry/asymmetry.

The one possibility is that only an *ex lege* energy difference between two enantiomers should be present to enforce the parity violation resulting in the breaking of the symmetry.[40,41,42] However, the energy difference is in the order of 10^{-10} joule and it complicates the calculations on the actual molecules. So it is generally ignored by chemists and biologists. The other mechanisms proposed for the origin of symmetry are circularly polarized light and magnetochiral anisotropy.[43] On the other hand, the breaking of symmetry can be realized rather simple chemical methods. Kondepudi *et al*. [44] and McBride *et al*. [45] have reported that when crystals are grown under constant stirring same handed crystals can be obtained. In those studies, the formation of first crystals having only one type is a result of mere chance and the created nucleation centers directs the induced selectivity for one type.

It is known that many molecules, including chiral ones, can be formed in cosmic space and can be brought to Earth by meteorites. On Murchison and Murray meteorites, L-enantiomeric excess α-methyl amino acids are found.[46] These amino acids are resistant to racemization and it is possible that chirality has been preserved because of this reason. But of course it is arguable that whether the origin of homochirality on Earth is these chiral exogenous compounds.[47]

2.12 Self-Organization and Replication

Self-organization is a broad term which can have many meanings. One possible definition is that the self organization is a process in which structures form spontaneously from the components of a system. It is possible to find literature examples from different scientific disciplines, including processes occurring in the submicroscopic range.

Self-organization is the dynamic principle behind the emergence of rich world of biological, ecological, societal and cultural structures. As can be seen from the definition, self-organization processes are highly complex. They include formation of patterns, growth, various types of cyclic processes, multi-stability and reproduction. It is proposed that there are two types of self-organization schemes. Conservative self organization based on the structure-conserving self-organization and the dissipative self-organization is dominant in evolving systems. Systems with dissipative self-organization are important for processes which lead to biogenesis. These are open systems, the internal state of which is dominated by a disequilibrium far away from the equilibrium state.

The Belousov-Zhabotinskii reaction, Bénard cells, RNase reconstruction and the tobacco mosaic virus are some examples of chemical and biochemical self-organization processes. Although these examples involve completely different forces and mechanisms, they all lead to the same result: the formation of "structures" via phenomenon of self-organization. The term "structure" depends on the distribution of matter; we speak of structure when the distribution is not uniform, i.e., when it deviates from the most likely distribution.

The replication is one of the most essential ability of evolvable life, tough the question of how replication would have emerged during the origin of life could not be answered yet.[48,49] Experimental contributions are mainly focused on kinetically controlled autocatalysis where a molecule is capable of catalyzing its own formation from a set of precursors. These results have been achieved using both biological molecules such as DNA [50,51], RNA [52] and α-helical peptides [53,54] and non-biological molecules.[55,56,57,58] On the other hand, two or more sets of compounds can induce one another's synthesis in so called cross-catalytic systems.[59,60] These

relatively simple systems are still far from the complexity exhibited by contemporary organisms, which can undergo Darwinian evolution and exhibit a complex internal organization.

2.13 The Miller-Urey Experiment

Stanley L. Miller was a doctoral candidate under supervision of Harold Urey at the University of Chicago in 1953 when he carried out the famous experiment.[61] The experiment become as very well known as the Wöhler's urea synthesis and attracted great attention in public. In the experiment, a reducing primeval Earth atmosphere, suggested by Oparin and Haldane hypothesis, is electrically discharged to see what happens. This experiment can be considered as the first proof that origin of life questions can be tested with scientific methodology.

Miller used a mixture of methane, ammonia, water and hydrogen instead of the mixture of nitrogen, oxygen, carbon dioxide and water suggested by Oparin.[62] The apparatus used is shown in Figure 21. Water vapor formed in the boiling flask is mixed in the gas flask and passed through electrical sparks, condensed and trapped. U-tube prevented the circulation in opposite direction. Reaction carried out a few hours or a full week at 350-370K (near the reaction zone) 870-920K (at the center). The main products obtained in the order of highest yield were formic acid, glycine, lactic acid, α-alanine, β-alanine aspartic acid and α-amino-*n*-butyric acid. And a little amount of glutamic acid.

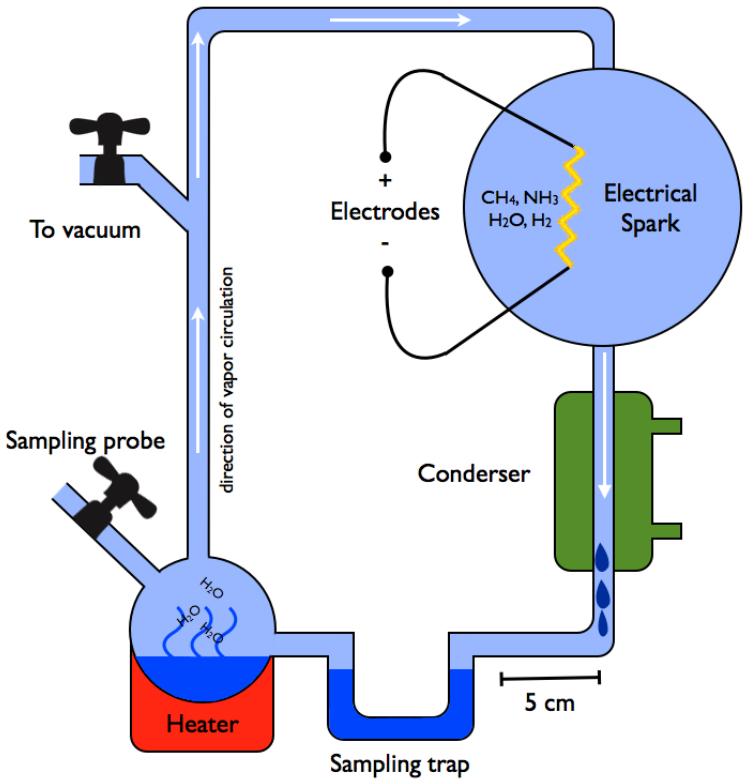

Figure 21. The Apparatus of Miller-Urey experiment.

In the reducing gas mixtures, kinetic studies showed that the concentration of ammonia decreases during the reaction while HCN first increases and then reaches a constant value. Formation of the amino acid steadily increases as the reaction time increases while aldehyde concentration remains constant.

Mechanism of amino acid formation follows the Strecker cyanohydrins synthesis from ammonia, hydrogen cyanide and aldehyde with subsequent hydrolysis.[63] It is also possible that the free radical reactions takes place since the formation of free radicals are likely under electrical discharges.

In a recent publication of Lazcano and Bada,[64] unreported archived samples from the Miller's 1958 experiment containing H_2S are analyzed. In the samples, which were produced via electrical discharge of H_2S, CH_4, NH_3 and CO_2, a total of 23 amino acids, 4 amines, 7 organosulfur compounds are detected. Amino acids were found as racemic mixtures indicating that samples are not contaminated during the

storage. This experiment is the first example of formation of sulfur containing amino acids using electrical discharge in a prebiotic atmosphere.

Abelson and co-workers carried out similar experiments under reducing atmosphere containing CO_2, CO, N_2, NH_3, H_2 and H_2O and detected formation of small amount of amino acids.[65] However with the addition of O_2, amino acid formation is not detected. In literature there can be found many variations of Miller-Urey experiment carried out in liquid and solid phase as well as gas mixtures using various energy sources. However, Miller-Urey experiment form a basis for prebiotic chemistry and biogenesis research and is only have a historic interest for recent works.

2.14 Current Models

2.14.1 The "Prebiotic" RNA World

The term "RNA World" becomes a keyword in origin of life studies and appears in many publications. The RNA World hypothesis was put forward about 20 years ago by W. Gilbert.[66] However, the predominant role of the particular nucleic acid was recognized by F. Crick [67] and L. Orgel.[68] This hypothesis postulates that RNA is the primeval macromolecule from with DNA and other proteins derived. Ribozymes, in vitro evolution of RNA and the self-replicating RNAs have sound literature in both modern biochemistry and molecular biology. However, the connection between prebiotic soup and the RNA is still an imaginary part of the hypothesis.

It is clear that there are examples in which partially random RNA libraries forms the basis of ribozymes. Among the many examples detecting the formation *of de novo* RNA with ligase activity,[69,70,71,72] in these examples RNAs are not produced under plausible prebiotic conditions. Moreover, RNA molecules are not totally random due to experimental considerations.

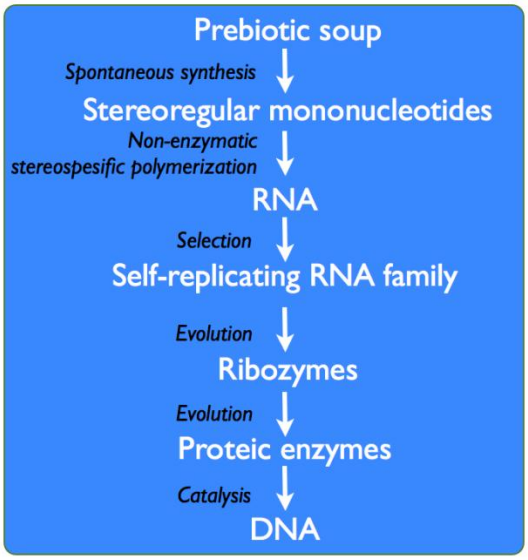

Figure 22. Origin of life in the "prebiotic" RNA world.

Although there are numerous problems related to this hypothesis, the presence of self replicating ribozymes that lead to formation of DNA and proteins and the power of RNA makes it still a good competitive model that can be supported experimentally.

2.14.2 Autocatalysis

The reaction in which the reaction product catalyzes the same reaction (i.e. the production of itself) is called autocatalytic reactions. In the origin-of-life point of view, Stuart Kauffman is first suggested that the life may have been started via autocatalytic reaction networks.[73] In 1990, J. Rebek and his coworkers reported an autocatalytic reaction[74] that involves the coupling of the amino adenosine with the pentafluorophenyl ester. This work demonstrated the very basic bits of natural selection due to creation of competition in a population of molecular entities.

2.14.3 Panspermia and Exogenesis

In 1908, Svante Arrhenius published a new version of Richter's Cosmozoa theory and gave it the name Panspermia which has been coined more than 22 centuries earlier by Anaxagoras. Richter, Kelvin and Helmholtz postponed alternative ideas to abiogenesis prior to Arrhenius. His main innovation was the introduction of theory

concerning the pressure exerted by solar radiation. He suggested that this pressure was the mechanism by which living germs are transported in space.

According to this hypothesis, bacterial cells had been formed in the universe like on planet Earth. Cosmic transport of living entities was assumed to be done by traveling units called bacterial spores. These spores are first transported by upward air currents to heights of 100 km. There, strong electrical discharges would push particles against gravity. Then, travel through interplanetary space was made possible by radiation pressure. When the spores entered another planet's gravitational field, they fall down being attached to interstellar dust that is big enough to resists solar radiation pressure. When the size and the weight of the spores are considered, frictional heat problem becomes negligible. The living spores could then germinate under appropriate conditions.

Exogenesis, which hypothesized the extraterrestrial formation of primitive life, is related to the notion Panspermia, but it is not the same. Studies on exogenesis extrapolate genetic complexity of organisms and results that life began 9.68 billion years ago, earlier than formation of Earth.

Both of these hypotheses actually lack of providing plausible explanation to origin of life but postulates it started in a certain location in space and spread out by impacts.

2.14.4 Extraterrestrial Organic Molecules

The extraterrestrial sources of organic molecules on Earth were first postulated as early as 1908 by Chamberlin [75] and Chamberlin was repeated quite independently by Oró [76] in 1961. It has been established since then a significant portion of organic carbon may have been imported to planet Earth from space, either by impact delivery or by interstellar dust. The list of organic molecules that can be derived from interstellar and cometary sources includes formaldehyde, acetaldehydes, hydrogen cyanide, and cyanamide.[77]

The Murchison meteorite that came down in Australia in 1969 contains additional information on the organic materials including amino acids.[78,79,80,81] It contains a wide variety of organic substances such as amino acids (proteogenic and non-proteogenic) hydroxyl acids, phosphonic acids, hydrocarbons, sulphonic acids etc. Over 15 amino acids have been identified on the meteorite.[82] Murchison meteorite dominantly contains amino acids glycine, alanine and glutamic acid in addition to unusual one like isovaline and α-aminoisobutyric acid.[83]

Compound Class	Concentration, ppm
Amino acids	17-60
Aliphatic hydrocarbons	>35
Aromatic hydrocarbons	3300
Fullerenes	>100
Carboxylic acids	>300
Hydrocarboxylic acids	15
Purines and Pyrimidines	1.3
Basic N-heterocycles	7
Amines	8
Amides (linear)	>70
Amides (cyclic)	>2
Alcohols	11
Aldehydes&Ketones	27
Sulphonic Acids	68
Phosphonic Acids	2

Table 3. Concentrations of organic compounds found in Murchison meteorite.[84]

2.15 Peptide Nanostructures

Well defined nanostructures can be constructed using the bottom-up approach of molecular self-assembly. It is known in literature that a large variety of organic or inorganic materials such as synthetic polymers, carbon, lipids, DNA, viral proteins can adopt nanotubular structures, can form nanotubular architectures. Although biological building blocks like DNA, proteins and viruses are very well studied; their high complexity makes the understanding of chemical and physical properties related with their self assembly difficult. On the other hand chemical, functional and conformational properties of peptides are extensively studied due to their high versatility.

The simplest nanotube forming peptides are dipeptides, namely diphenylalanine. It is reported that upon dilution of the dipeptide solutions from 100mg/mL to a final concentration of ≤ 2.0 mg/mL, multiwalled nanotubes are formed with a diameter of 80-300 nm diameter and length of 1.0μm. Cationic dipeptides like H_2N-Phe-Phe-NH_2 forms nanotubes with diameter of ~100nm at neutral pH and transforms into vesicular structures upon dilution below 8 mg/mL.[85] Size of the peptide nanotubes is highly dependent on the specific interaction between the aminoacids. For instance, diphenylglycine dipeptide forms more rigid nanotubes with a diameter of 10-100 nm under same conditions. Nanostructures and size can be controlled by external factors such as temperature, pH, solvent polarity or surfactants. On the other hand, formation of both tubular and vesicular structures from fundamentally similar peptides is possible (Figure 23). It is consistent with the fact that the formation of these structures are resulting from the folding two dimensional peptide stacks. In that way, mechanism of formation follows the same path as for carbon nanotubes and fulllerenes.

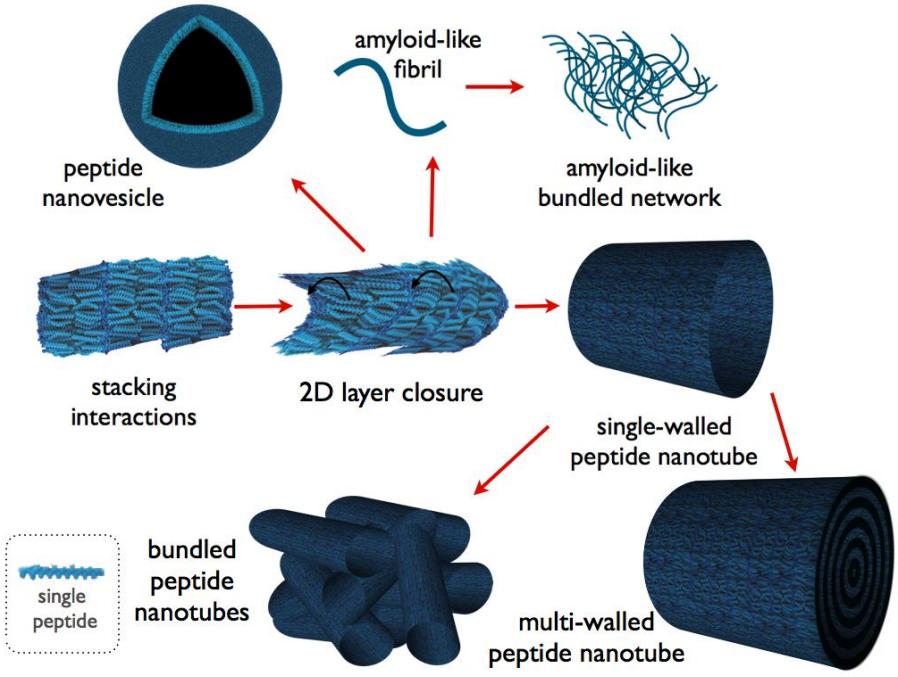

Figure 23. Possible peptide nanostructure formation routes via stacking interactions.

The peptide nanotubes can resist extreme conditions, they are stable in a wide range of pH and temperature [86] (CD spectra does not change up to 90 ºC and tubular structures are stable up to 150 ºC but degradation starts at 200 ºC). Mechanical properties are investigated using atomic force microscopy and resulted in estimated

average point stiffness [87] of 160 N/m and Young's modulus [88] of 27 Gpa. These results show that peptide nanotubes are the stiffest material among the known biological materials.

Amphiphilic peptide chains being 2-3 nm in length can form cationic or anionic open-ended nanotubular structures with a diameter of 30-50 nm in water at 4-5 mM concentration.[89,90,91] The walls are formed by a bilayer of peptides and hydrophobic effects play the key role in stabilization in addition to hydrogen bonding. These nanostructures are relatively more pH sensitive since the charge on the head groups needs to be maintained. It is possible design peptides in such a way that incorporated recognition elements deliver a wide range of substances inside the cell in a site specific manner.

The vesicular nanostructures can be encapsulated by cells through endocytosis. Recent studies have been demonstrated that the spontaneous formation of peptide nanovesicles is not restricted to an appropriate concentration of building blocks but it can be induced by incorporation of conformational rigidity which results in restriction of conformational entropy.[92,93,94,95,96,97] In aqueous media, short and medium-sized peptides can form nanovesicles and almost a decade ago it is demonstrated that dipeptide nanovesicles are stable in acidic and alkaline solutions.[98]

2.16 Solid State Peptide Synthesis

The pioneering method solid state peptide synthesis (SSPS) is developed by R. B. Merrifield [99] in 1963. In Merrifield method, the C-terminal of the amino acid is attached to the resin through formation of a benzyl ester. The *t*-butoxycarbonyl (Boc) group is used to protect α-amino group. Removal of this group is realized by trifluoroacetic acid. By activation of the amino acid with dicyclohexylcarbodiimide (DCC) in DCM, coupling of an amino acid to the resin is completed. Removal of the protecting groups and finally cleavage of the peptide chain from the resin is carried out with hydrofluoric acid.

In contrast to the Merrifield approach which uses acidolysis to achieve higher selectivity in the removal of protecting groups, Fmoc/*t*Bu method utilizes an orthogonal protecting group strategy. N-Fmoc groups are used for the protection of α-amino group taking advantage of its base-lability whereas acid labile protecting groups (such as *t*-butyl groups, chlorotrityl groups etc) used in side-chain protection. Milder acidic conditions are adequate for the removal of protecting groups and cleavage of the peptide chain and it provides an advantage over Merrifield method. In practice, t-butyl groups and trityl-based linkers can be removed by TFA. TFA can be used with standard laboratory glassware and it can be easily removed in *vacuo*.

Growth of a peptide chain on an insoluble solid support provides remarkable advantages over other methods. Namely, removal of the soluble reagents and solvents from the intermediate peptides can be easily done by filtration and washing. Use of excess reagents can force the reactions to completion. Possible physical losses can be minimized since growing peptide chains remain attached to the support during the synthesis.

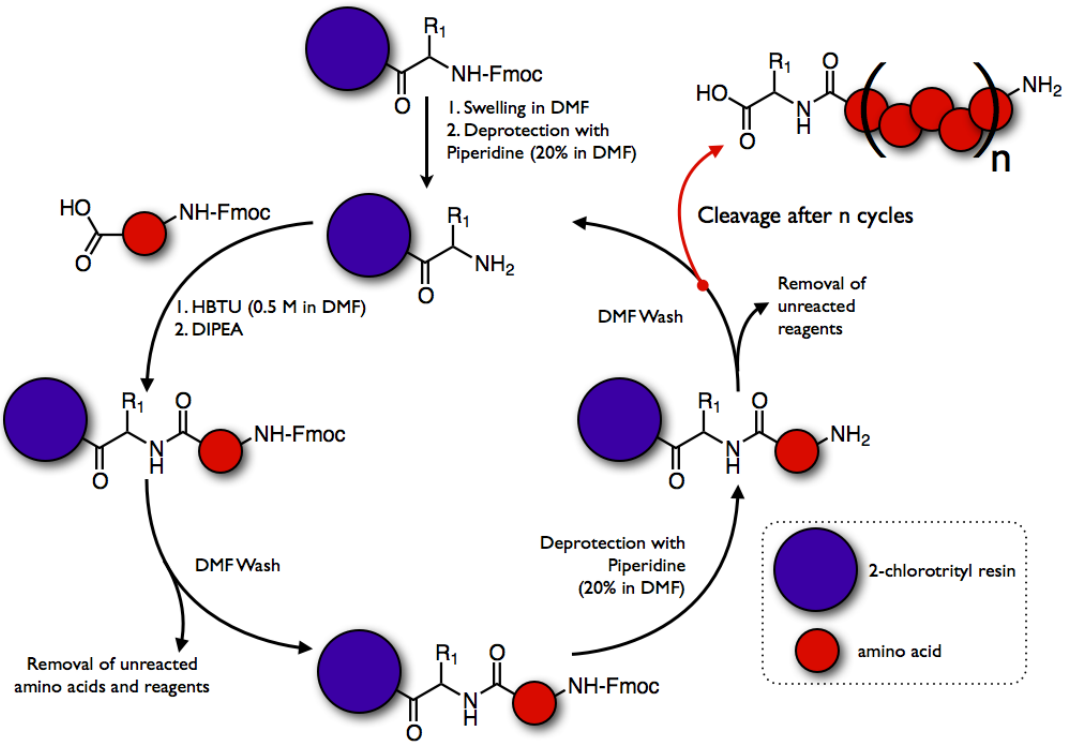

Figure 24. Synthetic cycle for solid state peptide synthesis (Fmoc/*t*Bu approach).

For batchwise synthesis, %1 divinylbenzene cross-linked polystyrene (PS) beads are in common use as base matrix. It is inexpensive and can be easily functionalized with chloromethyl and aminomethyl groups with Friedel-Crafts reaction. Another feature is that it can be swelled very easily in most common solvents used in peptide synthesis, namely DMF, DCM and NMP. Cross-linked PEG based resins are developed recently but it is not widely used.

The synthetic peptide and the solid support are connected to each other via reversible linkage. The α-amino group on the C-terminal is protected during the chain growth and C-terminal of the final product is also determined by the choice of linker. In general, acid labile linkers are used and peptide chain is released with the treatment of TFA. There are also found linkers cleaved by nucleophiles (for C-terminus modification) and light (for one-bead-one-compound libraries) for different applications. Among a wide variety of commercially available resins, four of the most commonly used resins are given in Figure 25. 2-Chlorotrityl resins have been widely used in both solid state peptide and organic chemistry. These resins are very acid labile and can be cleaved even with acetic acid. The bulky triphenylmethyl group, due to its steric hindrance, prevents premature cleavage due to possible cyclization on the linkage. PAM resins are another type of frequently used resins in SSPS. It utilizes Boc approach. PAM resins have higher stability to TFA, but it is harder to cleave final products. On the other hand Wang resins are the most commonly used solid supports for acid substrates. The phenyl ether bond provides high stability over a variety of reaction conditions. Nevertheless, it can be cleaved relatively moderate acid, TFA. The most popular solid support to get amide-functionalized C-terminus is Rink resin. It is designed to yield peptide amide using Fmoc strategy. These resins have one of the highest acid lability; it can be cleaved with 1% TFA. The amine group on the resin is protected with Fmoc group. So pretreatment with piperidine is required to render the free amine.

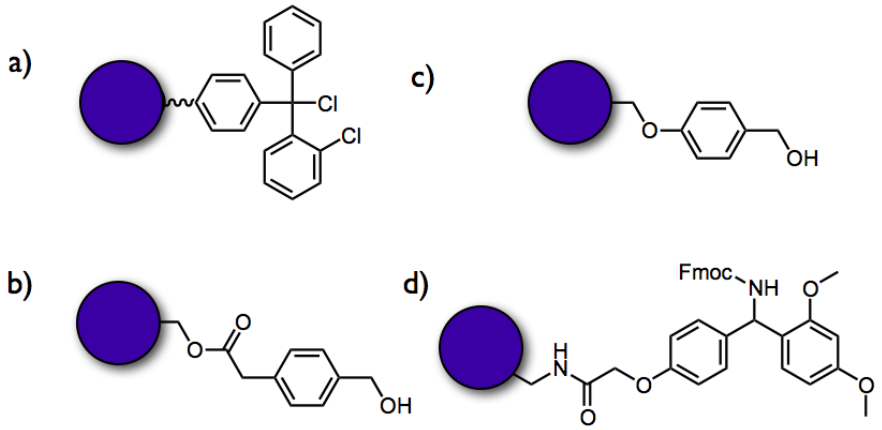

Figure 25. SSPS resins: a) 2-chlorotrityl resin b) PAM resin c) Wang d) Rink amide resin.

This approach does have limitations as any synthetic technique have. There are so many factors that can affect the overall yield and the purity of the final product. Side-products arising from incomplete reactions, side reactions or impure reagents accumulate on the resin in growing chain and will contaminate the desired final product. The analytical methods available for solution phase technique cannot be applicable to SSPS and qualitative color test such as Kaiser Test should be applied to detect the presence of residual amines on the solid support.

2.16.1 Mechanism

In solid state peptide synthesis, N-Fmoc deprotection is usually achieved by treatment with 20-50% v/v piperidine in DMF. The deprotection mechanism is shown in Figure 26. The most important step in the mechanism is the deprotonation of the fluorene ring and the generation of aromatic cyclopentadiene-like intermediate which forms dibenzofulvene by elimination. At the last stage, dibenzofulvene is scavenged by piperidine and forms an adduct that has a high UV absorption which facilitates monitoring the reaction.

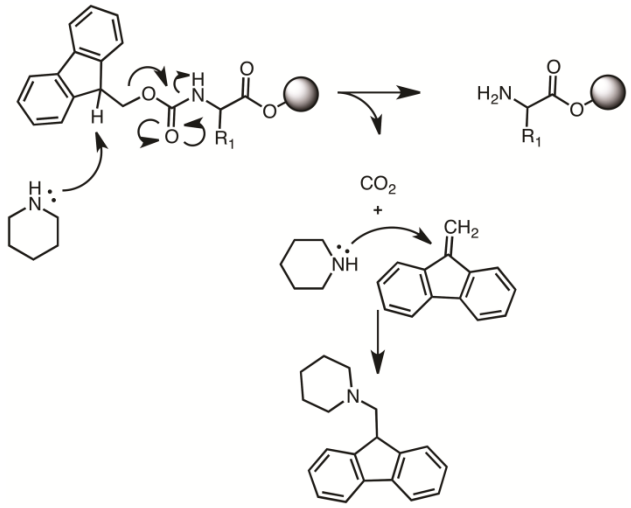

Figure 26. N-Fmoc deprotection mechanism.

This deprotection method is successful in most cases, but incomplete Fmoc deprotection may occur for long peptides even in high concentrations of piperidine. In such cases, deprotection may be extended or a stronger base such as 1,8-diazabicyclo[5.4.0]undec-7-ene (DBU) can be used.

Triazoles are introduced to solve the problem of racemization. In the recent developments carbodiimides are totally omitted. The active esters are introduced as an uronium salt of a non-nucleophilic anion (hexafluorophosphate). HBTU is such compound that is commonly used in peptide synthesis. It does react with only carboxylate anion. Diisopropylethylamine is emerged as a superior base. Once generated, acyloxycarbenium intermediate is formed by the attack of carboxylate to the reagent. The intermediate is either aminolyzed or converted to the benzotriazolyl ester. Peptide bond formation occurs rapidly after tetramethylurea is released.

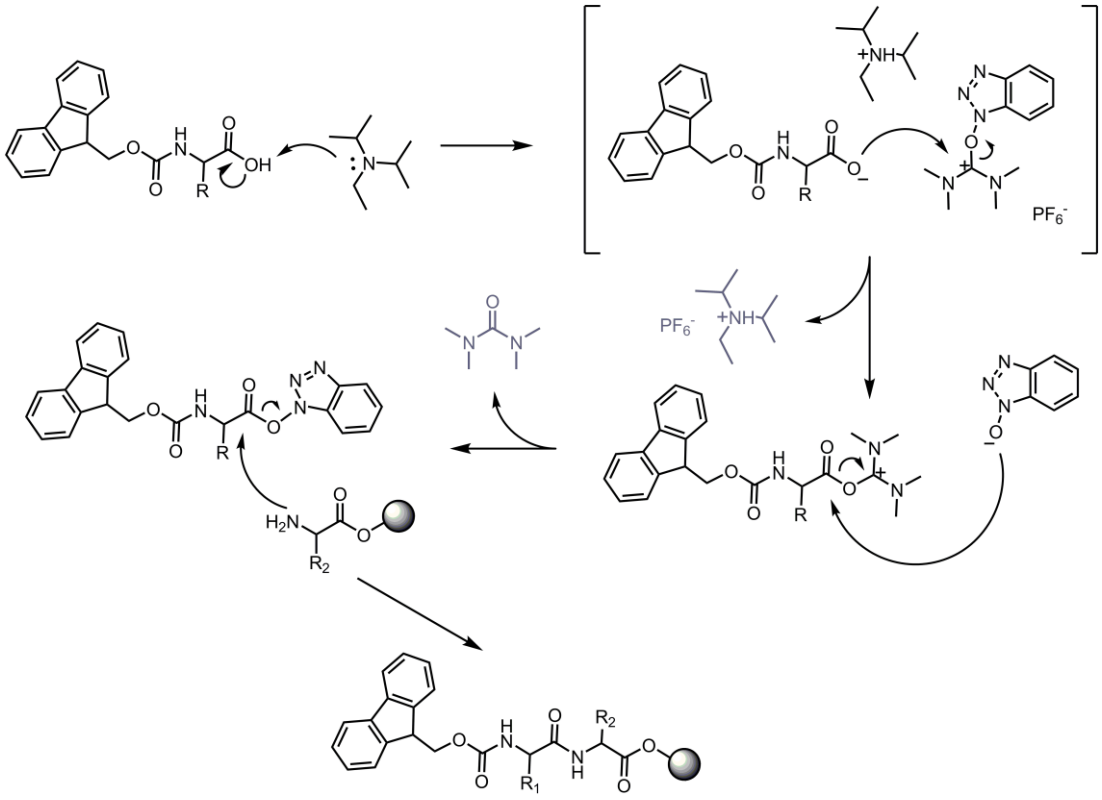

Figure 27. Mechanism of HBTU-DIEA activation of C-terminus.

CHAPTER 3

Designing a Gluthathione Selective Fluorescent Sensor: The Use of Multiple Modulators in Signal Transduction

3.1 Introduction

Chemosensor development has become an attractive field of study,[100] with large number of promising examples with worldwide participation. Nevertheless, the selective signal transduction highly dependent on the chance of "alignment" of the analyte-ligand characteristics and photophysical response of the chromophore. Any claim of design, therefore in many cases seem more like an afterthought or rationalization of the observed signal. Rational design of selectivity on the other hand, would benefit tremendously by the intelligent incorporation of multiple structural and electronic handles on the signal generation process.

Biological thiols such as cysteine [101] (Cys), homocysteine [102] (Hcy) and glutathione[103] (GSH) are known to be important parameters in health and disease states. High cysteine concentration is clearly associated with myocardial and cerebral infarctions, whereas elevated plasma Hcy level is an indicator of arterial and venous thrombosis. GSH on the other hand, is the major endogenous antioxidant with a number of biological roles. Consequently, great deal of recent effort has been placed on developing sensors and probes for each and every one of these three species. The substantial progress made in the field has been reviewed recently by Yoon and co-workers.[104,105] It is an interesting side note that a probe selective for GSH remained elusive until recently.[106,107]

3.2 Design

The design is mainly focused on advancing new strategies and/or tactics in sensing and signaling,[108,109] for that purpose it is found that BODIPY dyes are particularly useful and amenable to modification in accordance with any design requirements. [110] Their impressive spectroscopic properties (quantum yield, extinction coefficient,

tunability) coupled with the ease of modulation of these properties through, among other photophysical processes, photoinduced electron transfer [111] (PeT) and internal charge transfer [112] (ICT) made them a favorite among similar fluorophores. In designing a selective GSH sensor, we also noted that sensing of thiols is mostly based on their strong nucleophilic character even in aqueous solutions.[113] Conjugate addition reactions, altering the spectroscopic properties of the probe is a very common theme encountered in a large number of molecular sensor designs.[114] Our goal was to target GSH specifically, and we thought that could be achieved by incorporating an additional recognition site for the N-terminal ammonium group found in GSH. The structure of our target molecule is shown in Figure 28. We also thought the emission signal of the probe could be further modulated by the protonation state of the azacrown amine moiety which would alter the rate of PeT.

In our design we modified the fluorescent Boradiazaindacene (Bodipy) core with crown ether moiety at *meso* position. Crown moiety carries out the photo-induced electron transfer (PeT) to Bodipy core which quenches the fluorescence. Also it is a well known binding site for the ammonium end of the amino acids. In addition to that we incorporate nitro styryl group on the Bodipy core in order to achieve thiol binding via reaction between nitro and thiol moieties (Figure 28). First of all, our molecule is non-emissive at neutral pH 7.4 because of the PeT from crown ether. When we add thiol bearing compounds at pH 7.4, fluorescence enhancement is low because PeT mechanism is still effective. Weak ammonium binding to the crown causes only very minor enhancement in emission intensity and is not sufficient to effectively block electron transfer by itself at pH 7.4.

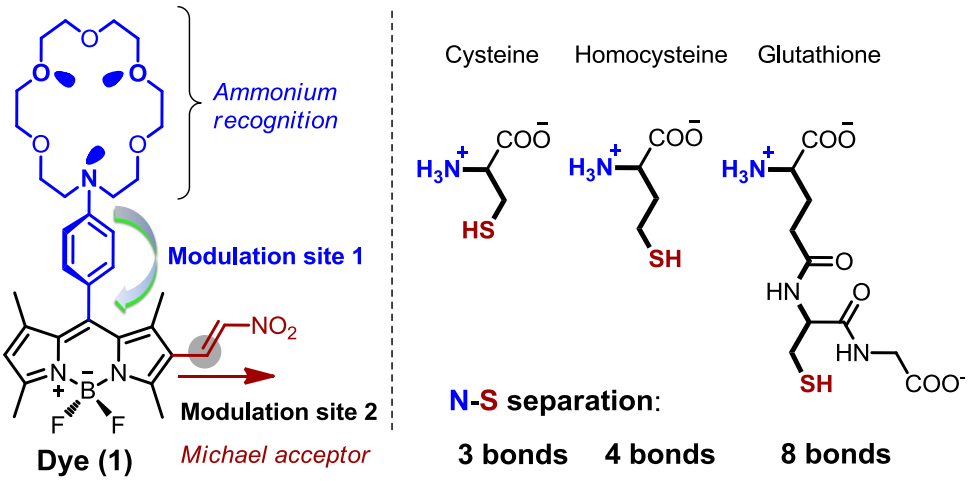

Figure 28. The structure and the signal modulation sites of the target probe.

Major and noticeable emission enhancement can be only seen when we make the pH slightly more acidic (pH 6 - which is the pH value of most of the cancer cells) and then add thiols. At that pH, PeT is blocked mostly due to the protonation of crown moiety. Now we have an emission but emission intensity increases are not identical for Cys, Hcy and GSH because of their molecular structure (Figure 30). GSH has more strong interaction with crown group due to its long structure than others. Ammonium end is more structurally suitable for interaction in the case of GSH. Thus, this coordination has more pronounced effect on PeT blocking at pH 6. Then Hcy has higher intensity and lowest intensity increase was observed with Cys as expected. Furthermore, other amino acids which do not contain thiol groups were tested and no emission enhancement was observed. This is the first study in which two biologically meaningful inputs (acidity and biological thiols) are used and more importantly one of the well known biological thiols are separated from each other in fluorescent sensing of thiols while GSH has the higher emission intensity.

3.3 Results and Discussion

The target molecule was synthesized in a couple of steps starting from corresponding aza-crown-substituted benzaldehyde. Formylation of the 2-position of the Bodipy core, followed by nitromethane condensation, yielded the desired product (see Section 3.4.2). It is very well known fact that electron donating and withdrawing groups on the BODIPY core alter both the ground state and the excited state properties and result in larger changes in dipole moment on excitation. Thus, dye **1**

shows a red-shifted absorbance with maximum at 518 nm and it is essentially nonfluorescent (fl < 0.01). A control reaction with mercaptoethanol causes an enhancement of the emission intensity with a concomitant blue-shift (-20 nm) in the absorption spectrum. Selected photophysical data are presented in Table 4.

Compounds	λ_{abs}[a] **(nm)**	ε_{max} $M^{-1}cm^{-1}$	λ_{ems}[a] **(nm)**	**fwhm** (cm^{-1})	φ_f[b] **(%)**	τ_f[c] **(ns)**
Dye **1**	518	76,000	522	1590	<1	3.0
Dye **1**+GSH (pH 6.0)	505	68,000	522	1523	24	3.9
Dye **1**+GSH (pH 7.4)	505	68,000	522	1505	2	3.9

Table 4. Selected photophysical parameters for the dye 1 and its conjugate adduct. [a] in buffer-acetonitrile (60:40) solutions [b] Quantum yields were determined in reference to Rhodamine 6G (0.95 in ethanol). [c] in MeOH.

Thus, it is obvious that the first criterion for the proposed GSH probe which is reactivity towards thiols and thus transforming the probe so that the typical green emission of an unaltered Bodipy core could be enhanced, was satisfied. This is simply a result of extended conjugation on the BODIPY core. The nitroethenyl substituent is in conjugation with the Bodipy core, and on reaction with a thiol, the nitro group becomes isolated from the Bodipy system, due to the formation of the thioether adduct. ^{1}H NMR data (Figure 29) strongly corroborates with the emission intensity changes, providing clear evidence for the conjugate addition.

It is also evident that, if there is any difference between the biological thiols in terms of the intensity of the emission signal, it should be most likely due to the relative rate of the reactions, perhaps in competition with any side reactions. Thus, unless there are other built-in structural selection criteria, cysteine and homocysteine should react faster than the larger/bulkier nucleophile GSH, and for shorter reaction (incubation) periods, they should generate larger emission responses.

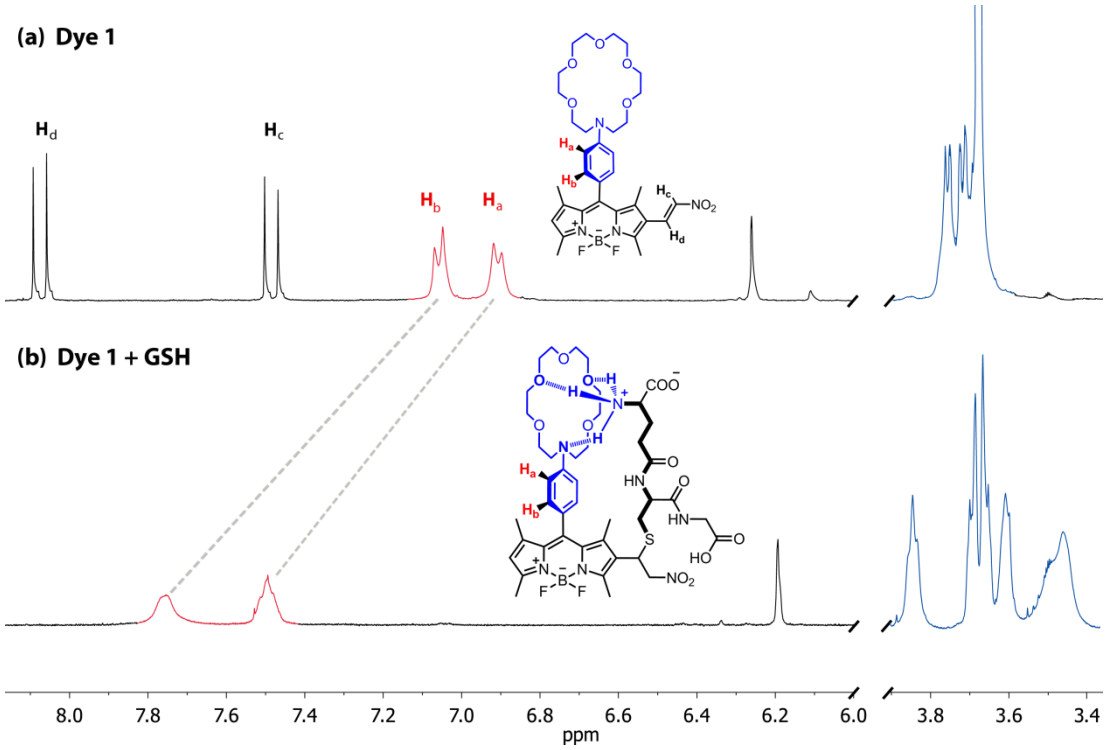

Figure 29. Partial ^{1}H-NMR (in CD_3OD) spectra depicting the changes on GSH conjugate addition to the dye 1: The adduct was isolated by preparative HPLC following a r.t. reaction of the probe and GSH in aqueous acetonitrile. Trans-coupled protons disappear in the product, and the azacrown peaks show a more spread out cluster of peaks, suggesting a non-covalent, non-symmetric interaction.

Next, the response of the probe to three biological thiols in aqueous solutions is tested. We carried out the first set of experiments in pH 7.4 buffered aqueous solutions. When the reactions are complete, we observed a turn on of fluorescence emission (Figure 30, top), together with a blue shift, just as it was in the case of simpler thiol, mercaptoethanol. However, when the reactions were repeated in slightly acidic solutions mimicking the typical pH values for tumor tissue (pH 6.0), in accordance with our design, the results showed a very clear cut preference for GSH for the strongest emission signal (Figure 30, bottom). Two conclusions can be drawn from this result, the steric fit of the protonated ammonium group at the N-terminal is optimal in GSH, and since the other two thiols, Cys and Hcy, are shorter and they cannot provide an ammonium group reaching the N-phenylazacrown receptor as the second recognition site (Figure 28), once the thiol adduct is formed. The second more important result is the PeT modulation: the N-phenylazacrown is a strong PeT donor. Its protonation would stop or slow down PeT leading to strong enhancement of the emission (off-on type). However, our expectation based on the

pK_a data of the aromatic amines, was such that the aromatic amine moiety should not be protonated to a significant extent at even pH 6.0, so no clear enhancement should be seen in the case of Cys or Hcy. In addition, the protonation state would not be in any way linked to thiol reaction. In GSH however, N-terminal ammonium is in the right place for an effective ion-dipole and H-bonding interactions, which would change in the pK_a of the azacrown amine, and thus it will be mostly protonated at pH 6.0. We did not want to leave this issue as simple conjecture, and synthesized two control compounds to check this experimentally (Figure 32):

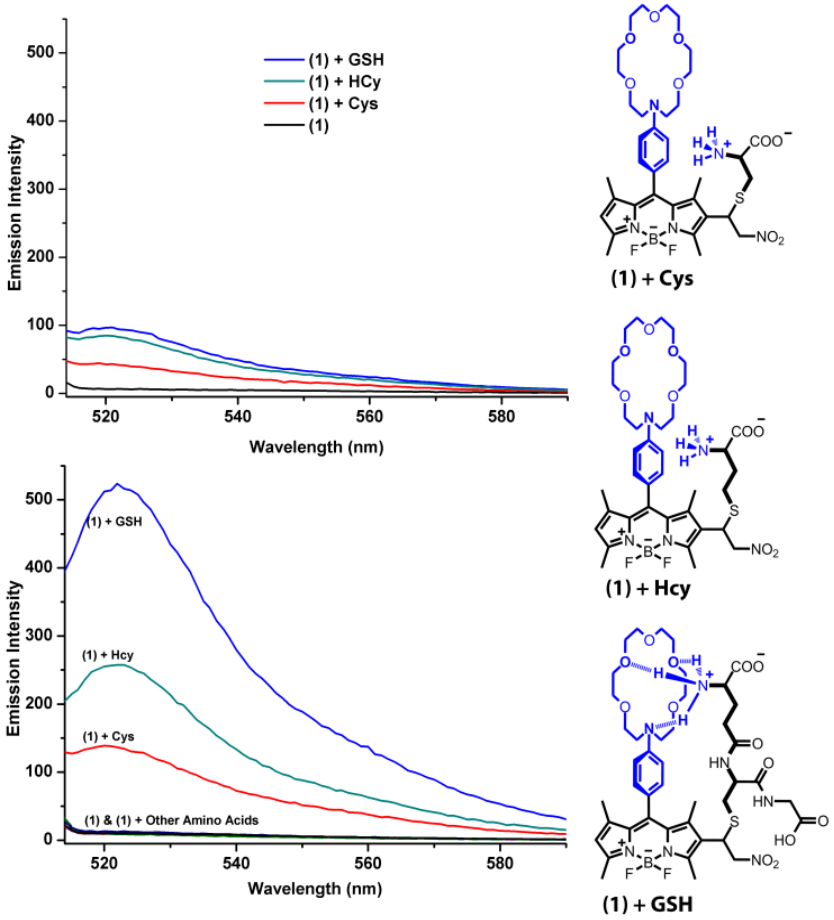

Figure 30. Emission response to biological thiols at two different pH values, 7.4 (top, 60:40, 30 mM MES buffer/acetonitrile) and 6.0 (bottom, 60:40, 30 mM MOPS buffer/acetonitrile). Small change in pH causes more than 5-fold increases in emission intensity for the GSH-1 adduct. For Cys and Hcy, the change is approximately 2.5 fold. The concentrations of the thiols and other amino acids (Gly, His, Ile, Leu, Met, Phe, Pro, Ser, Thr, Tyr, Val) were 1.6 mM and the dye 1 concentration was 8.0 μM. Excitation was at 500 nm, with 5 nm slit-widths.

Dye **2** is a simple phenylazacrown substituted Bodipy and dye **3** has nitroethenyl Michael acceptor and an amine function (Figure 32). These two compounds are to

serve as negative controls of our design. To our delight, control dye **2** showed essentially no response to either moderate change in pH (7.4 to 6.0) or to the thiols (Figure 32, top). Control dye **3** also as expected, did show a small enhancement in emission on reaction with thiols, with small discrimination in terms of signal intensity, but PeT from the dimethylaminophenyl substitituent showed no signs of change within the pH range mentioned, as expected (Figure 32, bottom).

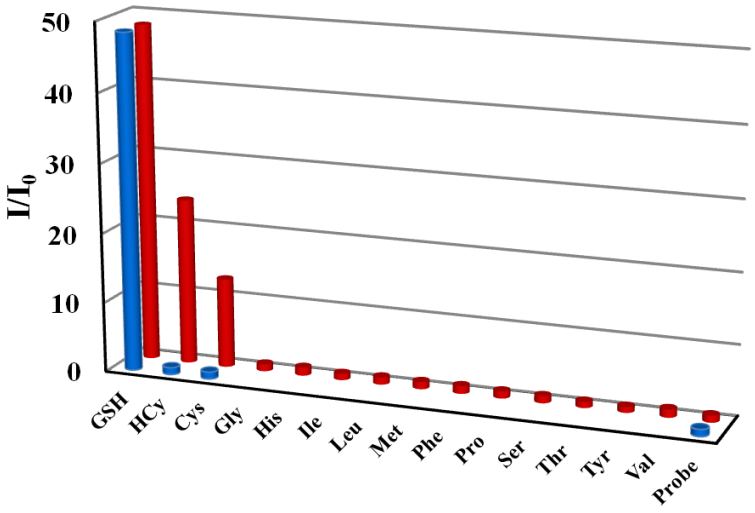

Figure 31. Selective emission response of the dye 1. Blue bars correspond to the emission enhancement ratios (I_o being the emission intensity of the probe) when biological thiols are introduced at their respective intracellular concentrations [11,12,13] in aqueous medium (60:40, pH 6.0 30 mM MOPS buffer/acetonitrile) with 8.0 μM dye 1 concentration. Red bars show the emission enhancement when all analytes are introduced at 1.6 mM, in the same solvent system and probe concentration. Excitation was at 500 nm, emission data at 522 nm (I and I_0) were used in calculations.

The control experiments prove that the designed dye **1**, has a strong steric differentiation between the GSH and the other two biologically relevant thiols, more so at pH 6.0. pH 6.0 versus pH 7.4 responses are important as pH difference in this range is one of the characteristics separating tumors from healthy tissues. GSH is known to be present at highly elevated concentrations in tumor cells compared to healthy tissues.[11]

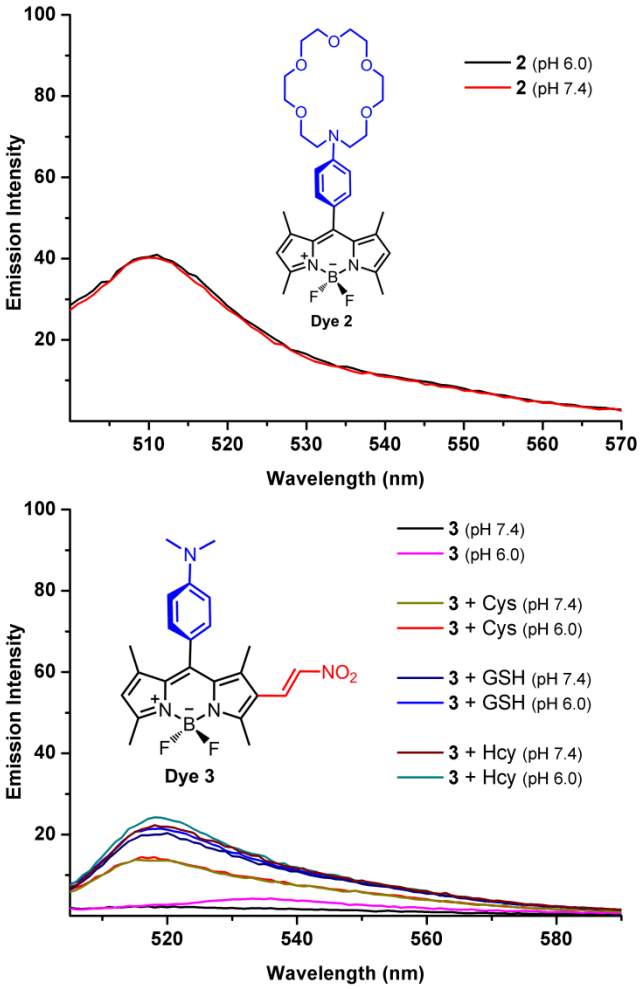

Figure 32. The structures of control Bodipy dyes 2 and 3. Dye 2 has a binding site for ammonium moiety, but no reactive group for thiols. Dye 3 is thiol reactive, but it does not have a site for ammonium. Dye 3 is thiol reactive, but it does not have a site for ammonium recognition. Dye concentrations were 8.0 μM, and the biological thiols were introduced at 1.6 mM. Aqueous buffer solutions were used as solvents, for pH 7.4 (top, 60:40, 30 mM MES buffer/acetonitrile) and for pH 6.0 (bottom, 60:40, 30 mM MOPS buffer/acetonitrile). Excitation was at 500 nm, with 5 nm slit-widths.

While this is already a demonstration of a remarkable multiparameter selectivity for GSH by making use simultaneous modulation of both ICT and PeT processes, we investigated the possibility of kinetic differentiation as well. The thiol reactions may have largely different rates (*vide supra*), and when all three biological thiols were reacted with the dye **1** in aqueous solutions (Supplementary Information), we observed, as expected a slower reaction rate with GSH and much faster in the case of Cys. When applied at equal concentrations, at t=5 min, more than 50% of the emission signal would be due to Cys. At t=100 min, the situation changes and more

than 50 % of the signal is then due to Hcy. On longer incubation times, slower but larger signal generating GSH reactions becomes the predominant factor, reaching more than 50% of the total signal near the completion of conversion. The single reaction based probe, in this way can kinetically differentiate between all three biological thiols.

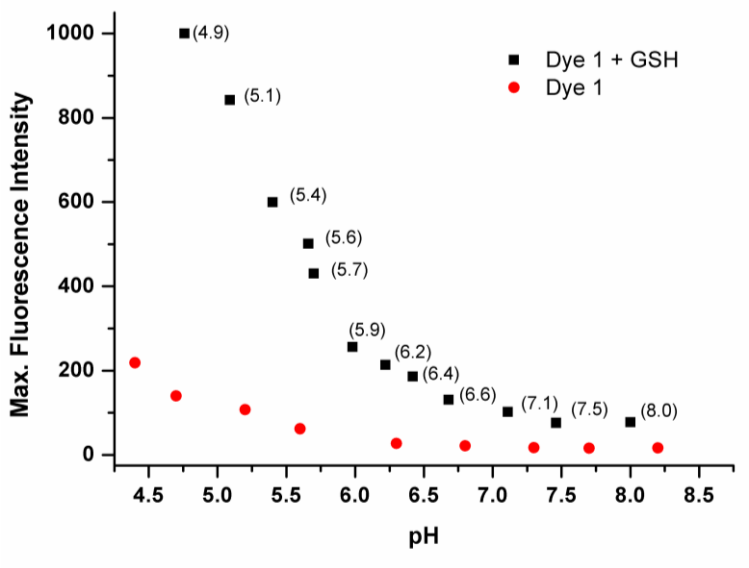

Figure 33. pH titration of GSH adduct in buffered solutions.

Table 4 shows the conjugated probe to undergo an almost 10-fold increase in fluorescence on going from pH 7.4 to pH 6.0. The intracellular pH of tumorous tissue is unknown and not always pH around 6.0. So the risk does exist that the probe reports on pH rather than on GSH, or indicates GSH levels that are much lower than the actual levels because of high pH. In order to test the possible malfunction of our probe, pH titration of both the dye and adduct is performed in the range of pH 8.0 and pH 5.0. Retro-Michael reactions are likely to happen above pH 8.0 and not in the therapeutic range, so excluded from the data. Results clearly shows that the maximum emission intensity of dye 1 stays almost constant with respect to the exponential increase of emission of the adduct. So that it is proved that our probe is reporting only GSH levels independent from pH.

Above all, the most important part of fluorescent probe design is to know well the dye or chromophore chosen and all the active photophysical processes. Meso-aniline-substituted BODIPYs are known to be quenched by an intramolecular charge transfer process in polar solvents.

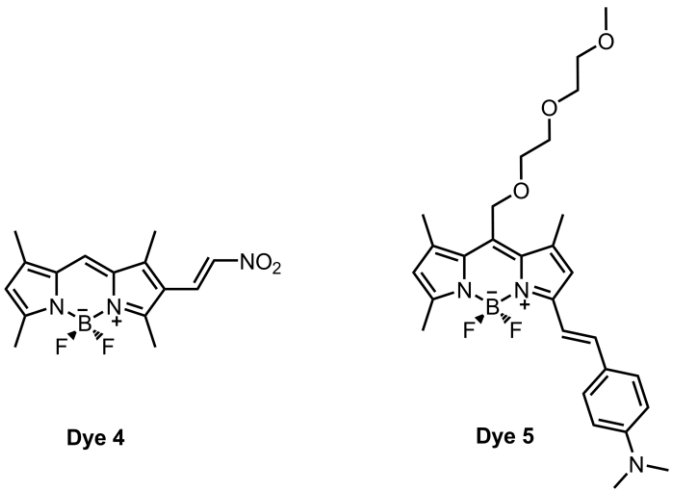

Figure 34. Structures of control molecules Dye 4 and 5.

PeT systems by definition do not show any PeT state-related fluorescence. On the other hand, the conjugation of further pi-electron moieties (like an ethenyl or vinyl bridge) and substituents with lone electron pairs (like a nitro group) to a cyanine chromophore (like BODIPY) is well known to produce bathochromic shifts. A simple test of recording absorption and emission spectra in three organic solvents of different polarity (such as diethyl ether, dichloromethane and acetonitrile) and an analysis of the Stokes shifts would give a very good first hint whether such an extension like in dye 1 is really the cause of an ICT process or whether it is simply a pi-extension. To clarify whether the process is an ICT or a PeT (or PET) process absorption and emission spectrum of additional control molecules (Dye 4 and 5) is recorded.

It is hard to understand the actual mechanism acting on the Dye 1. So as a starting point, dyes of known dominant mechanism are used. It is certainly known that the dominant mechanism in Dye **2** is PeT and Dye **5** is ICT. Comparison of these dyes' photochemical properties with Dye **4** would help to understand the actual mechanism acting on Dye **1**.

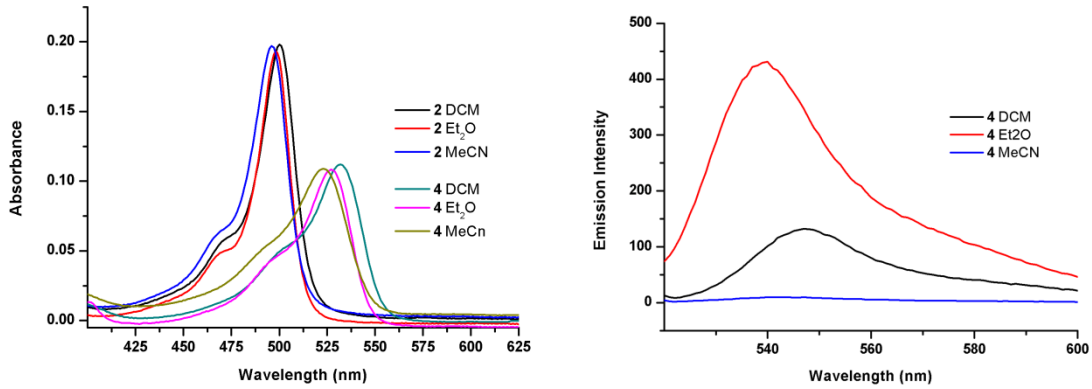

Figure 35. Absorption spectra of Dye 2 and 4 and emission spectra of Dye 4 in DCM, Et_2O and MeCN.

For Dye **5** (Figure 35), approximately 50 nm bathochromic shift is observed as expected due to effective ICT mechanism. In one hand, as the HOMO-LUMO gap in the fluorophore is decreased, number of possible transitions increases. On the other hand, as the solvent molecules having higher polarity or dielectric constant can contribute to the stabilization of the exited state. Because of these reasons increase in the solvent polarity results in decreased fluorescence emission of Dye **5** and become almost non-fluorescent in acetonitrile. Similarly, the emission intensity of Dye **4** decreased as the dielectric constant or solvent polarity is increased. Especially in acetonitrile no emission is observed. And the shift in the absorption spectrum of Dye **4** is almost negligible with respect to the Dye **5**.

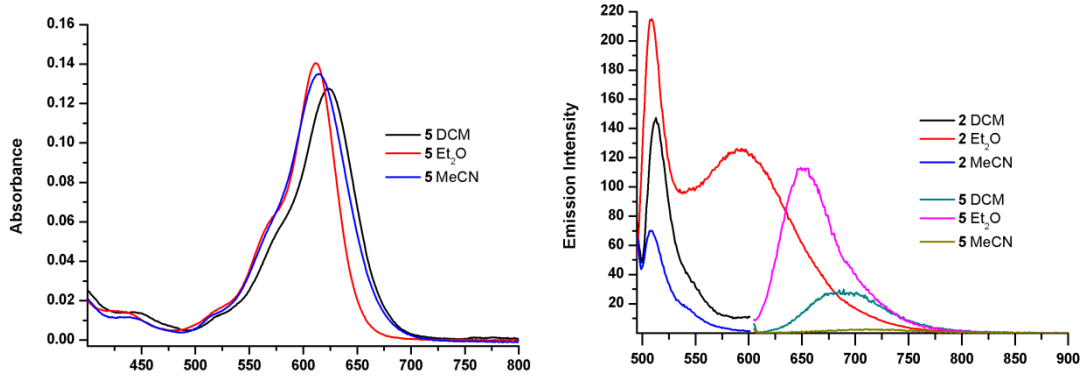

Figure 36. Absorption spectra of Dye 5 and emission spectra of Dye 2 and 5 in Et_2O, DCM and MeCN.

Considering the ICT mechanism, formation of charge separated excited state is important. From these results it can be concluded that nitrosytrene moiety has no

significant contribution to the fluorescence enhancement via ICT process. It only represents a pi-conjugation extension attached to BODIPY core.

The addition of a nucleophile at the indicated position would then only lead to a disruption of the extended pi-conjugation, yet not in the modulation of an ICT process; again, evaluating the Stokes shifts of the reaction product in the same solvents would quickly provide evidence.

Finally, we wanted to demonstrate the feasibility of the designed probe for GSH imaging in intracellular medium using cell cultures. Figure 37 shows time lapse images of dye **1** incubated cells. Within 2 hours, strong green emission of the GSH adduct is clearly visible in the cytosol of the cells. Considering intracellular concentrations of all biological thiols, the green emission is clearly resulting from the reaction with intracellular GSH.

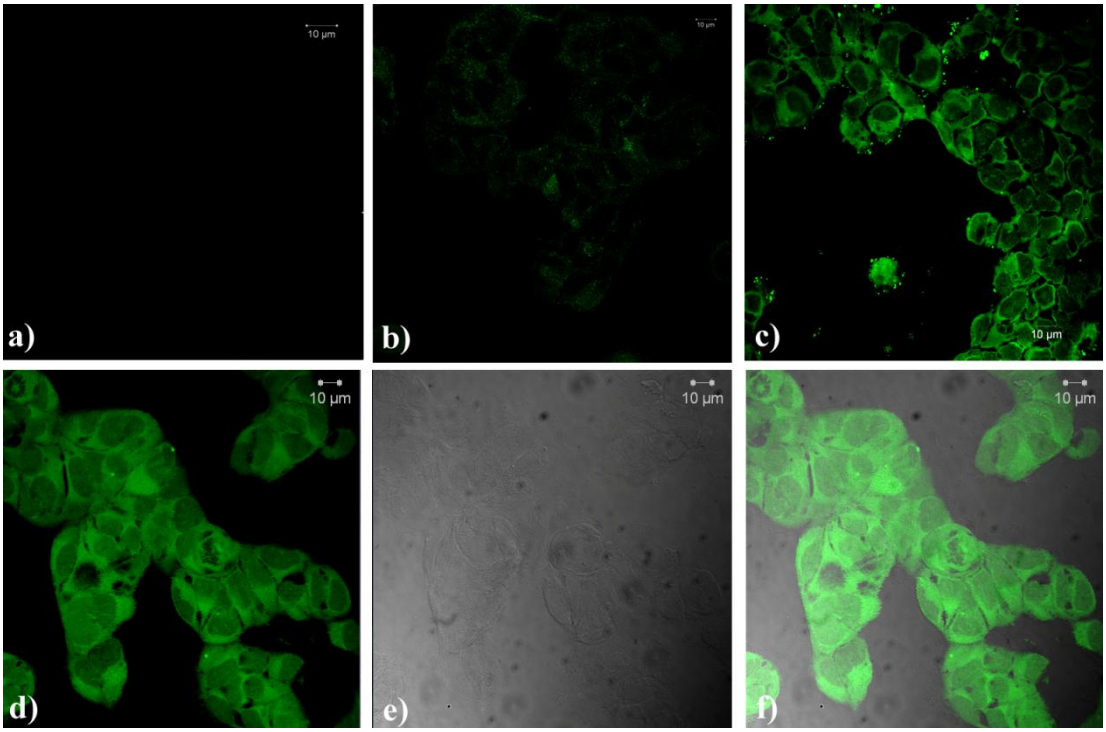

Figure 37. Time lapse (a-c) confocal microscopy pictures of Human breast adenocarcinoma cells (MCF-7) cells incubated with Dye 1 at 0.5 µM (a: 0 min, b: 1 min, c: 120 min). Bottom series of pictures were all acquired following 120 min incubation. d: fluorescence, e: differential interference contrast and f: merged image.

3.4 Experimental Details

3.4.1 General

^{1}H NMR and ^{13}C NMR spectra were recorded on Bruker Spectrospin Avance DPX 400 spectrometer using $CDCl_3$ as the solvent. Chemical shifts values are reported in ppm from tetramethylsilane as internal standard. Spin multiplicities are reported as the following: s (singlet), d (doublet), m (multiplet). HRMS data were acquired on an Agilent Technologies 6530 Accurate-Mass Q-TOF LC/MS. UV-Vis Absorption spectra were taken on a Varian Cary-100 spectrophotometer. Fluorescence measurements were conducted on a Varian Eclipse spectrofluorometer. Flash column chromatography (FCC) was performed by using glass columns with a flash grade silica gel (Merck Silica Gel 60 (40–63 μm)). Reactions were monitored by thin layer chromatography (TLC) using precoated silica gel plates (Merck Silica Gel PF-254), visualized by UV-Vis light and DNP stains as appropriate. All organic extracts were dehydrated over anhydrous Na_2SO_4 and concentrated by using rotary evaporator before being subjected to FCC. N-(4-Formylphenyl)-aza-18-crown-6[1,2] was synthesized following reported literature procedures. All other chemicals and solvents were supplied from commercial sources and used as received.

Kinetic studies of Dye 1 were subjected to exponential fit and the fitted data iterated until it is converged. Entire data set were used for fitting.

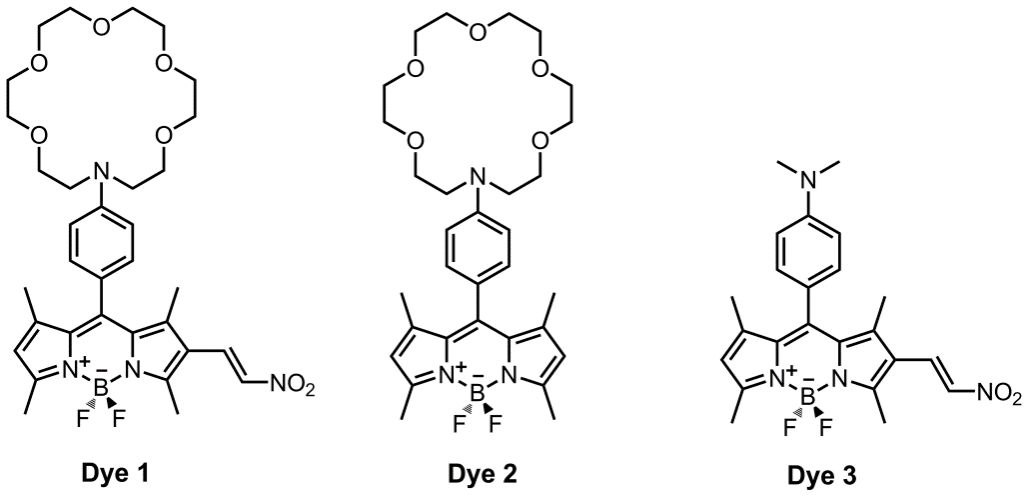

Figure 38. Structures of Dye 1,2 and 3.

3.4.2 Synthesis Scheme of Dye 1:

Following synthetic route was pursued to get the target glutathione (GSH) sensor Dye **1**.

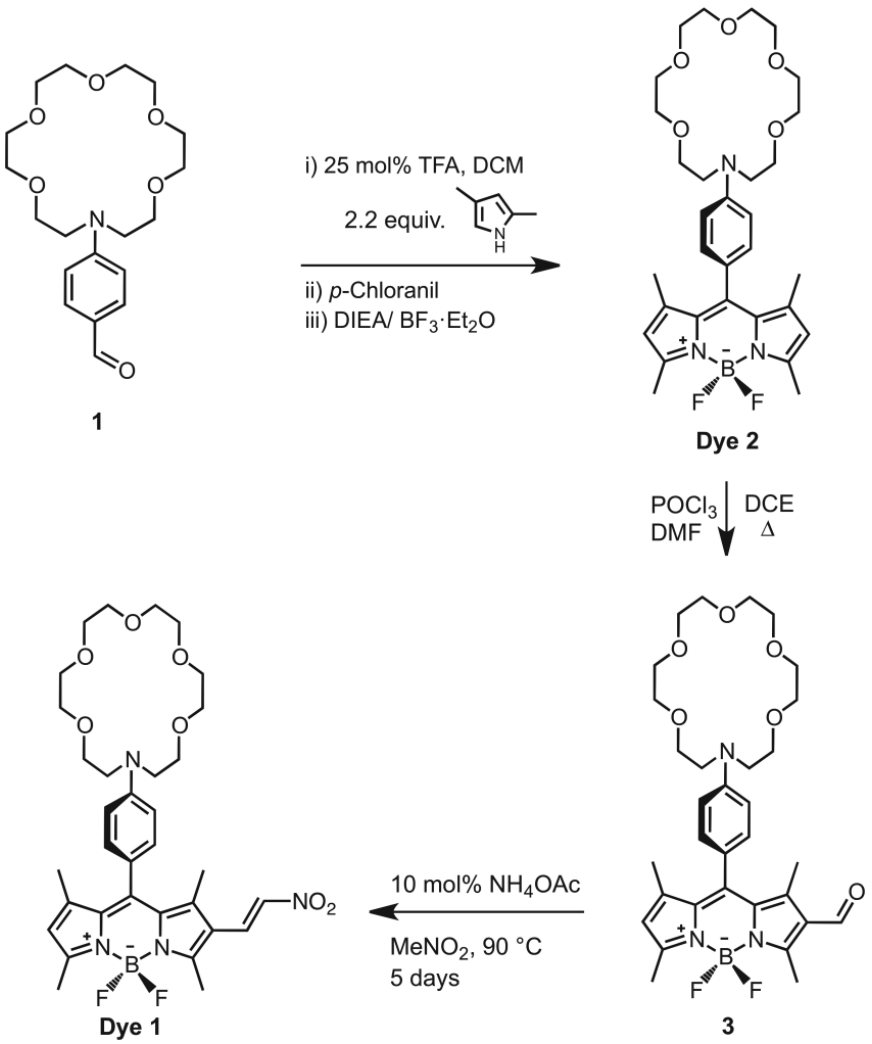

Figure 39. Synthesis scheme of Dye 1.

Synthesis of 4,4-difluoro-8-(*N*-Phenylaza-18-crown-6)-1,3,5,7-tetramethyl-4-bora-3a,4a-diaza-s-indacene (Dye **2**).

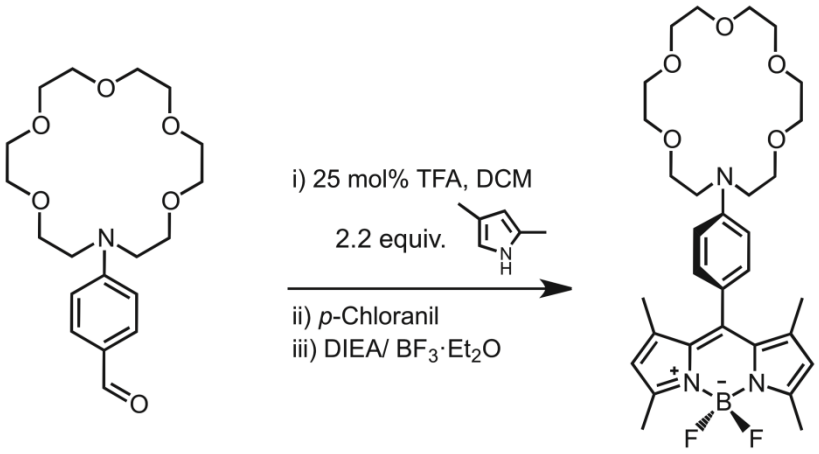

Dye 2

Trifluoroacetic acid (TFA; 57µL, 0.75 mmol) was added dropwise to a vigorously stirring solution of N-(4-Formylphenyl)-aza-18-crown-6[1,2] (1102 mg, 3.0 mmol) and 2,4-dimethylpyrrole (627 mg, 6.6 mmol) in 350 mL Ar-deaerrated dichloromethane (DCM). The resulting red solution was stirred at room temperature in the dark for 1 day. *p*-Chloranil (738 mg, 3.0 mmol) was then added in one portion and reaction was stirred for an additional hour. Diisopropylethyl amine (DIEA) (9.0 mL) was then added dropwise to this mixture over a period of 15 min, and the resulting dark brown solution was allowed to stir for an additional 15 min. BF_3•OEt_2 (9.0 mL) was then added dropwise over a period of 15 min., and the resulting dark red solution was allowed to stir further for 2h at rt. The slurry reaction mixture was washed with water (3 × 300 mL) and dried over anhydrous Na_2SO_4. The solvent was evaporated and the residue was purified by silica gel flash column chromatography (FCC) using $CHCl_3$:MeOH (95:5) as the eluant. Standing on air, compound **2** was solidified as a dark orange solid (790 mg, 45% yield).

^{1}H NMR (400 MHz, CDCl3) δ 7.01 (d, J = 8.4 Hz, 2H), 6.75 (d, J = 8.4 Hz, 2H), 5.96 (s, 2H), 3.81 – 3.51 (m, 24H), 2.54 (s, 6H), 1.49 (s, 6H). ^{13}C NMR (100 MHz, CDCl3) δ 154.6, 148.4, 143.2, 132.2, 128.9, 121.8, 120.8, 111.9, 70.9, 70.8, 70.7, 68.6, 51.3, 43.5, 14.7, 14.5.

MS (TOF-ESI): m/z: Calcd: 585.3191 $[M-H]^+$, Found: 585.3365 $[M-H]^+$, Δ=29.72 ppm.

Synthesis of 4,4-difluoro-8-(*N*-Phenylaza-18-crown-6)-1,3,5,7-tetramethyl-2-formyl-4-bora-3a,4a-diaza-s-indacene (**3**).

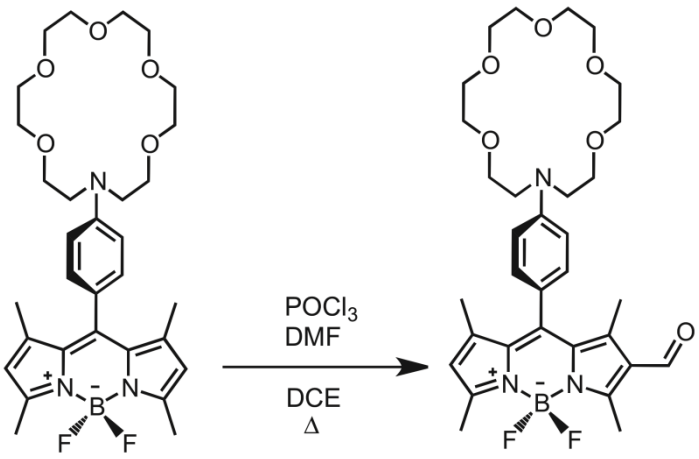

Dye 2 **3**

$POCl_3$ (1 mL) was added dropwise to a vigorously stirring anhydrous DMF (1 mL) which was kept in ice bath under N_2. Resulting pale yellow viscous liquid was allowed to stir at room temperature for additional 30 min. To this, 1,2-dichloroethane (DCE) (50 mL) solution of compound **2** (585 mg, 1.0 mmol) was then slowly introduced and the resultant brown solution was heated at 60 °C for 3 h. (Attention!: 60 °C is critical to get mono-formylated product **3** as the major, side product formation was observed otherwise at higher temperatures.) Reaction was cooled to room temperature, and poured into ice-cold sat'd $NaHCO_3$ solution. This mixture was extracted thrice with DCM (100 mL portions) and dried over anhydrous Na_2SO_4. Solvent was evaporated in vacuo and compound was purified by silica gel FCC using DCM:MeOH (98:2) as the eluent. Product **3** was obtained as dark brown waxy solid with a green luster (521 mg, 85% yield).

^{1}H NMR (400 MHz, $CDCl_3$) δ 9.98 (s, 1H), 6.97 (d, J = 8.8 Hz, 2H), 6.76 (d, J = 8.8 Hz, 2H), 6.11 (s, 1H), 3.71 – 3.63 (m, 24H), 2.78 (s, 3H), 2.56 (s, 3H), 1.75 (s, 3H), 1.53 (s, 3H). ^{13}C NMR (100 MHz, $CDCl_3$) δ 185.9, 160.6, 155.8, 148.9, 147.4, 145.2, 142.8, 134.7, 130.6, 128.8, 126.1, 123.6, 120.6, 112.0, 70.8, 70.7, 70.6, 68.4, 51.2, 25.6, 15.3, 15.0, 12.9, 12.0.

MS (TOF-ESI): m/z: Calcd: 613.3135 $[M-H]^+$, Found: 613.3324 $[M-H]^+$, Δ= 30.81 ppm.

Synthesis of 4,4-difluoro-8-(*N*-Phenylaza-18-crown-6)-1,3,5,7-tetramethyl-2-nitrovinyl-4-bora-3a,4a-diaza-s-indacene (Dye 1).

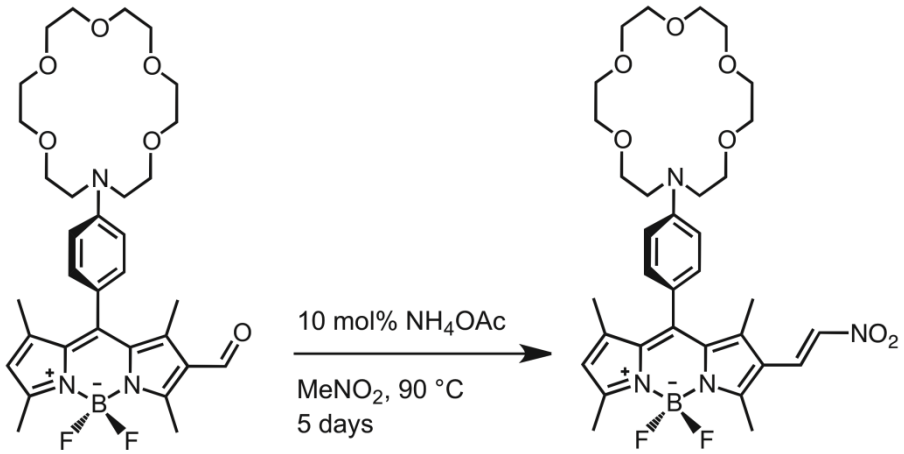

NH_4OAc (3.8 mg, 0.049 mmol) was added to a nitromethane (5 mL) solution of compound **3** (300 mg, 0.49 mmol) and the solution was left to stir at 90 ^oC for 5 days. Product formation was monitored with TLC using DCM:MeOH (99:1) as the eluant. At the end of reaction, nitromethane was removed in vacuo and obtained crude mixture was subjected to silica gel FCC using DCM:MeOH (99:1) as the eluent. Product **1** was obtained as a wine-red waxy solid (288 mg, 89% yield).

^1H NMR (400 MHz, $CDCl_3$) δ 8.07 (d, J = 13.7 Hz, 1H), 7.37 (d, J = 13.7 Hz, 1H), 7.03 (d, J = 8.6 Hz, 2H), 6.81 (d, J = 8.6 Hz, 2H), 6.15 (s, 1H), 3.82 – 3.64 (m, 24H), 2.71 (s, 3H), 2.62 (s, 3H), 1.62 (s, 3H), 1.57 (s, 3H). ^{13}C NMR (100 MHz, $CDCl_3$) δ 213.7, 160.6, 153.8, 148.9, 147.4, 145.3, 144.3, 140.3, 134.3, 131.6, 131.2, 129.0, 123.6, 120.6, 112.0, 70.9, 70.8 , 70.7 , 68.5, 51.2, 15.4, 15.0, 13.8, 13.3, 1.0.

MS (TOF-ESI): m/z: Calcd: 656.3193 $[M-H]^+$, Found: 656.3240 $[M-H]^+$, Δ= 7.16 ppm.

3.4.3 Synthesis of Dye 3

Following synthetic route was pursued to get Dye **3**.

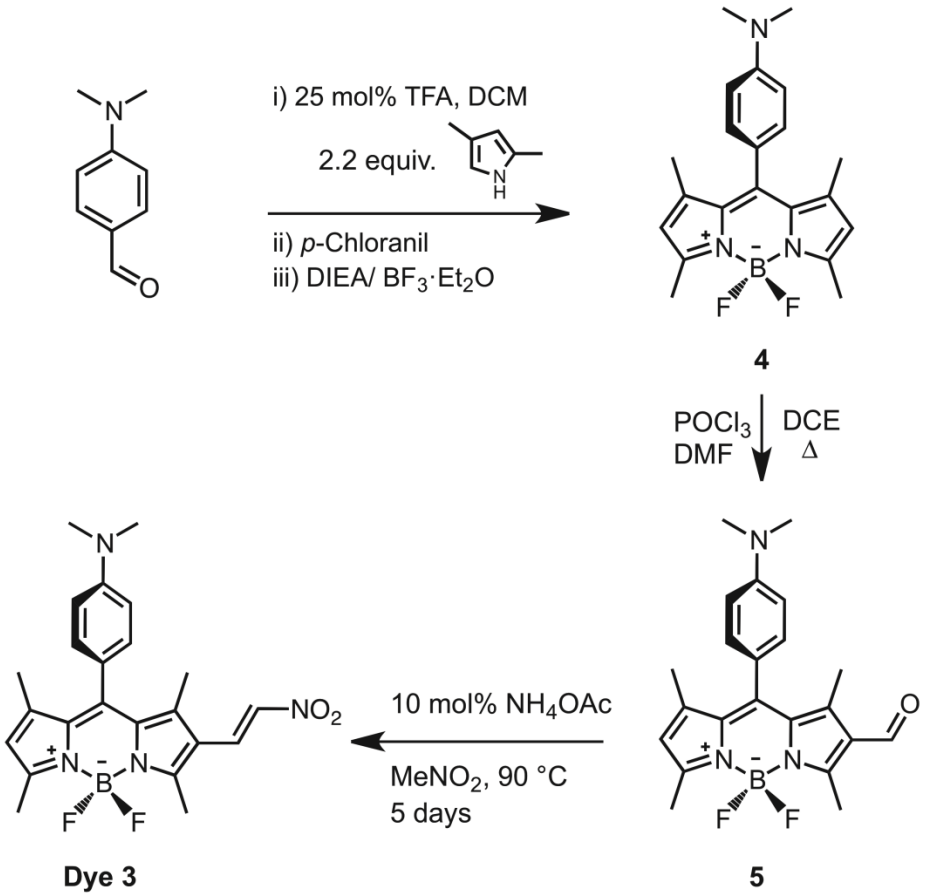

Figure 40. Synthesis scheme of Dye 3.

Synthesis of 4,4-difluoro-8-(*N*,*N*-dimethylamino)-1,3,5,7-tetramethyl-4-bora-3a,4a-diaza-s-indacene (4).

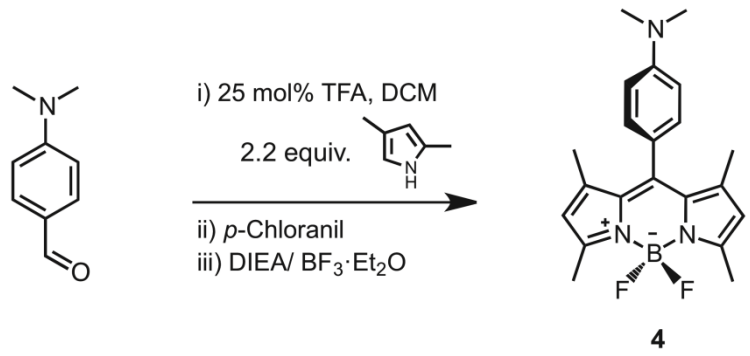

Compound for synthesized according to the literature protocols.[115] Trifluoroacetic acid (TFA; 57µL, 0.75 mmol) was added dropwise to a vigorously stirring solution of N-N-dimethylamino benzaldehyde (447.5 mg, 3.0 mmol) and 2,4-dimethylpyrrole

(627 mg, 6.6 mmol) in 350 mL Ar-degassed dichloromethane (DCM). The resulting red solution was stirred at room temperature in the dark for 1 day. *p*-Chloranil (738 mg, 3.0 mmol) was then added in one portion and reaction was stirred for an additional hour. Diisopropylethyl amine (DIEA) (9.0 mL) was then added dropwise to this mixture over a period of 15 min, and the resulting dark brown solution was allowed to stir for an additional 15 min. BF_3•OEt_2 (9.0 mL) was then added dropwise over a period of 15 min., and the resulting dark red solution was allowed to stir further for 2h at rt. The slurry reaction mixture was washed with water (3 × 300 mL) and dried over anhydrous Na_2SO_4. The solvent was evaporated and the residue was purified by silica gel flash column chromatography (FCC) using $CHCl_3$:MeOH (95:5) as the eluant. Standing on air, compound **4** was solidified as a dark orange solid (716 mg, 65% yield).

MS (TOF-ESI): m/z: Calcd: 368.2079 $[M-H]^+$, Found: 368.2022 $[M-H]^+$, Δ=15.48 ppm.

Synthesis of 4,4-difluoro-8-(*N,N*-dimethylamino)-1,3,5,7-tetramethyl-2-formyl-4-bora-3a,4a-diaza-s-indacene (5).

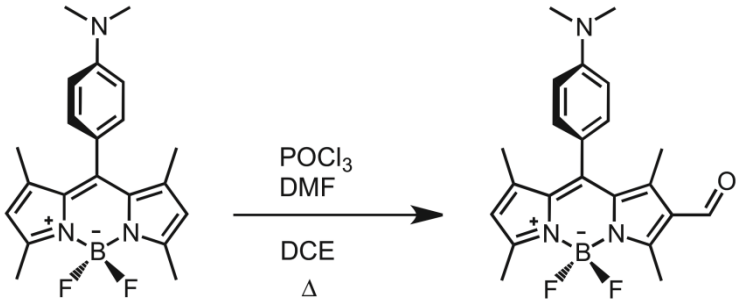

4 **5**

$POCl_3$ (1 mL) was added dropwise to a vigorously stirring anhydrous DMF (1 mL) which was kept in ice bath under N_2. Resulting pale yellow viscous liquid was allowed to stir at room temperature for additional 30 min. To this, 1,2-dichloroethane (DCE) (50 mL) solution of compound **4** (367 mg, 1.0 mmol) was then slowly introduced and the resultant brown solution was heated at 60 °C for 3 h. (Attention!: 60 °C is critical to get mono-formylated product **5** as the major, side product formation was observed otherwise at higher temperatures.) Reaction was cooled to room temperature, and poured into ice-cold sat'd $NaHCO_3$ solution. This mixture was extracted thrice with DCM (100 mL portions) and dried over anhydrous Na_2SO_4.

Solvent was evaporated in vacuo and compound was purified by silica gel FCC using DCM:MeOH (98:2) as the eluent. Product **5** was obtained as dark brown waxy solid with a green luster (335 mg, 85% yield).

^{1}H NMR (400 MHz, $CDCl_3$) δ 10.04 (s, 1H), 7.07 (d, J = 8.7 Hz, 2H), 6.82 (d, J = 8.7 Hz, 2H), 6.15 (s, 1H), 3.06 (s, 6H), 2.84 (s, 3H), 2.62 (s, 3H), 1.79 (s, 3H), 1.56 (s, 3H). ^{13}C NMR (100 MHz, $CDCl_3$) δ 185.9, 160.6, 156.01, 150.9, 147.3, 145.2, 128.6, 123.5, 112.4, 77.3, 77.0, 76.6, 40.2, 15.2, 15.0, 12.9, 11.9.

MS (TOF-ESI): m/z: Calcd: 394.1980[M-H]+, Found: 394.1917 [M-H]+ , Δ= 15.98 ppm.

Synthesis of 4,4-difluoro-8-(*N*,*N*-dimethylamino)-1,3,5,7-tetramethyl-2-nitrovinyl-4-bora-3a,4a-diaza-s-indacene (Dye 3).

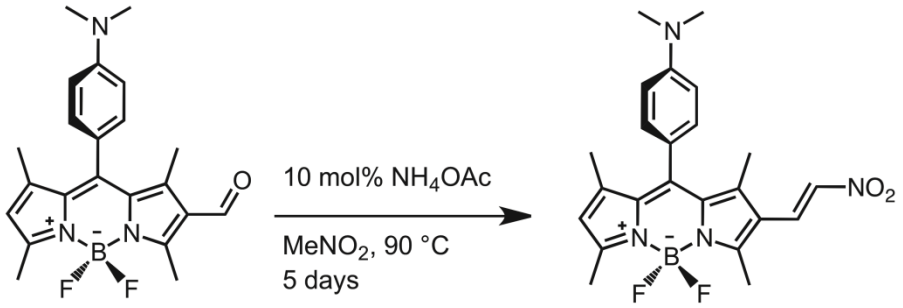

5 **Dye 3**

NH_4OAc (3.8 mg, 0.049 mmol) was added to a nitromethane (5 mL) solution of compound **5** (193 mg, 0.49 mmol) and the solution was left to stir at 90 ^{o}C for 5 days. Product formation was monitored with TLC using DCM:MeOH (99:1) as the eluant. At the end of reaction, nitromethane was removed in vacuo and obtained crude mixture was subjected to silica gel FCC using DCM:MeOH (99:1) as the eluent. Product **Dye 3** was obtained as a wine-red solid (194 mg, 90% yield).

^{1}H NMR (400 MHz, $CDCl_3$) δ 8.07 (d, J = 13.7 Hz, 1H), 7.37 (d, J = 13.7 Hz, 1H), 7.11 – 7.01 (m, 2H), 6.82 (d, J = 8.8 Hz, 2H), 6.16 (s, 1H), 3.07 (s, 6H), 2.72 (s, 3H), 2.62 (s, 3H), 1.61 (s, 3H), 1.57 (s, 3H). ^{13}C NMR (100 MHz, $CDCl_3$) δ 160.6, 153.6, 151.0, 147.4, 144.3, 140.3, 134.2, 131.1, 128.7, 123.6, 120.9, 112.3, 77.3, 77.0, 76.7, 40.2, 15.2, 15.0, 13.7, 13.2.

MS (TOF-ESI): m/z: Calcd: 437.2039 [M-H]+, Found: 437.1973 [M-H]+, Δ= 15.09 ppm.

3.4.4 Absorbance and Fluorescence Spectra

Uv-Vis & Fluorescence Experiments

Analytical and preparative HPLC separations of Dye 1 + GSH adduct were performed on Agilent Technologies HPLC-1200 Series with multi-wavelength detector (MWD) and Agilent Technologies Preparative HPLC-1200 Series with diode array detector (DAD). In the case of analytical separation Agilent Technologies Zorbax Eclipse XDB-C18 analytical 4.6 x 150 mm 5- micron column was employed and for preparative separation Agilent Technologies PrepHT XDB-C18 preparative Cartridge 21.2 x 150 mm 5 micron column was used. For analytical resolution, adduct was dissolved in distilled water (0.1% TFA), filtered and injected to the column. The flow rate was 1 mL/min and UV detection wavelengths were 250, 370 and 520 nm. This separation was performed on a 4.6 x 150 mm column. Only one injection was done (10µL). In the case of preparative resolution of adduct, again it was dissolved in distilled water (0.1% TFA), filtered and injected to the column. The flow rate was adjusted as 20 mL/min and UV detection wavelength was 505 nm. This separation was performed on a 21.2 x 150 mm column. In preparative separation 5 injections were done (5 mg/injections, 2000µL/injections), in order to get reasonable amount of the pure adduct.

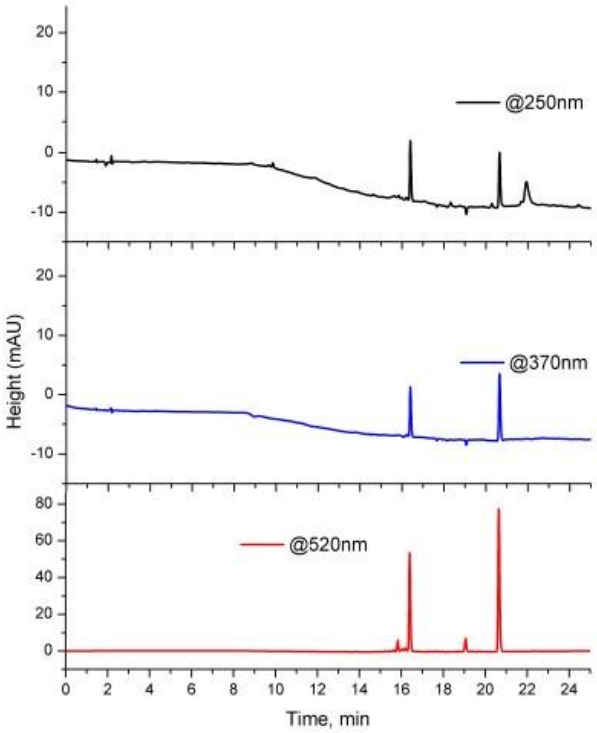

Figure 41. HPLC spectrum of dye 1.

All Uv-Vis absorption and fluorescence spectra were recorded upon addition of 200 equivalents (1.6 mM) of analytes on to 8 μM of probes, dye **1**, **2**, and **3**. Each mixture (probes + analytes) was kept for 15 hours prior to spectrophotometric measurements. All data were collected in aqueous solutions (buffer-acetonitrile, 60:40). To adjust the pH to 7.4 and 6.0, 30 mM of MES and MOPS buffers were prepared, respectively.

3.4.5 Absorbance and Fluorescence Spectra

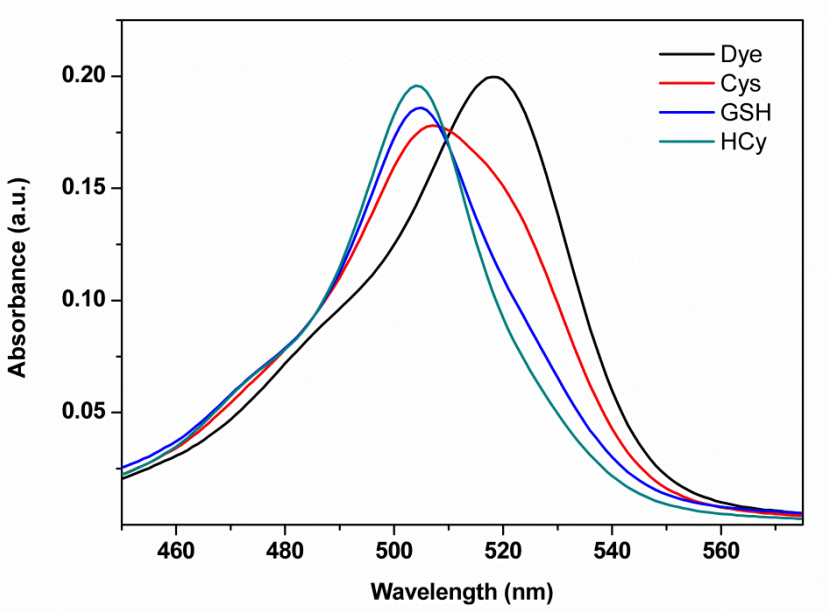

Figure 42. Absorbance spectra of Dye 1 (8.0×10^{-6} M) and Dye 1 + Thiols (200 equivalents) at pH 7.4 in 60% MOPS Buffer (30 mM) / 40% MeCN.

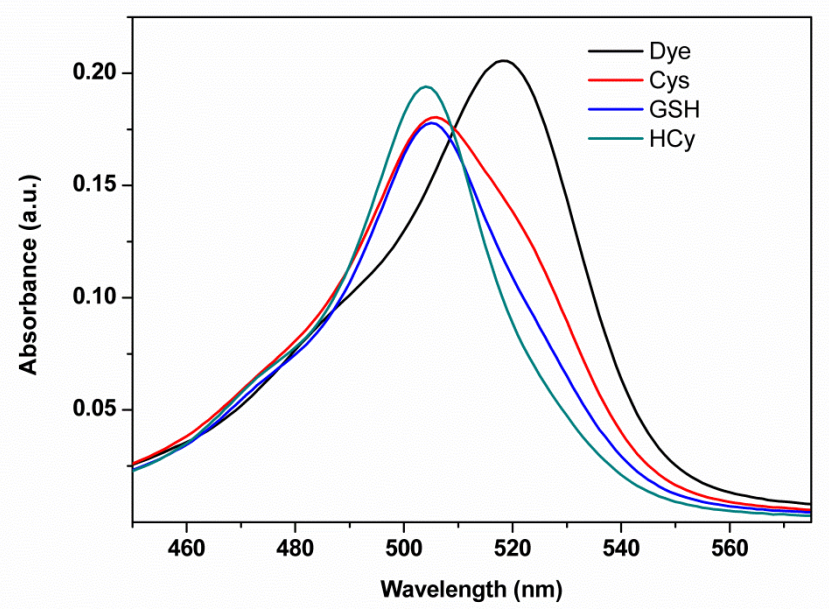

Figure 43. Absorbance spectra of Dye 1 (8.0×10^{-6} M) and Dye 1 + Thiols (200 equivalents) at pH 6.0 in 60% MES Buffer (30 mM) / 40% MeCN.

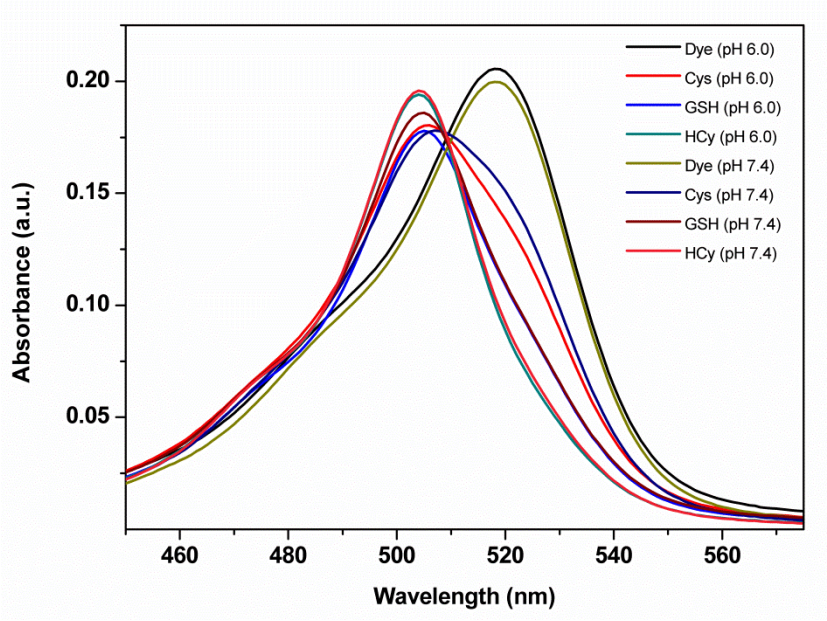

Figure 44. Absorbance spectra of Dye 1 (8.0×10^{-6} M) and BODIPY 1 + Thiols (200 equivalents) at pH 6.0 in 60% MES Buffer (30 mM) / 40% MeCN and at pH 7.4 in 60% MOPS Buffer (30 mM) / 40% MeCN.

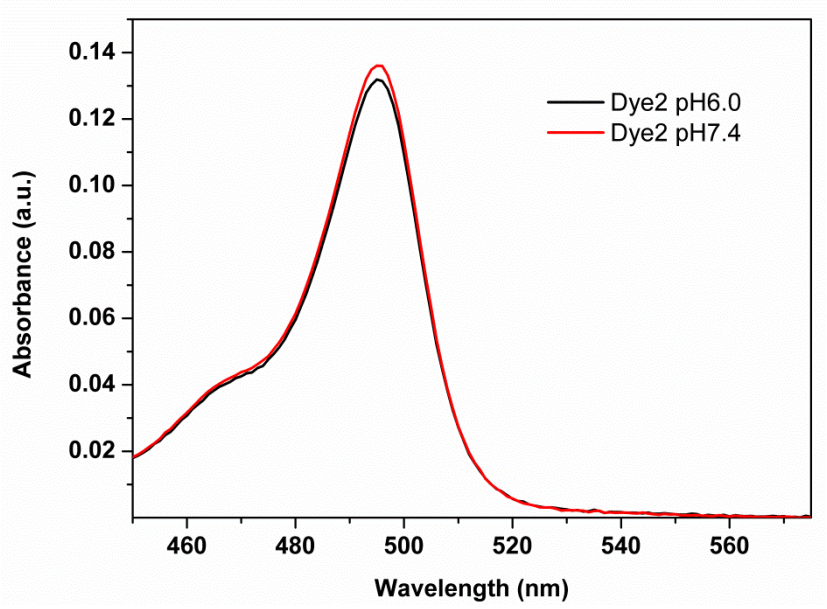

Figure 45. Absorbance spectra of Dye 2 (8.0×10^{-6} M) at pH 6.0 in 60% MES Buffer (30 mM) / 40% MeCN and at pH 7.4 in 60% MOPS Buffer (30 mM) / 40% MeCN.

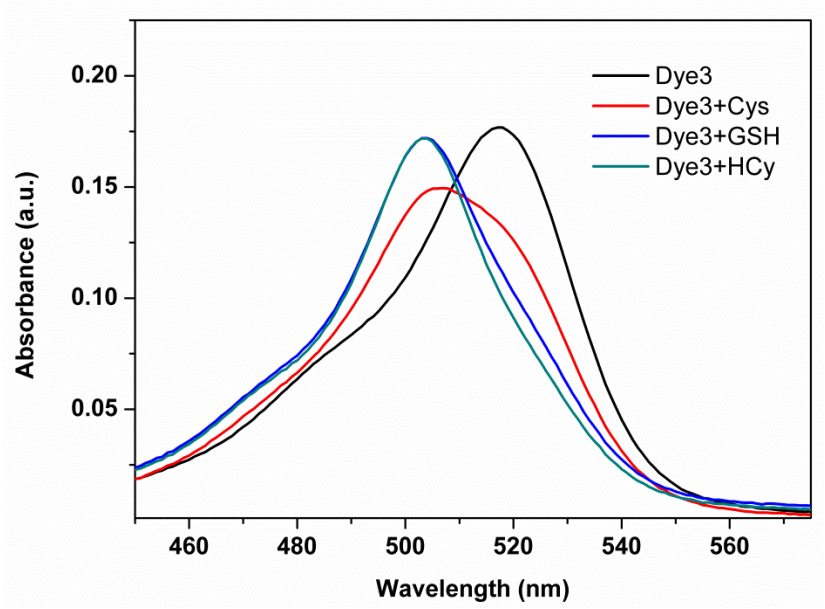

Figure 46. Absorbance spectra of Dye 3(8.0×10^{-6} M) and BODIPY 3 + Thiols (200 equivalents) at pH 7.4 in 60% MOPS Buffer (30 mM) / 40% MeCN.

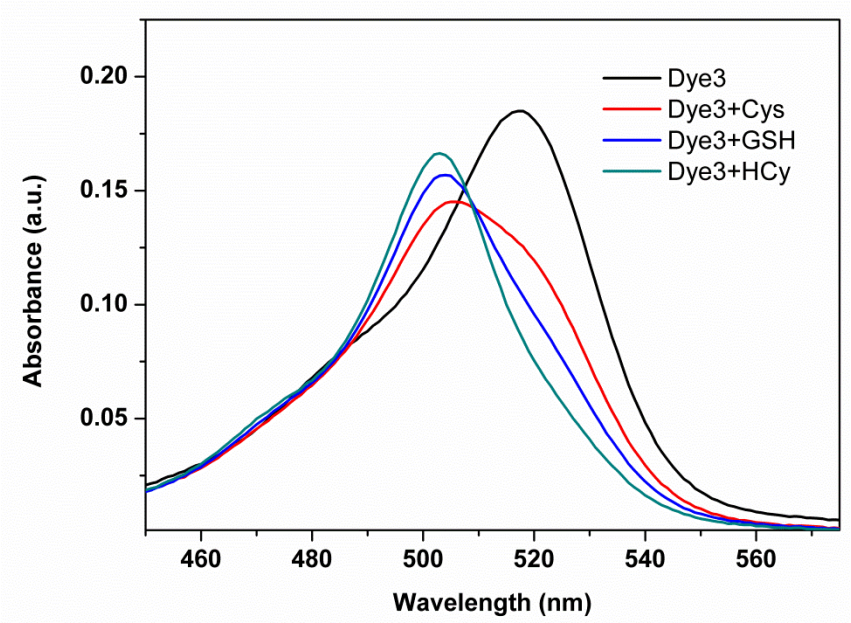

Figure 47. Absorbance spectra of Dye 3 (8.0×10^{-6} M) and BODIPY 3 + Thiols (200 equivalents) at pH 6.0 in 60% MES Buffer (30 mM) / 40% MeCN

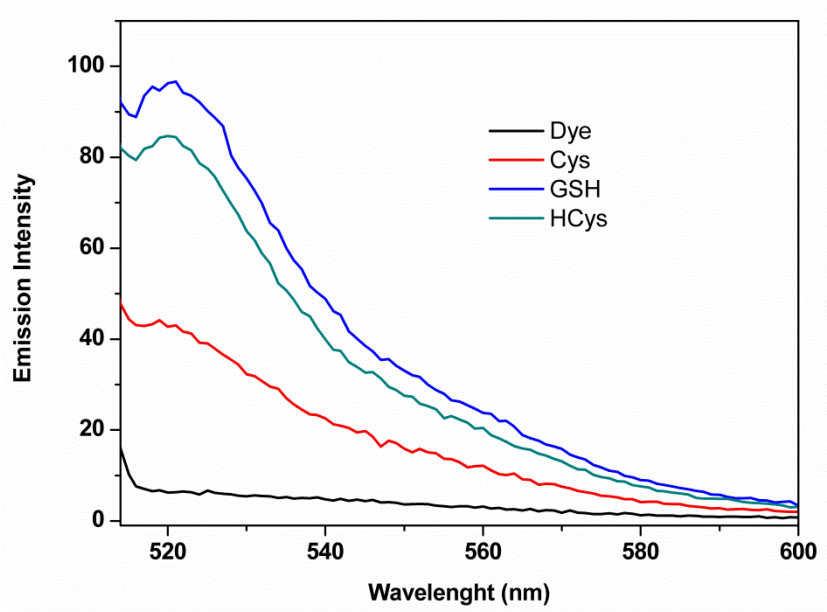

Figure 48. Emission spectra of Dye 1 (8.0×10^{-6} M) and Dye 1 + Thiols (200 equivalents) at pH 7.4 in 60% MOPS Buffer (30 mM) / 40% MeCN (exct @ 510 nm)

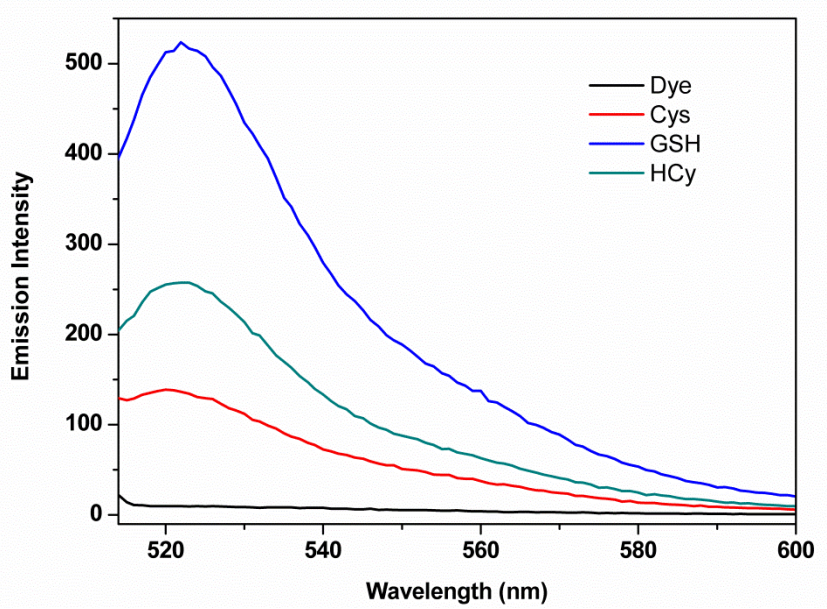

Figure 49. Emission spectra of Dye (8.0×10^{-6} M) and BODIPY 1 + Thiols (200 equivalents) at pH 6.0 in 60% MES Buffer (30 mM) / 40% MeCN (exct @ 510 nm)

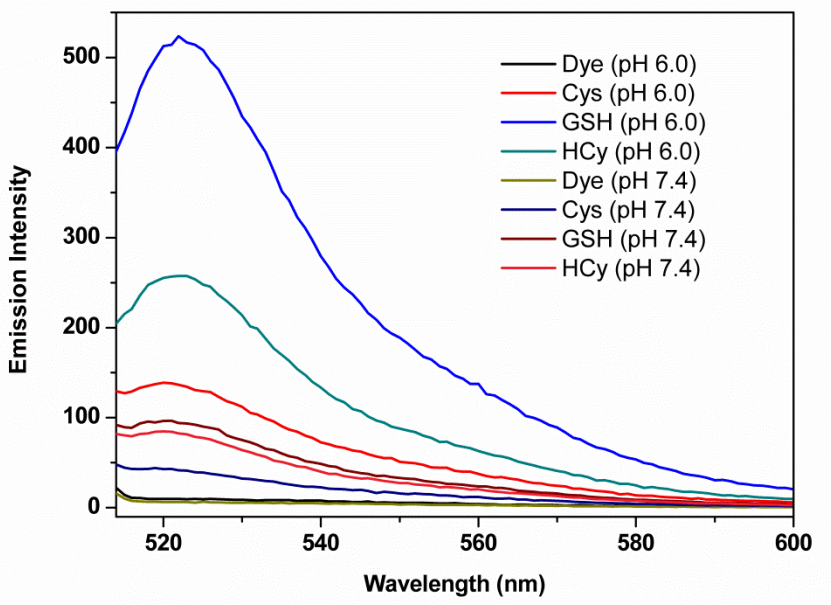

Figure 50. Emission spectra of Dye 1 (8.0×10^{-6} M) and Dye 1 + Thiols (200 equivalents) at pH 6.0 in 60% MES Buffer (30 mM) / 40% MeCN (exct @ 510 nm) and at pH 7.4 in 60% MOPS Buffer (30 mM) / 40% MeCN (exct @ 510 nm)

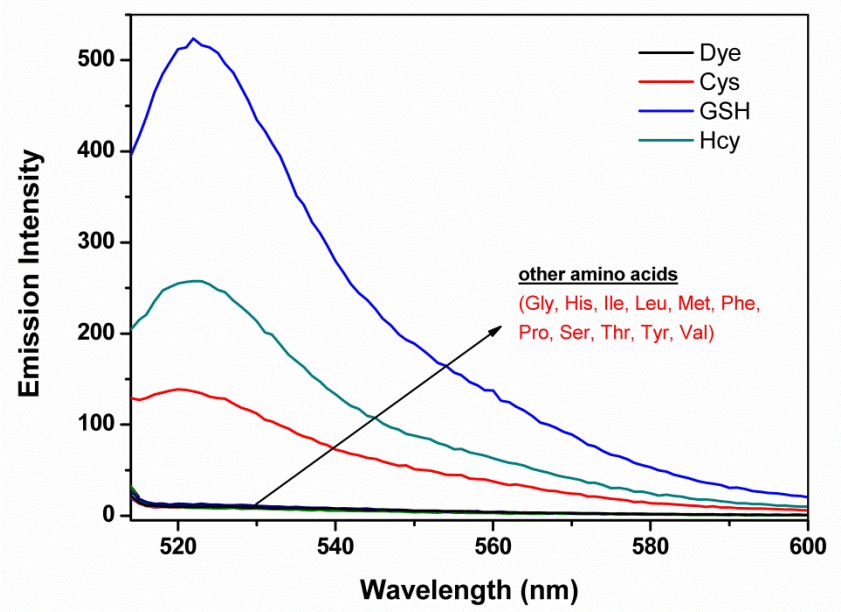

Figure 51. Emission spectra of Dye 1 (8.0×10^{-6} M), BODIPY 1 + Thiols (200 equivalents) and BODIPY 1 + Amino acids (200 equivalents) at pH 6.0 in 60% MES Buffer (30 mM) / 40% MeCN (exct @ 510 nm).

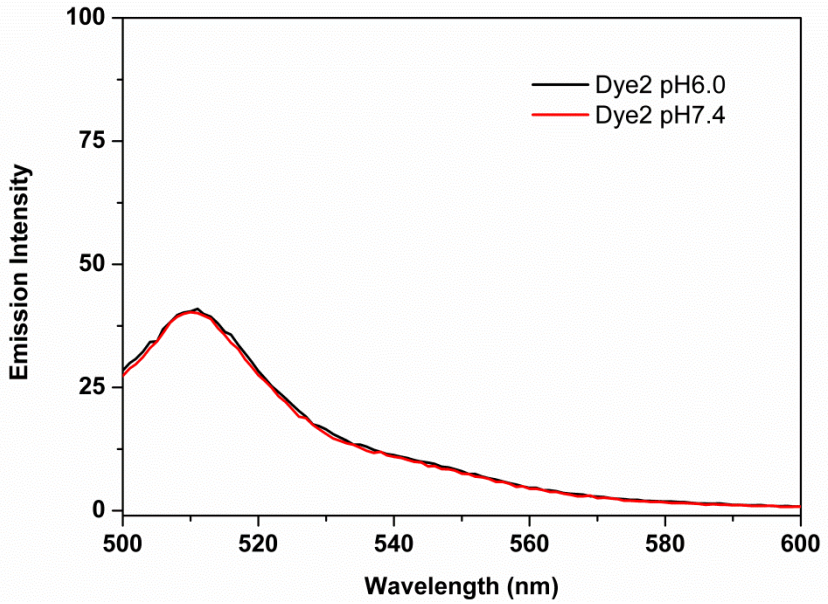

Figure 52. Emission spectra of Dye 2 (8.0×10^{-6} M) at pH 6.0 in 60% MES Buffer (30 mM) / 40% MeCN (exct @ 500 nm) and at pH 7.4 in 60% MOPS Buffer (30 mM) / 40% MeCN (exct @ 500 nm).

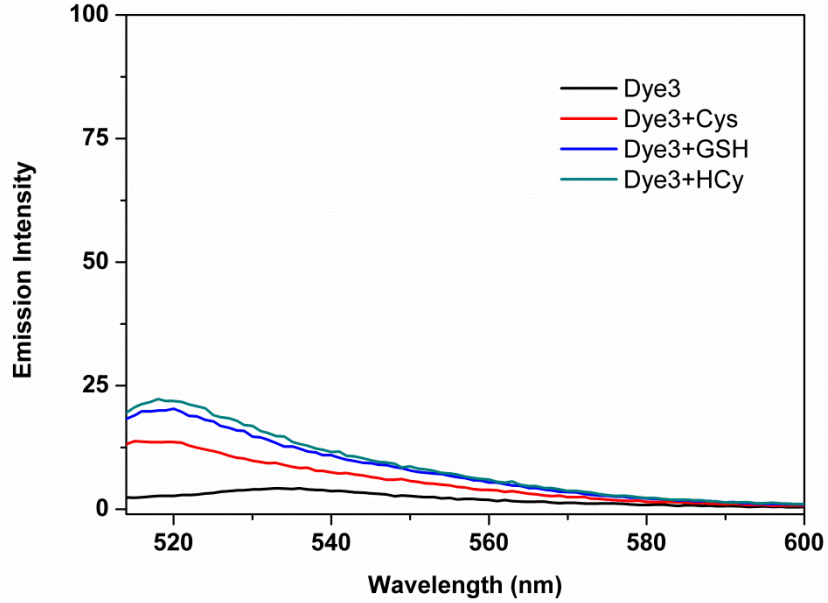

Figure 53. Emission spectra of Dye 3 (8.0×10^{-6} M) and Dye 3 + Thiols (200 equivalents) at pH 7.4 in 60% MOPS Buffer (30 mM) / 40% MeCN (exct @ 500 nm)

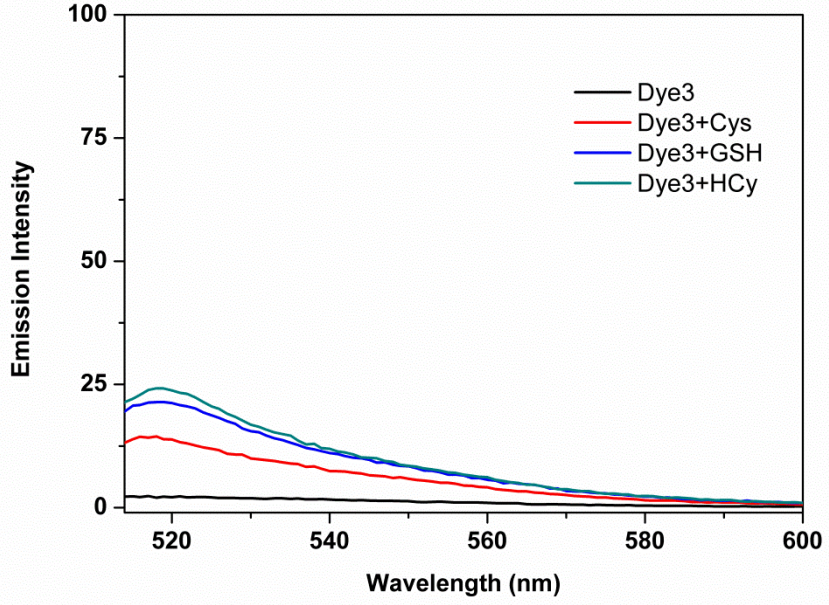

Figure 54. Emission spectra of Dye 3 (8.0×10^{-6} M) and Dye 3 + Thiols (200 equivalents) at pH 6.0 in 60% MES Buffer (30 mM) / 40% MeCN (exct @ 500 nm).

3.4.6 Kinetic Studies

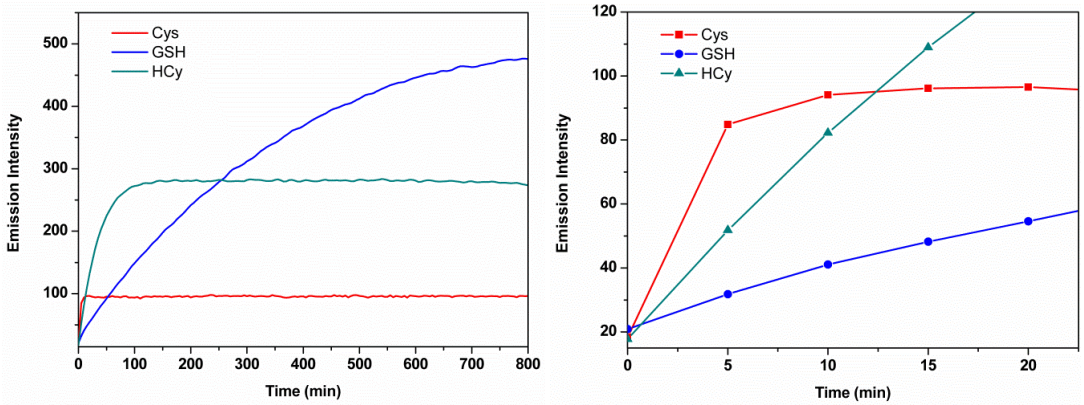

Figure 55. Fluorescence kinetic studies of Dye 1 + Thiols (200 equivalents) at pH 6.0 in 60% MES Buffer (30 mM) / 40% MeCN (exct @ 510 nm).

GSH		Value	STD
	y_0	541,46686	1,49029
	A	-517,37746	1,24239
	R_0	-0,00275	$1,99652x10^{-5}$
	R^2=0,99945		
HCy		**Value**	**STD**
	y_0	279,4373	0,24049
	A	-268,84207	2,19099
	R_0	-0,03189	$4,10935x10^{-4}$
	R^2=0,99187		
Cys		**Value**	**STD**
	y_0	113,06288	0,15583
	A	-76,62715	0,91394
	R_0	-0,40936	0,0181
	R^2=0,99509		
$y=y_0+Ae^{R0t}$			

Table 5. Exponential fit of the kinetic studies of Dye 1 + Thiols (200 equivalents) in the form of $y=y_0+Ae^{R0t}$ at pH 6.0 in 60% MES Buffer (30 mM) / 40% MeCN.

3.4.7 Cell Culture and Confocal Microscopy

Human breast adenocarcinoma cells (MCF-7) were grown to confluence at 37°C under 5% CO_2 in Dulbecco's Modified Eagle Serum (DMEM) containing 1% penicillin/streptomycin, 10% fetal bovine serum (FBS) and 2mML-glutamine. The cells were seeded in 24-well plates at $5x10^3$cells/well. After a 24 h incubation period, the cells were treated with 0.5 μM of dye **1** at 37°C for 2h in a humidified incubator. Cells were washed three times with phosphate-buffered saline (PBS), fixed with 4% paraformaldehyde in PBS, covered with mounting medium and stored at -20°C.

The samples were analyzed with Zeiss LSM-510 confocal microscope with an oil-immersion 63x objective lens. An argon laser of 488 nm wavelength was used with NFT 515 filter. The pinhole diameter was 94 μm and pixel dwell times were 1.27 μs.

CHAPTER 4

The Catalytic Activity of Short Peptide Amphiphile Nanostructures: Implications on the Origin of Life

4.1 Introduction

One of the most fundamental questions in the intersection between modern biology and chemistry is the molecular basis of life. There is a big gap in our knowledge considering the early steps of the formation of complex molecules (RNA, DNA, proteins and etc.). It is essential to assume that the spontaneous formation of RNA oligonucleotides is practically impossible. The recent works in the field demonstrated that peptide molecules as short as dipeptides can self-assemble into nanostructures in the form of tubes, closed-cages and fibrils. The ability of dipeptides to act as catalysts and the capability of other peptides, as short as tripeptides, to serve as a template for nucleotide binding and orientation, are confirmed by the other studies. In contrast to complex RNA molecules, the possibility of spontaneous generation of functional short peptides in the primordial earth conditions is very high. We propose a novel mechanism for the origin of life that is based on the ability of amphiphilic short peptides to form nanostructures and catalyze a chemical reaction. This model may help to explain the early events that led to the formation of the current biochemical machinery which combines the intricate and coordinated interaction between nucleic acids and proteins to allow the function of living organisms.

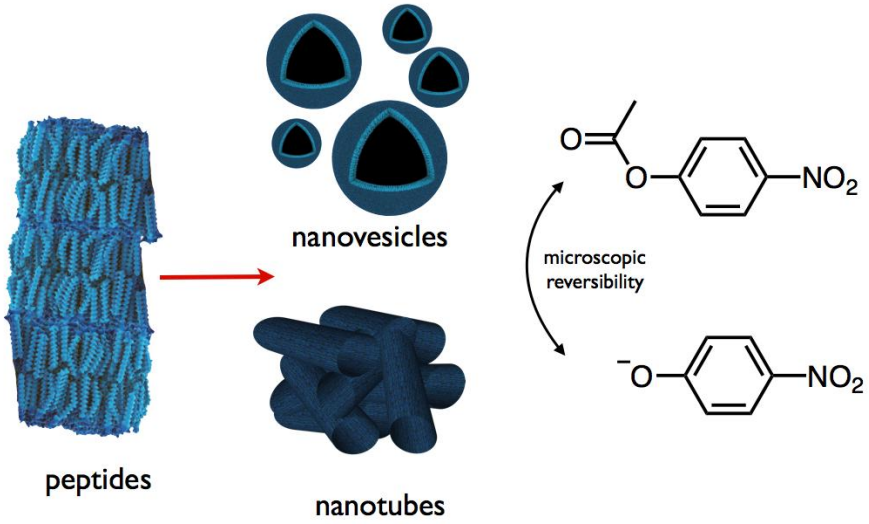

Figure 56. Schematic representation of the mechanism of our model.

Following “protein world” hypothesis, formation processes of various prebiotic amino acids were demonstrated under the primordial earth conditions. Alternatively, amino acids could be distributed from the universe to the primitive earth by falling meteorites. In the presence of these building blocks, short peptide formation in the primordial soup and its survival in very harsh conditions are widely accepted. Formation of nanostructures at neutral pH and their catalytic activity on hydrolysis of p-nitrophenyl acetate at acidic, neutral and basic mediums are studied.

4.2 Design

It is very unlikely to predict peptide sequences that are capable of forming nanostructures, namely nanotubes and nanovesicles by just looking the amino acids and their sequence in the peptide. However, the number can be minimized by rational design strategies.

The first peptide library constructed was containing peptides having alternating series of four amino acids. Eight of these peptides are synthesized manually using solid state peptide synthesis strategy and initial experiments are conducted with them. Considering these initial results, peptide library in Figure 57 is constructed and purchased.

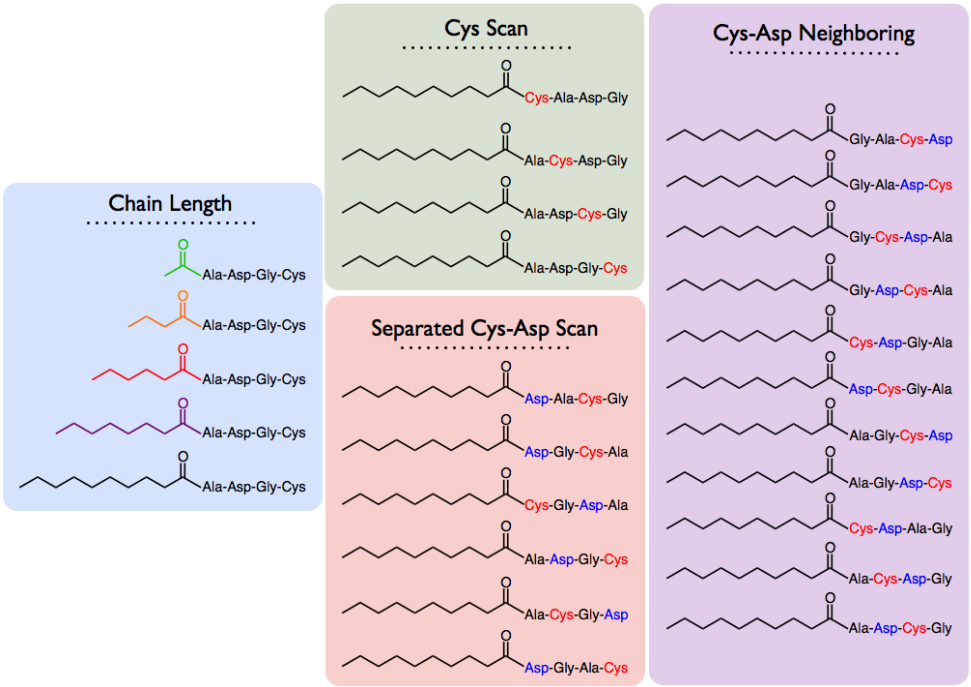

Figure 57.Peptide amphiphiles synthesized in this study.

In this study, peptide library is constructed consisting amino acids alanine (Ala), glycine (Gly), aspartic acid (Asp) that are most abundantly found in many prebiotic synthesis experiments and cysteine (Cys) that is found in most of the active sites of proteins and enzymes. These peptides are decorated with hydrophobic hydrocarbon chains found in stardust and meteorites ranging between two to ten carbons long.

Peptide library constructed with 21 peptides amphiphiles is used to scan different parameters. Effect of chain length is scanned with peptides having decoration of the N-terminus with ethanoyl, butanoyl, hexanoyl, octanoyl and decanoyl functionalities. In one series, position of the cysteine is scanned since its position likely to affect the catalytic activity of peptide. Position of the aspartic acid and relative distance to cysteine might also affect the catalytic activity of peptide. So that, in last two series, seperated cysteine-aspartic acid and neighboring cysteine-aspartic acids are preferred in the design of peptide sequences. All the peptide sequences can be seen in Figure 57.

4.3 Results and Discussion

It is expected to observe structural variation depend on the sequential differences. First a few peptides are synthesized manually following general procedure. For the nanostructure formation, peptide solutions (1.0 mg/mL concentration) are aged to according to a common procedure found in experimental section. Among all of the sequences, only one peptide sequence, decanoyl-DACG-COOH, successively formed nanostructures. In Figure 58, both nanovesicles (left-most image) and the nanotubes formations can be observed (right-most image) at different formation conditions. Additionally, the intermediate structure (middle image) shows the transformation from nanotubes to nanovesicles upon concentration. It is observed that when the 1.0 mg/mL solution of the same peptide in 9:1 methanol:water system aged for 24 hour in an ambient condition, only nanovesicles are formed. As the solutions are diluted both vesicular and tubular structures are obtained where the tubular structures are more dominant.

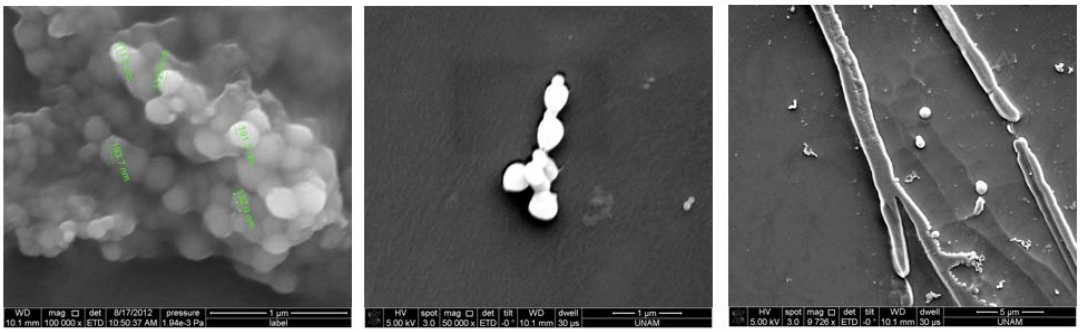

Figure 58. Scanning electron microscope (SEM) micrograph of peptide nanostructures formed by Decanoyl-DACG-COOH peptide.

Each single parameter may have significant importance for the nanostructure formation. Peptide concentration in solution, solvent composition, aging time, aging temperature, and nanostructure formation method and peptide sequence are among the most important parameters. So, all the parameters are fixed according to these preliminary studies. Among the solutions of 21 peptides, in only four of them nanostructure formation is observed: Decanoyl-GDCA-COOH, Decanoyl-AGCD-COOH, Decanoyl-CADG-COOH and Decanoyl-ACGD-COOH.

Decanoyl-GDCA-COOH formed spherical nanostructures with an average diameter of 155 nm whereas Decanoyl-AGCD-COOH nanospheres have an average diameter of 3.6 μm. Decanoyl-CADG-COOH and Decanoyl-ACGD-COOH formed needle-like and nanotubular structures. When the cysteine and aspartic acid located in neighboring positions, peptides preferred to adopt spherical structures. In contrast, as the distance between cysteine and aspartic acid increased, more open forms such as needle like or tubular structures are adopted. For example Decanoyl-DGAC-COOH where the cysteine and aspartic acid located at the two ends, no nanostructure formation is observed. On the other hand, it is observed that peptides adopting at least 80% of beta-sheet conformation successfully formed nanostructures. Peptides with lower beta-sheet character constructed no special structure.

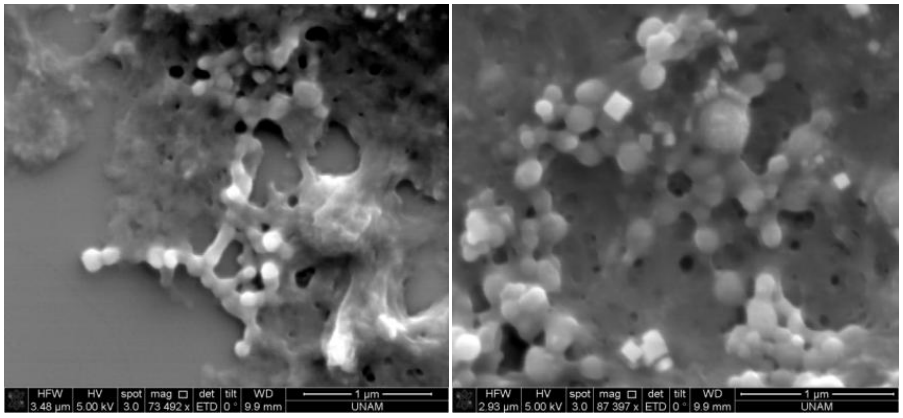

Figure 59. SEM images of peptide Decanoyl-GDCA-COOH

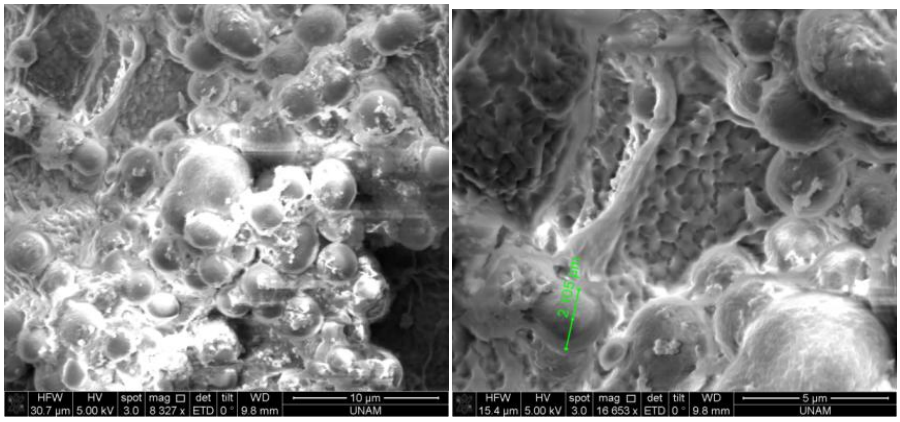

Figure 60. SEM images of peptide Decanoyl-AGCD-COOH

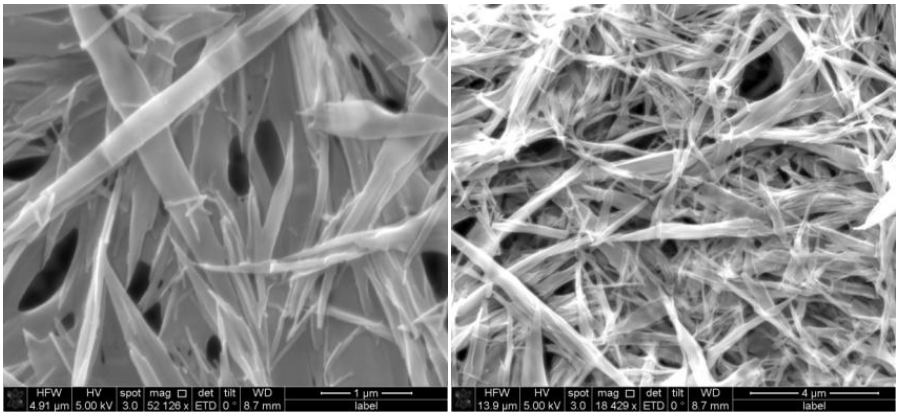

Figure 61. SEM images of peptide Decanoyl-CADG-COOH

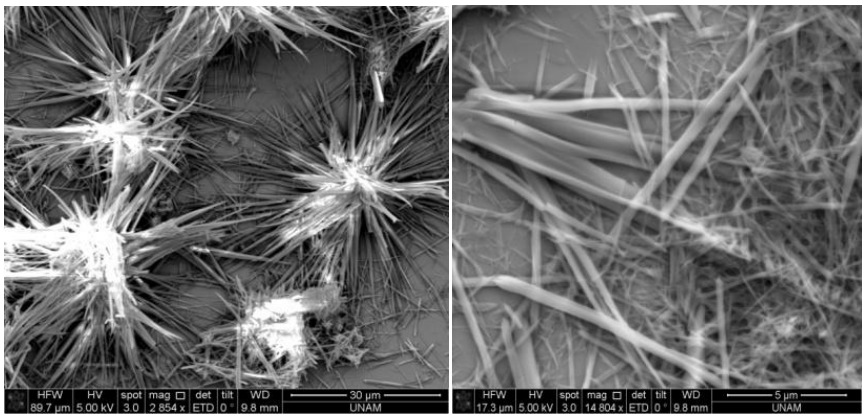

Figure 62. SEM images of peptide Decanoyl-ACGD-COOH

	Peptide Sequence (N- to C-terminus)	Nanostructure Formation	Gel Formation	Peptide Chain Conformation		
				β-sheet	α-helix	random chain
Chain Length	Ethanoyl-ADGC	-	-	2%	23%	75%
	Butanoyl-ADGC	-	-	4.5%	20%	75.5%
	Hexanoyl-ADGC	-	-	22%	3.5%	74.5%
	Octanoyl-ADGC	-	-	1%	3%	96%
	Decanoyl-ADGC[1]	-	-	25%	2%	73%
Cys-Asp Neighboring	Decanoyl-GACD	-	-	40%	0%	60%
	Decanoyl-GADC	-	-	0%	20%	80%
	Decanoyl-GCDA	-	yes	61%	14%	25%
	Decanoyl-GDCA	vesicular	-	83%	5%	12%
	Decanoyl-CDGA	-	-	20%	0%	80%
	Decanoyl-DCGA	-	-	40%	0%	60%
	Decanoyl-AGCD	vesicular	-	80%	8%	12%
	Decanoyl-AGDC	-	-	16%	14%	70%
	Decanoyl-CDAG	-	-	20%	0%	80%
	Decanoyl-ACDG[2]	-	-	8%	22%	70%
	Decanoyl-ADCG[3]	-	-	12%	15%	73%
Cys Scan	Decanoyl-CADG	tubular	yes	93%	2.5%	4.5%
	Decanoyl-ACDG[2]	-	yes	59%	22%	19%
	Decanoyl-ADCG[3]	-	-	12%	15%	73%
	Decanoyl-ADGC[1]	-	-	25%	2%	73%
Seperated Cys-Asp	Decanoyl-DACG	vesicular	-	82%	8%	10%
	Decanoyl-DGCA		-	36%	0%	64%
	Decanoyl-CGDA	-	-	34.5%	5.5% %	60%
	Decanoyl-ADGC[1]	-	-	25%	2%	73%
	Decanoyl-ACGD	needle-like	-	84%	10%	6%
	Decanoyl-DGAC	-	-	0%	20%	80%

Table 6. Characteristics of peptide amphiphiles.

Following to the characterization of the peptides, successful sequences are used to study the catalytic activity on the hydrolysis of p-nitrophenylacetate (pNPA).

$$k_0^{water}(neutral) = k_{H_2O} + k_{H^+}[H_3O^+] + k_{OH^-}[OH^-]$$
$$k_0^{water}(acidic) = k_{H_2O} + k_{H^+}[H_3O^+]$$
$$k_0^{water}(basic) = k_{H_2O} + k_{OH^-}[OH^-]$$

The hydrolysis of an ester may occur through base-catalyzed, pH-independent and acid-catalyzed reaction pathways. Hine has demonstrated that these reaction pathways are independent of each other. Thus, the observed pseudo-first-order rate constant for the hydrolysis of the ester is made up of the sum of products of the catalyst concentration and a second-order rate constant. The latter rate constant represents the inherent ability of the catalyst to catalyze the reaction. In distilled water, the observed rate constants are in Figure 65. For the ester p-nitrophenylacetate at neutral pH the where k_{HnO} is the pH-independent rate constant, observed pseudo-first-order rate constant may be described as in Table 7. Yates and McClelland have shown that in aqueous sulfuric acid, the mechanism of p-nitrophenylacetate hydrolysis is second order, acid-catalyzed with acyl-cleavage. It is presented evidence that acid-catalyzed p-nitrophenylacetate hydrolysis may also occur at neutral pH. The hydrolysis of p-nitrophenylacetate is generally followed spectrophotometrically at 270 nm for p-nitrophenylacetate loss or 400 nm for p-nitrophenoxide ion appearance or 300nm for p-nitrophenol appearance. The spectroscopic data may yield rate constants. Although the application of pseudo first-order kinetics requires mathematically an infinite excess of hydroxyl reactant, a reactant/reagent ratio of more than 15 was found to be satisfactory from a practical standpoint.[116]

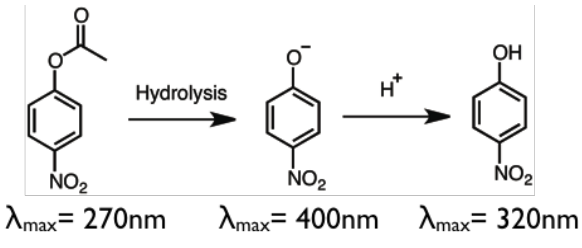

Figure 63. Maximum absorption wavelengths of products of pNPA hydrolysis.

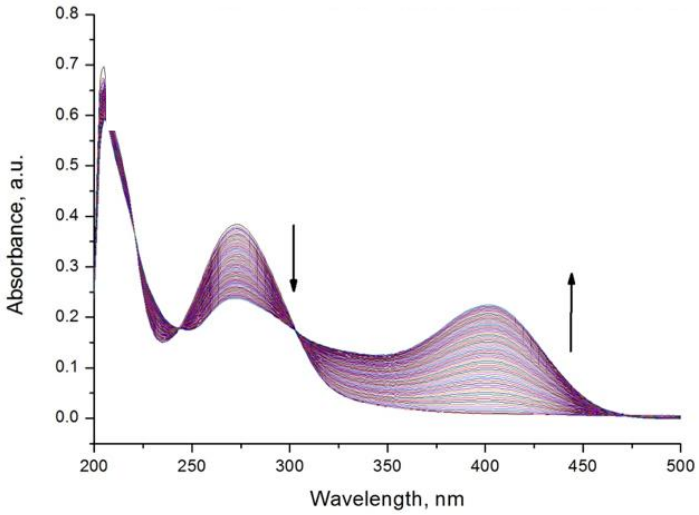

Figure 64. Hydrolysis of pNPA in phosphate buffer pH 7.0 in the presence of peptide.

UV-vis measurement is used to study the hydrolysis of PNPa. Spectra taken at every 15 min for 15 hours (Figure 64). It can be clearly seen that the p-nitrophenol peak at 270nm continuously decreases as the peak at the 400 nm which belongs to the p-nitrophenoxide increases suggesting a pseudo-first order catalytic reaction mechanism.

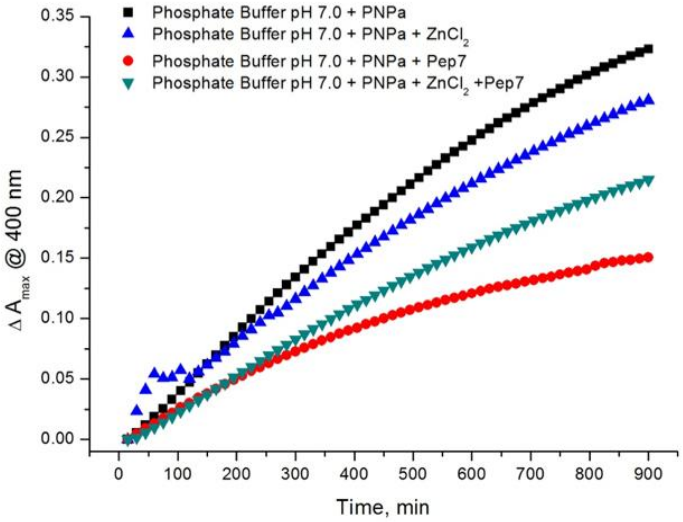

Figure 65. Plot of the absorption maximum at 400 nm vs time for phosphate buffer pH 7.0.

Additional experiments are conducted with $ZnCl_2$ since the presence of Zn(II) and Fe(II)/Fe(III) are known in prebiotic conditions. It has been thought of their presence may affect the catalysis of elementary reactions and in our case the hydrolysis of pNPA. However, the results were not very promising and so excluded from the further studies.

Peptide Sequence (N- to C-terminus)	Equations of Exponential Fit	R^2
pNPA (blank)	$A = 0.55 - 0.567e^{-0.00103t}$	0.999
+$ZnCl_2$	$A = 0.65 - 0.641e^{-0.00061t}$	0.999
+Peptide	$A = 0.19 - 0.002e^{-0.00162t}$	0.999
Peptide + $ZnCl_2$	$A = 0.44 - 0.447e^{-0.00079t}$	0.999

Table 7. Exponential fit equations of Decanoyl- DACG-COOH in phosphate buffer pH 7.0.

Hydrolysis experiment repeated with several control experiments that can be seen in Figure 65. The rate constants calculated from the exponential fit data and there is a distinguishable difference between peptide catalyzed and uncatalyzed reaction. The difference is not so significant when the reaction medium made slightly basic. Base catalyzed hydrolysis become more dominant then the catalysis by the peptide, but it can still be observed.

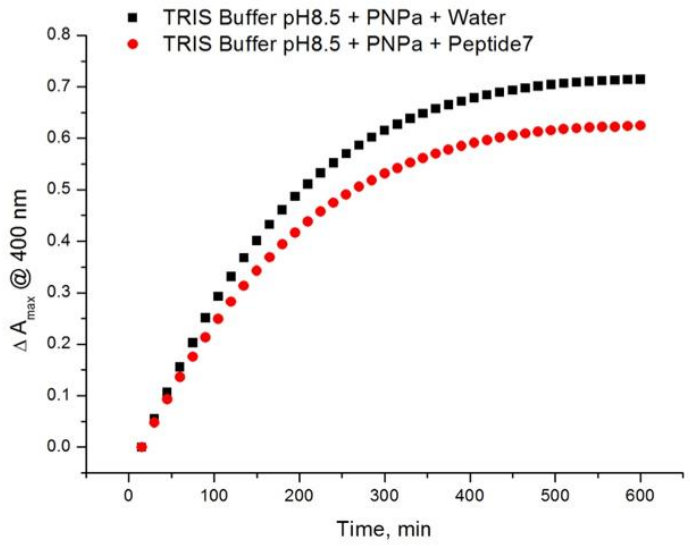

Figure 66. Plot of the absorption maximum at 400nm vs time for TRIS buffer pH 8.5.

Peptide Sequence (N- to C-terminus)	Equations of Exponential Fit	R^2
pNPA (blank)	$A = 0.74 - 0.839e^{-0.00597t}$	0.999
Decanoyl-DACG	$A = 0.66 - 0.732e^{-0.00569t}$	0.999

Table 8. Exponential fit equations of Decanoyl- DACG-COOH in TRIS buffer pH 8.5

After the catalysis studies, it is determined to use pH 7.2 phosphate buffer to eliminate the effect of hydrolysis by the hydroxide ion. *Para*-nitrophenyl acetate hydrolysis is carried out in the presence of peptides that are capable of forming nanostructures. When the normalized relative rates of these reactions are compared, almost 6-fold acceleration is observed (Table 11 and Figure 68). When it is compared to the catalytic activity of enzymes which are capable of accelerate reactions up to 10^{17} fold (see Table 9 for examples), 6-fold increase seems insignificant. However, universe has time and it is probable that even 6-fold increase in the rate may lead to trigger the initial steps in the origin of life in the time period of hundreds and billions of years.

Enzyme	Nonenzymatic rate	Enzymatic rate	Rate acceleration
Cyclophilin[117]	2.8×10^{-2}	1.3×10^{4}	4.6×10^{5}
carbonic anhydrase[116]	1.3×10^{-1}	10^{6}	7.7×10^{6}
chorismate mutase [116]	2.6×10^{-5}	50	1.9×10^{6}
Chymotrypsin [118]	4×10^{-9}	4×10^{-2}	10^{7}
triosephosphate isomerase [117]	6×10^{-7}	2×10^{3}	3×10^{9}
Fumarase [117]	2×10^{-8}	2×10^{3}	10^{11}
ketosteroid isomerase [116]	1.7×10^{-7}	6.6×10^{4}	3.9×10^{11}
carboxypeptidase A [116]	3×10^{-9}	578	1.9×10^{11}
adenosine deaminase[116]	1.8×10^{10}	370	2.1×10^{12}
Urease [117]	3×10^{-10}	3×10^{4}	10^{14}
alkaline phosphatase [117]	10^{-15}	10^{2}	10^{17}
orotidine 5'-phosphate decarboxylase [116]	2.8×10^{-16}	39	1.4×10^{17}

Table 9. Examples of Enzymatic Rate Acceleration

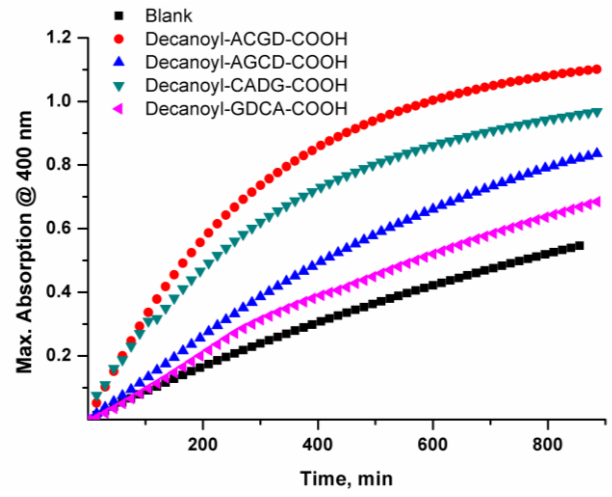

Figure 67. Plot of the absorption maximum at 400nm vs time for pNPA hydrolysis in phosphate buffer pH 7.2.

Peptide Sequence (N- to C-terminus)	Equations of Exponential Fit	R^2
pNPA (blank)	$A = 1.16385 - 1.15792e^{-0.000738795t}$	0.99998
Decanoyl-ACGD	$A = 1.1577 - 1.16649e^{-0.00338t}$	0.99995
Decanoyl-AGCD	$A = 1.25977 - 1.27614e^{-0.00126t}$	0.99969
Decanoyl-CADG	$A = 1.03717 - 1.01282e^{-0.00294t}$	0.99962
Decanoyl-GDCA	$A = 1.07124 - 1.08778e^{-0.00115t}$	0.99888

Table 10. Exponential fit equations of the nanostructure forming peptides, catalysis by nanostructures.

Peptide Sequence (N- to C-terminus)	t_{max} (min)	k (s^{-1})
pNPA (blank)	9800	$1.19x10^{-4}$
Decanoyl-ACGD	1700	$6.89x10^{-4}$
Decanoyl-AGCD	5300	$2.38x10^{-4}$
Decanoyl-CADG	2000	$5.21x10^{-4}$
Decanoyl-GDCA	5900	$1.82x10^{-4}$

Table 11. Time required to reach complete hydrolysis and calculated rate constants of the nanostructure forming peptides, catalysis by nanostructures.

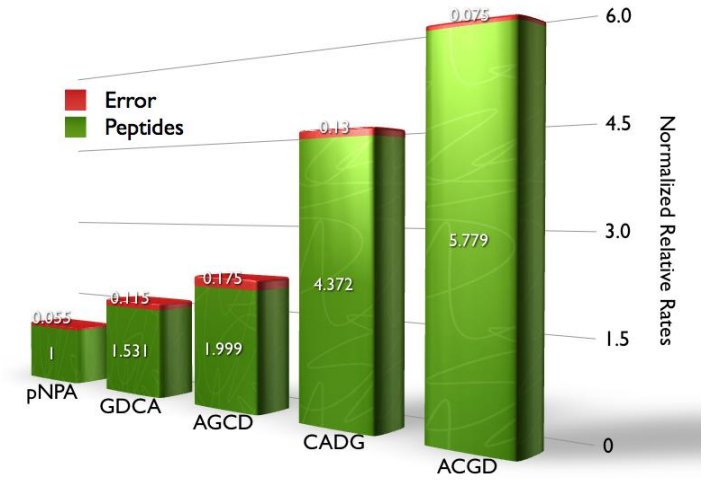

Figure 68. Normalized relative rates of nanostructure forming peptides.

It is also important to see that not the peptides but their nanostructures are capable of catalyzing a reaction. To test this hypothesis, catalysis is studied by the same amount (within the range of probable weighting errors) of peptide and their corresponding nanostructures.

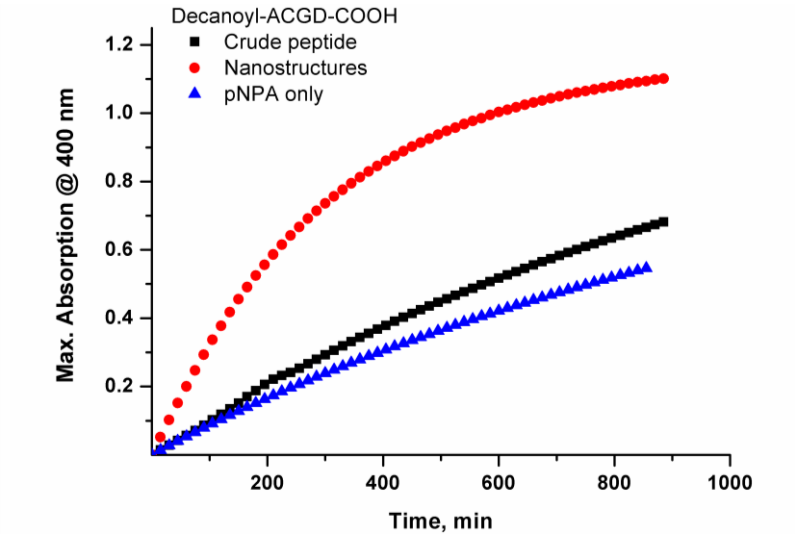

Figure 69. Plot of the absorption maximum at 400 nm vs time for pNPA hydrolysis by Decanoyl-ACGD-COOH in the form of peptide and nanostructures in phosphate buffer pH 7.2.

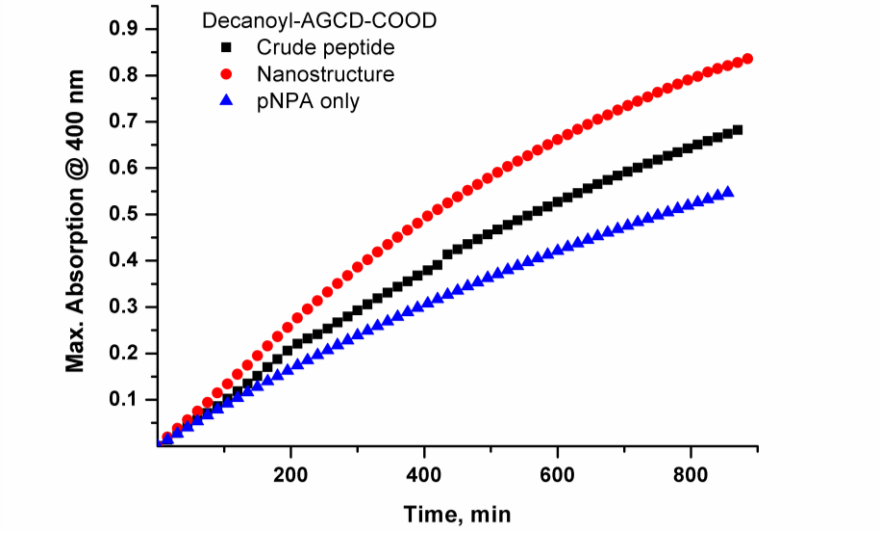

Figure 70. Plot of the absorption maximum at 400 nm vs time for pNPA hydrolysis by Decanoyl-ACGD-COOH in the form of peptide and nanostructures in phosphate buffer pH 7.2.

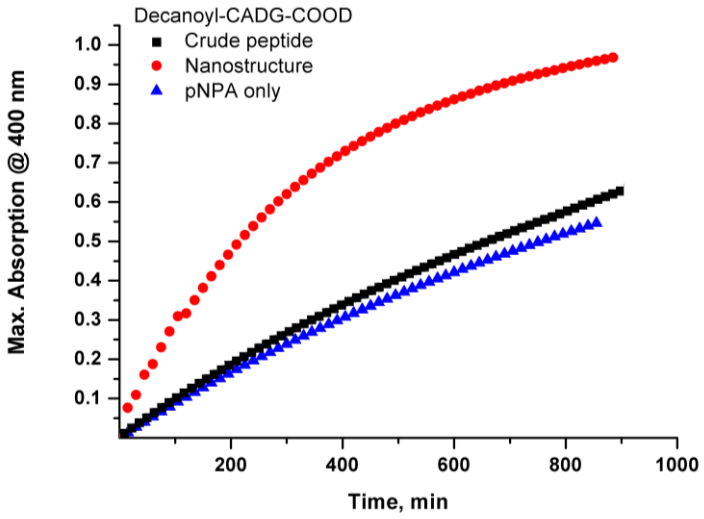

Figure 71. Plot of the absorption maximum at 400 nm vs time for pNPA hydrolysis by Decanoyl-CADG-COOH in the form of peptide and nanostructures in phosphate buffer pH 7.2.

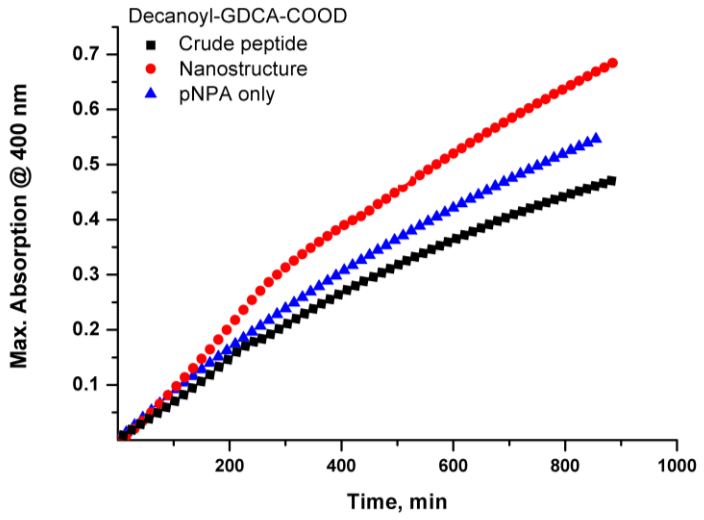

Figure 72. Plot of the absorption maximum at 400 nm vs time for pNPA hydrolysis by Decanoyl-GDCA-COOH in the form of peptide and nanostructures in phosphate buffer pH 7.2.

Peptide Sequence (N- to C-terminus)	**Equations of Exponential Fit**	**R^2**
Decanoyl-ACGD	$A = 1.11341 - 1.1001e^{-0.00085673t}$	0.9998
Decanoyl-AGCD	$A = 1.22515 - 1.23434e^{-0.000946872t}$	0.9997
Decanoyl-CADG	$A = 1.18496 - 1.19803e^{-0.000849321t}$	0.9998
Decanoyl-GDCA	$A = 1.05345 - 1.0798e^{-0.000956723t}$	0.9996
Decanoyl-GACD	$A = 1.203 - 1.2101e^{-0.00094874t}$	0.99980

Table 12. Exponential fit equations of the nanostructure forming peptides, catalysis by peptides. (*Decanoyl-GACD does not form nanostructures).

Peptide Sequence (N- to C-terminus)	t_{max} (min)	k (s^{-1})
Decanoyl-ACGD	8300	$1.35x10^{-4}$
Decanoyl-AGCD	7300	$1.67x10^{-4}$
Decanoyl-CADG	7800	$1.43x10^{-4}$
Decanoyl-GDCA	7600	$1.45x10^{-4}$
Decanoyl-GACD*	7400	$1.64x10^{-4}$

Table 13. Time required to reach complete hydrolysis and calculated rate constants of the nanostructure forming peptides, catalysis by peptides. (*Decanoyl-GACD does not form nanostructures).

Catalysis experiments clearly showed the nanostructures are more effective in catalysis of hydrolysis of pNPA. Corresponding rate constants can be found in Table 13 and the difference between peptide catalyzed and nanostructure catalyzed normalized relative rates in Figure 73. Depending on the results, it can be concluded that peptides showed no catalytic activity on the hydrolysis reaction whereas their corresponding nanostructures are capable of catalyzing the same reaction up to almost 6-fold. With this result, one of the main goals of the study is achieved.

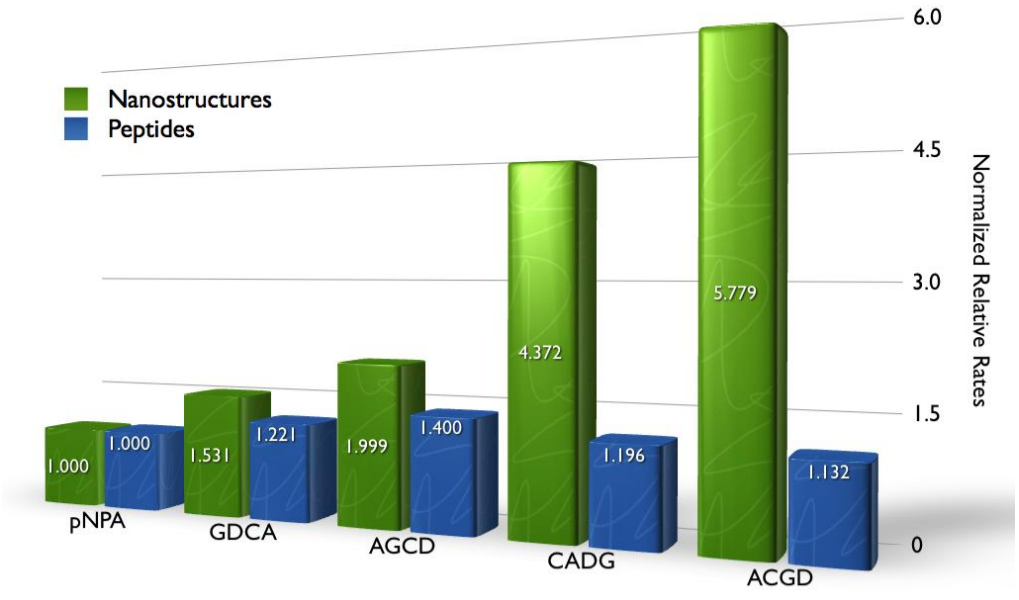

Figure 73. Normalized relative rates of nanostructure and peptide catalyzed hydrolysis of pNPA.

After these successful measurements, a chaotic combinatorial synthesis is completed to observe the major product formed in a mixture that can represent the prebiotic conditions (Figure 74). To the Gly-attached resin, Asp, Ala and Cys is coupled simultaneously and the N-termini is decorated with 5 different long chain hydrocarbons namely, ethanoyl, butanoyl, hexanoyl, octanoyl and decanoyl. Possible 240 different peptide sequences are formed (Figure 75).

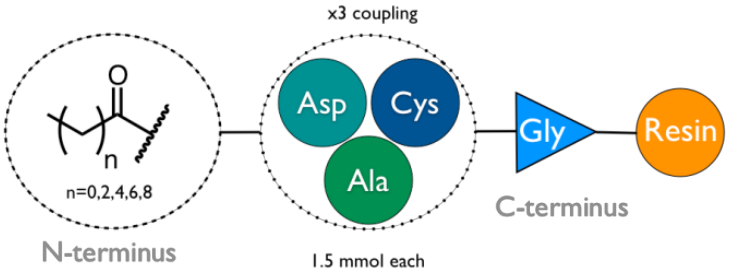

Figure 74. Chaotic combinatorial synthesis scheme.

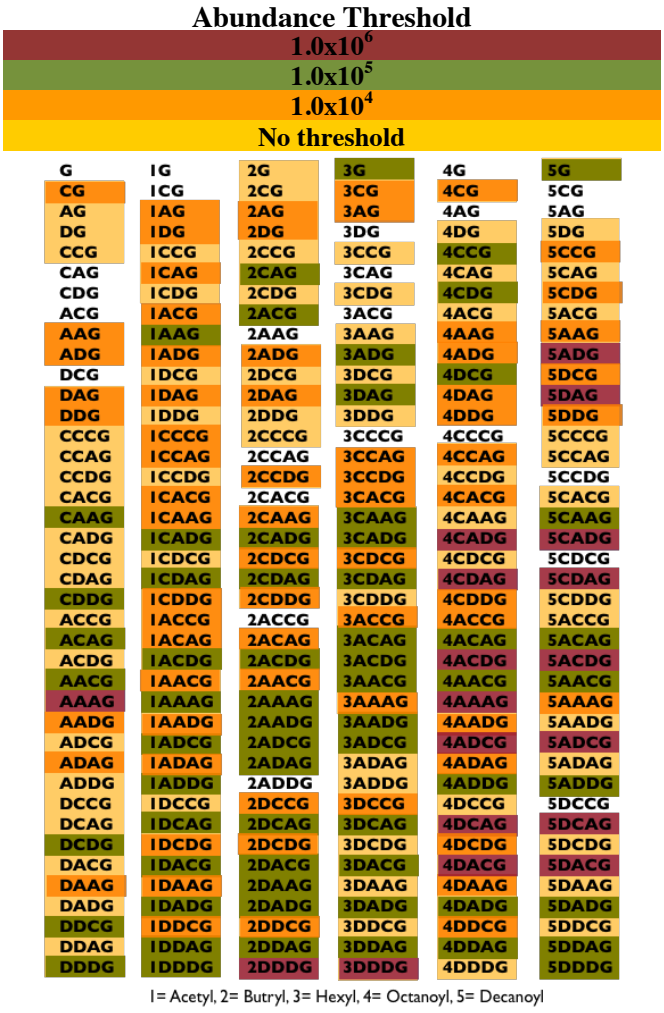

Figure 75. Possible products formed by the chaotic synthesis.

When the abundance threshold kept at the highest level, $1.0x10^6$, it is observed that the longer chain ended peptides are dominated the mixture. However in such a mixture, nanostructure formation could not be observed. Synthesis of the most abundant species will be completed manually and then kinetic studies will be completed.

4.4 Experimental Details

4.4.1 General

Solvents used in synthesis were reagent grade. CH_2Cl_2, DMF and DIEA were used without further purification. Reagents were purchased from Sigma-Aldrich, Merck, Fluka, or Acros and used as received. Preloaded resins and Fmoc-protected amino acids are purchased from Chem-Impex and Merck. Designed peptide library (in Figure 57) is purchased from Selleck-Chem with > 95% purity.

4.4.2 General Procedure for Solid State Peptide Synthesis

Preloaded resins should be swollen in DMF for 30 min prior to initial deprotection or coupling.

Deprotection:

The Fmoc protecting group is removed by treating the pre-swollen resin with a solution of 20% piperidine in DMF for 10 min (2x10 mL). Then the solution is drained and the resin washed with DMF (4 × 10 mL).

Coupling with a Fmoc-Protected Amino Acid:

Fmoc-protected amino acid (0.4 mmol, 4 eq.) dissolved in HBTU (800 μL, 0.5 M in DMF) then DIPEA (160 μL) is added. After addition of DIPEA solution is mixed and added to the resin in 30 seconds at max. Mixture allowed to stand for 1 hour and agitated in 10 min time intervals. Then the solution is filtered off and the resin

washed with DMF (4 × 10 mL), and DCM. The reaction progress is checked with the Kaiser test.

Final Deprotection:

Finally, after the last deprotection step, wash the resin with DMF (4 × 2 mL), DCM (4 × 2 mL), MeOH (1 × 2 mL), DCM (4 × 2 mL), then dry the resin under vacuum.

Cleavage:

The cleavage cocktail is prepared with 98% TFA, 1% DCM and 1% TIPS. This cocktail (2 x 1 mL) added to the resin and waited for 1 hour. Then the solvent is drained and collected. The peptide is precipitated by addition of ice-cold diethylether and the resulting emulsion is centrifuged at 8500 rpm for 20 min. The solid is filtered off. The product is dissolved in distilled water and lyophilized.

Kaiser Test:

A few dry resin beads are taken into a test tube, and 2 drops of ninhydrin, phenol and KCN solutions are added. Test is carried out at 110 ºC for 10 min. Positive test is indicated by blue/purple resin beads which means that the coupling was not complete and that there are still uncoupled amines left on the beads. Negative test is indicated by pale yellow/brown color.

4.4.2 Nanostructure Formation and Kinetic Studies

A peptide sample is taken from -80 ºC and waited for 30 min to equilibrate room temperature. Then, 1.0 ± 0.1 mg of sample is weighted and taken into a mass vial with a hollow glass rod. Sample dissolved in 1.0 mL of 9:1 water:methanol solution. Mass vials are vortexed for 2 min and stayed undisturbed for 3.5 hours and vortexed again for 2 min. After in total of 6 hours, one drop of sample is placed on a silicon wafer of dimensions 1.0 cm x 1.0 cm and left as is to slowly evoporate at ambient temperature.

Kinetic studies are performed in Varian Carry 5000 and Varian Carry 100 UV-Vis-NIR Spectrophotometers. Data collected between 600 nm - 200 nm. In all measurements 1.0 mM pH 7.2 phosphate buffer is used. For all measurements, pNPA

(in acetonitrile) concentration is 2.0 μM, nanostructure or peptide concentration is less than 1.0 μM.

4.4.3 Scanning Electron Microscopy

SEM and EDX studies were carried out using Quanta 200 FEG SEM (FEI, Hillsboro, OR) equipped with AmetekApollo X silicon drift detector (EDAX Inc., Mahwah, NJ).Samples used for EDX were uncoated, whereas those used for SEM imaging were coated with ~5 nm Au/Pd alloy.

4.4.4 Circular Dichroism

All spectra were collected in a Jasco J-815 CD spectrophotometer using a circular quartz cuvette with a path length of 1.0 mm from 260 nm to 190 nm at room temperature. The spectra were an average of five scans recorded at a scan rate of 50 nm/min with a 1 nm step interval and measured in mdeg.

CD data are analyzed in Dichroweb [119,120] using K2d neural-network-based analysis algorithm and Set 7 as a reference set which is optimized for the interval of 190-240 nm. The normalized root mean square deviation is lower than 0.1 for all calculations.

4.4.5 LC-MS

Analytical LC-MS-QTOF and preparative HPLC separations of synthesized peptides were performed on Agilent Technologies High Resolution Mass Time-of-Flight (TOF) LC/MS 1200 series and Agilent Technologies Preparative HPLC-1200 Series with diode array detector (DAD). In the case of analytical separation Agilent Technologies Zorbax Eclipse XDB-C18 analytical 4.6 x 150 mm 5- micron column was employed and for preparative separation Agilent Technologies PrepHT XDB-C18 preparative Cartridge 21.2 x 150 mm 5 micron column was used. For analytical resolution, peptide was dissolved in distilled water (%0.1 TFA), filtered and injected to the column. The flow rate was 0.65 mL/min and UV detection wavelengths were 210, 280 and 330 nm. This separation was performed on a 4.6 x 150 mm column. Only one injection was done (10μL). In the case of preparative resolution of peptides, again it was dissolved in distilled water (%0.1 TFA), filtered and injected to the column. The flow rate was adjusted as 20 mL/min and UV detection

wavelength was same. This separation was performed on a 21.2 x 150 mm column. Peptides obtained have purity of > 95%.

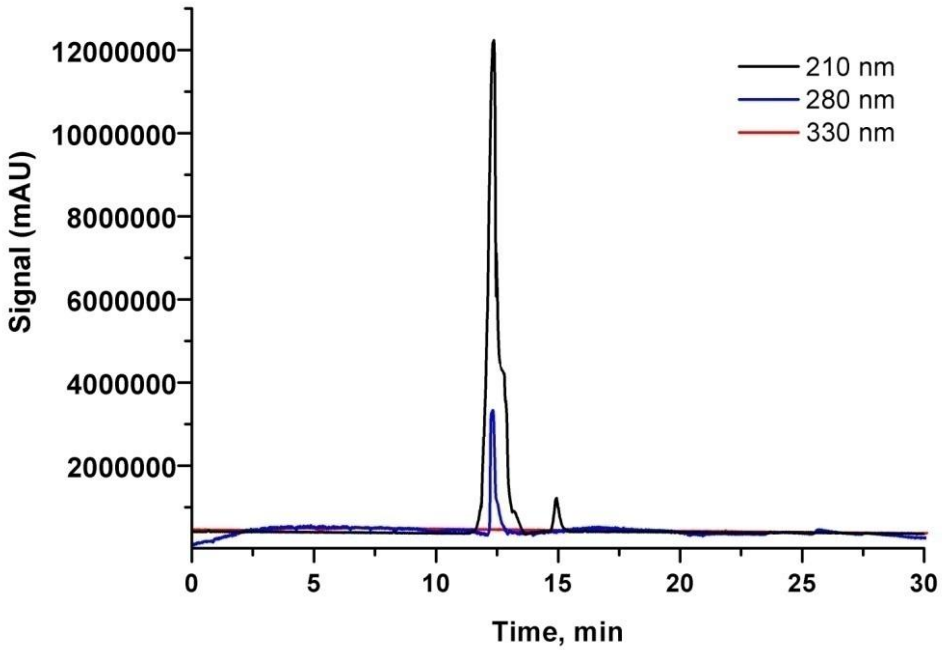

Figure 76. LC-MS profile of peptide Decanoyl-DAGC-COOH.

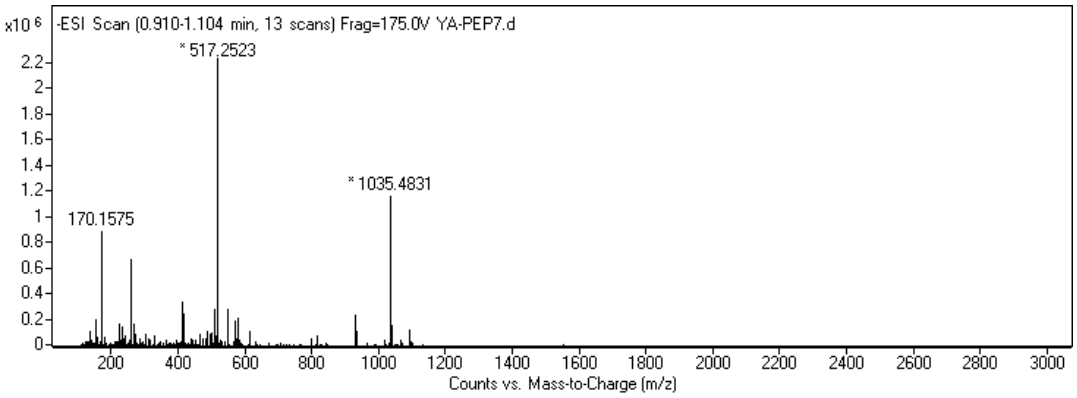

Figure 77. QTOF-ESI-MS spectrum of peptide Decanoyl-DAGC-COOH.

CHAPTER 5
CONCLUSION

In conclusion, we have shown in chapter 3 that selectivity for reaction based probes can be improved by applying additional photophysical manipulation sites. In this work, this was made possible by the simultaneous modulation of ICT and PeT processes, as adduct was generated. Large response to small pH difference in the biologically important range is particularly impressive considering practical applications. While the probe discussed here required a cosolvent (acetonitrile) for better solubility, the idea described in this work is perfectly transferable to other fluorophores and even to other reactions to be used in sensory systems. And when large differences in reaction rates for competing analytes are obtained, kinetic selectivity can be considered as a useful practical methodology. Such differentiation can be obtained by producing steric bulk around the reaction center(s). Work along these lines is in progress.

In chapter 4, it is shown that small amphiphilic peptides containing four amino acids, of which their presences are known under prebiotic conditions, can form tubular or vesicular nanostructures. In addition only these nanostructures are capable of catalyzing hydrolysis reaction whereas the peptide of the same sequences does not have such capability. In this work, this was made possible by scanning certain parameters such as hydrophobic chain length, position of the cysteine and separation between cysteine and aspartic acid. Observed rate acceleration is almost 6-fold with respect to the self-hydrolysis of pNPA. It might be considered as insignificant contribution to the catalysis if it is compared to the enzymes. However, when its implications on origin of life are considered, the results are quite impressive, indeed. Even small differences in reaction rates might trigger the initial steps of evolution. The work presented in this thesis forms an infrastructure of such small systems and helps to provide a route map for further studies.

BIBLIOGRAPHY

[1] R. C. Tolman, *The Principles of Statistical Mechanics*. Oxford University Press, London, UK, 1938.

[2] F. Wöhler, "Ueber künstliche Bildung des Harnstoffs" *Annalen der Physik und Chemie*, vol. 88, no. 2, pp. 253-256, 1828.

[3] R. B. Woodward, "The total synthesis of vitamin B_{12}" *Pure Appl*. *Chem*., vol. 33, no. 1, pp. 145-178, 1973.

[4] A. Eschenmoser, "Post-B_{12} problems in corrin synthesis" *Chem Soc*. *Rev*., vol. 5, no.1, pp. 377-410, 1976; *Quart*. *Rev*., vol. 24, pp. 336, 1970; *Nova Acta Leopoldina*, vol. 55, pp. 5, 1982.

[5] J.-M. Lehn, "Design of Organic Complexing Agents. Strategies towards Properties" *Struct*. *Bonding*, vol. 16, pp. 1-69, 1974.

[6] M. Eigen and L. De Maeyer, "Chemical Means of Information Storage and Readout in Biological Systems" *Naturwiss*, vol. 53, pp. 50, 1966.

[7] J.-M. Lehn, "Supramolekulare Chemie – Moleküle, Übermoleküle und molekulare Funktionseinheiten" *Angew*. *Chem*., vol. 100, no. 1, pp. 91, 1988.

[8] J.-M. Lehn, "Perspektiven der Supramolekularen Chemie – von der molekularen Erkennung zur molekularen Informationsverarbeitung und Selbstorganisation" *Angew*. *Chem*., vol. 102, no. 11, pp. 1347, 1990.

[9] E. Fischer, "Einfluss der Configuration auf die Wirkung der Enzyme" *Ber*. *Deutsch*. *Chem*. *Ges*., vol. 27, no.3, pp. 2985, 1894.

[10] J.-M. Lehn, *Perspectives in Coordination Chemistry*, VCH, Weinheim, pp. 447, 1992.

[11] B. Dietrich, J.-M. Lehn and J.-P. Sauvage, "Diaza-polyoxa-macrocycles et macrobicycles" *Tetrahedron Lett*., no. 10, vol. 34, pp.2885-2888, 1969.

[12] D. E. Koshland, "The active site and enzyme action" *Adv*. *Enzym*., vol. 22, pp. 45-97, 1960.

[13] J.-M. Lehn, "Supramolecular Chemistry: Receptors, Catalysts, and Carriers" *Science*, vol. 227, no. 4689, pp. 849, 1985.

[14] J.-M. Lehn, "Cryptate inclusion complexes, effects on solute-solute and solute-solvent interactions and on ionic reactivity" *Pure Appl*. *Chem*., vol. 52, no. 10, pp. 2303-2319, 1980.

[15] J.-M. Lehn, "Cryptates: macropolycyclic inclusion complexes" *Acc. Chem. Res.*, vol. 11, no. 2, pp. 49-57, 1978.

[16] Y. A. Ovchinnikov, V. T. Ivanov and A. M. Skrob, *Membrane Avtive Complexones*, Elsevier, New York, 1974.

[17] B. T. Kilbourn, J. D. Dunitz , L. A. R. Pioda and W. Simon, "Structure of the K+ complex with nonactin, a macrotetrolide antibiotic possessing highly specific K+ transport properties" *J. Mol. Biol.*, vol.30, no. 3, pp.559-563, 1967.

[18] C. J. Pedersen, "Cyclic polyethers and their complexes with metal salts" *J. Am. Chem. Soc.*, vol.89, no. 26, pp.7017-7036, 1967.

[19] C. J. Pedersen, "Die Entdeckung der Kronenether (Nobel-Vortrag)" *Angew. Chem.*, vol.100, no. 8, pp. 1053-1059, 1988.

[20] C. J. Pedersen, H. K. Frensdorff, "Makrocyclische Polyäther und ihre Komplexe" *Angew. Chem.*, vol. 84, no. 1, pp. 16-26, 1972.

[21] B. Diederich, J.-M. Lehn and J.-P. Sauvage, *"*Diaza-polyoxa-macrocycles et macrobicycles*" Tetrahedron Lett., no. 10, vol. 34, pp.2885-2888, 1969*.

[22] B. Diederich, J.-M. Lehn, J.-P. Sauvage and J. Blanzat, "Cryptates—X: Syntheses et proprietes physiques de systemes diaza-polyoxa-macrobicycliques" *Tetrahedron*, vol.29, no.11, pp. 1629-1645,1973.

[23] D. J. Cram, "Präorganisation – von Solventien zu Sphäranden" *Angew. Chem.*, vol. 98, no. 12, pp. 1041-1060, 1986.

[24] D. J. Cram, "Von molekularen Wirten und Gästen sowie ihren Komplexen" *Angew. Chem.*, vol. 100, no. 8, pp. 1041-1052, 1988.

[25] B. Valeur and I. Leray, "Design principles of fluorescent molecular sensors for cation recognition" *Coord. Chem. Rev.*, vol. 205, no.1, pp. 3-40, 2000.

[26] P. A. Panchenko, Y. V. Fedorov, O. A. Fedorova and G. Jonusauskas, "Comparative analysis of the PET and ICT sensor properties of 1,8-naphthalimides containing aza-15-crown-5 ether moiety" *Dyes and Pigments,* vol. 98, no. 3, pp. 347-357, 2013.

[27] S. Delmond, J. F. Le´tard, R. Lapouyade, R. Mathevet, G. Jonusauskas, and C. Rulliere, "Cation-triggered photoinduced intramolecular charge transfer and fluorescence red-shift in fluorescence probe" *New J. Chem.*, vol. 20, no. 7-8, pp. 861-869, 1996.

[28] Y. Zhou, Y. Xiao, S. Chi and X. Qian, "Isomeric Boron−Fluorine Complexes with Donor−Acceptor Architecture: Strong Solid/Liquid Fluorescence and Large Stokes Shift" *Org.Lett*., vol. 10, no. 4, pp. 633-636, 2008.

[29] Y. Dong, A. Bolduc, N. McGregor and W. G. Skene, "Push−Pull Aminobithiophenes — Highly Fluorescent Stable Fluorophores" *Org.Lett*., vol. 13, no.7, pp. 1844-1847, 2011.

[30] S. R. Marder, B. Kippelen, A. K. Y. Jen and N. Peyghammbarian, "Design and synthesis of chromophores and polymers for electro-optic and photorefractive applications" *Nature*, vol. 388, no. 6645, pp. 845-851, 1997.

[31] H. Burckstummer, N. M. Kronenberg, K. Meerholz and F. Wurtner, "Near-Infrared Absorbing Merocyanine Dyes for Bulk Heterojunction Solar Cells" *Org.Lett*., vol. 12, no.16, pp. 3666-3669, 2010.

[32] A. P. de Silva, H. Q. N. Gunaratne and C. P. McCoy, "A molecular photoionic AND gate based on fluorescent signaling" *Nature*, vol. 364, no. 6432, pp. 42-44, 1993.

[33] P. Ghosh, P. K. Gharadway, J. Roy and S. Ghosh, "Transition Metal (II)/(III), Eu(III), and Tb(III) Ions Induced Molecular Photonic OR Gates Using Trianthryl Cryptands of Varying Cavity Dimension" *J. Am. Chem. Soc*., vol. 119, no. 49, pp. 11903-11909, 1997.

[34] B. O. Küppers, *Information and the origin of life*, MIT Press, Cambridge, 1990.

[35] H. Girvetz, G. Geiger, H. Hantz, and B. Morris, *Science, Folklore and philosophy*. Harper & Row, New York, 1966.

[36] D. W. Deamer and G. R. Fleischaker (eds) *Origins of life: The central concepts*. Jones and Bartlet Publishers, Boston, 1994.

[37] R. F. Fox, *Energy and the evolution of life*, W. H. Freeman and Company, New York, 1988.

[38] S. Chang, *Prebiotic synthesis in plenatary environments*. In: J. M. Greenberg, C. X. Mendoza-Gomez, and V. Pirronello (eds.) *The chemistry of life's origins*. Kluwer Academic Press, Dordrecth, pp. 259-299, 1993.

[39] J. F. Kasting, "Earth's early atmosphere" *Science*, vol. 259, no. 259, pp. 920-926, 1993.

[40] S. F. Mason and G. E. Tranter, "The parity violating energy difference between enantiomeric molecules" *Chem. Phys. Lett.,* vol. 94, no. 1, pp. 34-37, 1983.

[41] G. E. Tranter, "The parity-violating energy difference between enantiomeric reactions" *Chem. Phys. Lett.*, vol. 115, pp. 286-287, 1985.

[42] M. Quack, and J. Stohner, "Molecular chirality and the fundamental symmetries of physics: influence of parity violation on rotovibrational frequencies and thermodynamic properties" *Chirality*, vol. 15, no. 4, pp. 375–376, 2003.

[43] G. L. Rikken, and E. Raupach, "Enantioselective magnetochiral photochemistry" *Nature*, vol. 405, no. 6789, pp. 895–896, 2000.

[44] D. K. Kondepudi, R. Kaufman and N. Singh, "Chiral symmetry breaking in sodium chlorate crystallization" *Science*, vol. 250, no.4983, pp. 975-976, 1990.

[45] J. M. McBride and R. L. Carter, "Spontaneous resolution by stirred crystallization" *Angew. Chem. Int. Ed.*, vol. 30, no. 3, pp. 293–295, 1991.

[46] J. R. Cronin and S. Pizzarello, "Enantiomeric excesses in meteoritic amino acids" *Science*, vol. 275, no.5302, pp. 951–955, 1997.

[47] J. L. Bada, "Meteoritics – extraterrestrial handedness?" *Science*, vol. 275, vol.5302, pp. 942–943, 1997.

[48] L. E. Orgel, "Molecular Replication" *Nature*, vol. 358, pp. 203-209, 1992.

[49] E. Szathmary, and J. M. Smith, "From Replicators to Reproducers: the First Major Transitions Leading to Life" *J. Theor. Biol.,* vol. 187, no.4, pp. 555-571, 1997.

[50] G. von Kiedrowski, "A Self-Replicating Hexadeoxynucleotide" *Angew. Chem. Int. Ed.*, vol. 25, no.10, pp. 932935, 1986.

[51] G. von Kiedrowski, B. Wlotzka, J. Helbing, M. Matzen, S. Jordan, "Parabolic Growth of a Self-Replicating Hexadeoxynucleotide Bearing a 3'-5'-Phosphoamidate Linkage*" Angew. Chem. Int. Ed.*, vol. 30, no.4, pp. 423, 1991.

[52] N. Paul, and G. F. Joyce, "A self-replicating ligase ribozyme" *Proc. Natl. Acad. Sci. U.S.A,*. vol. 99, pp. 12733-12740, 2002.

[53] D. H. Lee, J. R. Granja, J. A. Martinez, K. Severin, M. R. Ghadri, "A self-replicating peptide" *Nature*, vol. 382, pp.525-528,1996.

[54] S. Yao, I. Ghosh, R. Zutshi, J. Chmielewski, "A pH modulated self-replicating peptide." *J. Am. Chem. Soc.*, vol. 119, pp. 10559-10560, 1997.

[55] A. Vidonne, D. Philp, "Making molecules make themselves–the chemistry of artificial replicators." *European Journal of Organic Chemistry,* vol.5, pp. 593-610, 2009.

[56] T. Tjivikua, P. Ballester, J. Rebek, "Self-replicating system" *J. Am. Chem. Soc.* vol. 112, no.3, pp.1249-1250, 1990.

[57] V. Rotello, J. I. Hong, J. Rebek, "Sigmoidal Growth in a Self-Replicating System" *J. Am. Chem. Soc.,* vol. 113, pp. 9422-9423, 1991.

[58] B. Wang, I. O. Sutherland, "Self-replication in a Diels–Alder reaction" *Chem. Commun.*, vol. 2, no. 16, pp.1495-1496, 1997.

[59] R. J. Pieters, I. Huc, J. Rebek, "Reciprocal Template Effectsin a Replication Cycle" *Angew. Chem. Int. Ed.*, vol. 33, pp. 1579-1581, 1994.

[60] D. H. Lee, K. Severin, Y. Yokobayashi, M. R. Ghadiri, "Emergence of symbiosis in peptide self-replication through a hypercyclic network" *Nature*, vol. 390, pp. 591-593, 1997.

[61] S. L. Miller, "A production of amino acids under possible primitive earth conditions." *Science*, vol. 117, no. 2046, pp. 528-529, 1953.

[62] A. Oparin, *The Origin of Life* Macmillan, New York, 1938.

[63] A. Strecker, "Ueber die Künstliche Bildung der Mitchsaüre und einen Neuen, dem Glycocoll Homologen Körper" *Liebigs. Ann. Chem.,* vol. 75, pp. 27, 1850.

[64] E. T. Parker, H. J. Cleaves, J. P. Dworkin, D. P. Glavin, M. Callahan, A. Aubrey, A. Lazcano and Jeffrey Bada, " Primordial synthesis of amines and amino acids in a 1958 Miller H2S-rich spark discharge experiment." *PNAS*, vol. 10, no. 14, pp. 5526-5531, 2011.

[65] P. H. Abelson, "National Academy of Sciences: Abstracts of Papers Presented at the Autumn Meeting, 8-10 November 1956, Washington, D.C" *Science*, vol. 124, no.3228, pp. 935-941, 1956.

[66] W. Gilbert, "Origin of life: The RNA world" *Nature*, vol. 319, no. 6055, pp. 618, 1986.

[67] F. H. C. Crick, "The origin of the genetic code" *J. Mol. Biol.,* vol. 38, no. 3, pp. 367-379, 1968.

[68] L. E. Orgel, "Evolution of the genetic apparatus" *J. Mol. Biol.,* vol. 38, no. 3, pp. 381-393, 1968.

[69] L. Jager, M. C. Wright and G. F. Joyce, “A complex ligase ribozyme evolved in vitro from a group I ribozymes domain” *Proc. Natl. Acad. Sci.*, vol. 96, no. 26, pp. 14712–14717, 1999.

[70] K. B. Chapman and J. W. Szostak, “Isolation of a ribozyme with 5’-5’ ligase activity” *Chem. Biol.*, vol. 2, no. 5, pp. 325–333, 1995.

[71] N. Teramoto, Y. Imanishi and I. Yoshihiro, “In vitro selection of a ligase ribozymes carrying alkylamino groups in the side chains” *Bioconjugate Chem.*, vol. 11, no. 6, pp. 744–748, 2000.

[72] L. F. Landweber and I. D. Pokrovskaya, “Emergence of a dual-catalytic RNA with metal-specific cleavage and ligase activities: the spandrels of RNA evolution.” *Proc. Natl. Acad. Sci.*, vol. 96, no. 1, pp. 173–178, 1999.

[73] S. Kauffman, *At Home in the Universe: The Search for the Laws of Self-Organization and Complexity*. Oxford University Press, 1995.

[74] T. Tjivikua, P. Ballester, and J. Rebek, “A Self-Replicating System.” *J. Am. Chem. Soc.*, vol. 112, no. 3, pp.1249–1250, 1990.

[75] T. C. Chamberlin and R. T. Chamberlin, “Early terrestrial conditions that may have favored organic synthesis”, *Science*, vol. 28, no.730, pp. 897-911, 1908.

[76] J. Oró, “Comets and the formation of biochemical compounds on the primitive earth”, *Nature*, vol. 190, no. 4774, pp. 389-390, 1961.

[77] J. Oró, “Early chemical stagesin the origin of life.” In: S. Bengston (ed.) *Early life on Earth. Nobel Symposium 84*. New York: Columbia University Press. pp. 48-59, 1994.

[78] S. Epstein, R. V. Krishnamurthy, J. R. Cronin, S. Pizzarello, and G. U. Yuen, “Unusual stable isotope ratios in amino acid and carboxylic-acid extracts from the Murchison meteorite” *Nature*, vol. 326, no. 6112, pp. 477–479, 1987.

[79] S. Pizzarello, X. Feng, S. Epstein, and J. R. Cronin, “Isotopic N-lyses of nitrogenous compounds from Murchison meteorite: ammonia, amines, amino acids, and polar hydrocarbons”. *Geochim. Cosmochim. Acta*, vol. 58, no. 24, pp. 5579–5587, 1994.

[80] S. Pizzarello, and J. R. Cronin, “Non-racemic amino acids in the Murray and Murchison meteorites” *Geochim. Cosmochim. Acta*, vol. 64, no. 2, pp. 329–338, 2000.

[81] S. Pizzarello, and A. L. Weber, “Prebiotic amino acids as asymmetric catalysts” *Science*, vol. 303, no. 5661, pp. 1151, 2004.

[82] K. Kvenvolden, J. Lawless, K. Pering, E. Peterson, J. Flore, C. Ponnamperuma, I. R. Kaplan, and C. Moore, “Nonprotein Amino Acids from Spark Discharges and Their Comparison with the Murchison Meteorite Amino Acids”, *Proc*. *Nat*. *Acad*. *Sci*.,vol. 69, no. 4, pp. 809-811, 1972.

[83] K. A. Kvenvolden, J. Lawless, K. Pering, E. Peterson, J. Flores, C. Ponnamperuma, I. R. Kaplan, C. Moore, "Evidence for extraterrestrial amino-acids and hydrocarbons in the Murchison meteorite", *Nature*, vol. 228, no. 5275, pp. 923–926, 1970.

[84] O. Botta and J. L. Bada, “Extraterrestrial organic compounds in meteorites” *Surv*. *Geophys*., vol. 23, no. 1-4, pp. 411-467, 2002.

[85] X. H. Yan, “Transition of Cationic Dipeptide Nanotubes into Vesicles and Oligonucleotide Delivery” *Angew*. *Chem*. *Int*. *Ed*., vol. 46, no. 14, pp. 2431-2434, 2007.

[86] S. Scanlon and A. Aggeli, “Self-assembling peptide nanotubes” *Nanotoday*, vol. 3, no. 3-4, pp.22-30, 2008.

[87] N. Kol, L. A. Abramovich, D. Barlam, R. Z. Shneck, E. Gazit, and I. Rousso “Self-Assembled Peptide Nanotubes Are Uniquely Rigid Bioinspired Supramolecular Structures” *Nano Lett, vol*. 5, no. 7, pp. 1343-1346, 2005.

[88] L. Niu, X. Chen, S. Allen, and S. J. B. Tendler “Using the Bending Beam Model to Estimate the Elasticity of Diphenylalanine Nanotubes” *Langmuir,* vol. 23, no. 14, pp. 7443-7446, 2007.

[89] S. Vauthey, S. Santoso, H. Gong, N. Watson, and S. Zhang, “Molecular self-assembly of surfactant-like peptides to form nanotubes and nanovesicles” *Proc*. *Natl*. *Acad*. *Sci USA*, vol. 99, no. 8, pp. 5355-5360, 2002.

[90] S. G. Zhang and X. J. Zhao, “Design of molecular biological materials using peptide motifs” *J*. *Mater*. *Chem*., vol. 14, no.14, pp. 2082-2086, 2004.

[91] X. J. Zhao and S. G. Zhang, “Self-Assembling Nanopeptides Become a New Type of Biomaterial” In *Polymers for regenerative medicine*, pp. 145-170, Springer, 2006,.

[92] M. Antonietti and S. Förster, “Vesicles and Liposomes: A Self-Assembly Principle Beyond Lipids” *Adv*. *Mater*., vol. 15, no.16, pp. 1323-1333, 2003.

[93] S. Förster, M. Schmidt, “Polyelectrolytes in solution” *Adv*. *Polym*. *Sci*., vol. 120, pp. 51-133, 1995.

[94] N. Hermsdorf, Ph.D. Thesis, University of Potsdam, Germany, 1999.

[95] S. A. Jenekhe, and X. L. Chen, “Self-Assembly of Ordered Microporous Materials from Rod-Coil Block Copolymers” *Science,* vol. 283, no. 5400, pp. 372-375, 1999.

[96] S. A. Jenekhe, X. L. Chen, “Self-Assembled Aggregates of Rod-Coil Block Copolymers and Their Solubilization and Encapsulation of Fullerenes” *Science* , vol.279, no. 5358, pp. 1903-1907, 1998.

[97] S. J. Holder, N. A. J. M. Sommerdijk, S. J. Williams, R. J. M. Nolte, R. C. Hiorns, N. A. J. M. Sommerdijk and R. G. Jones, “The first example of a poly(ethylene oxide)–poly(methylphenylsilane) amphiphilic block copolymer: vesicle formation in water” *Chem*. *Commun*., no. 14, pp.1445, 1998.

[98] M. Reches, and E. Gazit, “Formation of Closed-Cage Nanostructures by Self-Assembly of Aromatic Dipeptides” *Nano Lett*., vol.4, no.4, pp. 581-585, 2004.

[99] R. B. Merrifield, "Solid Phase Peptide Synthesis. I. The Synthesis of a Tetrapeptide" *J*. *Am*. *Chem*. *Soc*., vol. 85, no.14, pp. 2149–2154, 1963.

[100] (a) J. Wu, W. Liu, J. Ge, H. Zhang, and P. Wang, “New sensing mechanisms for design of fluorescent chemosensors emerging in recent years” *Chem*. *Soc*. *Rev*., vol. 40, no. 7, pp. 3483, 2011.

(b) Z. C. Xu, J. Yoon, and D. R. Spring, “Fluorescent chemosensors for Zn^{2+},” *Chem*. *Soc*. *Rev*. vol. 39, no. 6, pp. 1996-2006, 2010.

(c) E. M. Nolan, S. J. Lippard, “Small-Molecule Fluorescent Sensors for Investigating Zinc Metalloneurochemistry” *Account*. *Chem*. *Res,*. vol. 42, no.1, pp. 193-203, 2009.

(d) J. L. Sessler, C. M. Lawrence, J. Jayawickramarajah, “Molecular recognition via base-pairing” *Chem*. *Soc*. *Rev*., vol. 36, no. 2, pp. 314-325, 2007.

(e) J. S. Kim, D.T. Quang, “Calixarene-Derived Fluorescent Probes” *Chem*. *Rev*. vol. 107, no. 9, pp. 3780-3799, 2007.

(f) P. D. Beer, P. A. Gale, "Anion Recognition and Sensing: The State of the Art and Future Perspectives" *Angew. Chem. Int. Ed.*, vol. 40, no. 3, pp. 486-516, 2001.

(g) B. Valeur, I. Leray, "Design principles of fluorescent molecular sensors for cation recognition" *Coord. Chem. Rev.*, vol. 205, no. 1, pp. 3-40, 2000.

[101] W. Dröge, H-P. Eck and S. Mihm, Immunology Today, 1992, 6, 211-214.

[102] P. J. Jacques, J. Selhub, A. G. Bostom, P. W. F. Wilson, I. H. Rosenberg, N. Engl. J. Med. 1999, 340, 1449.

[103] (a) Z.-B. Zheng, G. Zhu, H. Tak, E. Joseph, J. L. Eiseman, D. J. Creighton, Bioconjugate Chem. 2005, 16, 598. (b) C.-C. Yeh, M.-F. Hou, S.-H. Wu, S.-M. Tsai, S.-K. Lin, L. A. Hou, H. Ma, L.-Y. Tsai, Cell Biochem. Funct. 2006, 24, 555.

[104] Y. Zhou, and J. Yoon, "Recent progress in fluorescent and colorimetric chemosensors for detection of amino acids" *Chem. Soc. Rev.* vol. 41, no. 1, pp. 52-67, 2012.

[105] X. Chen, Y. Zhou, X. Peng, J. Yoon, "Fluorescent and colorimetric probes for detection of thiols"*Chem. Soc. Rev.*, vol. 39, no. 6, pp. 2120-2135, 2010.

[106] Y. Guo, X. Yang, L. Hakuna, A. Barve, J. O. Escobedo, M. Lowry, R. M. Strongin, "A Fast Response Highly Selective Probe for the Detection of Glutathione in Human Blood Plasma" *Sensors*, vol. 12, no. 5, pp. 5940-5950, 2012.

[107] L. Y. Niu, Y. S. Guan, Y. Z. Chen, L. Z. Wu, C. H. Tung, Q. Z. Yang, "BODIPY-Based Ratiometric Fluorescent Sensor for Highly Selective Detection of Glutathione over Cysteine and Homocysteine" *J. Am. Chem. Soc.* 2012, vol. 134, no. 46, pp. 18928-18931, 2012.

[108] M. Isik, T. Ozdemir, İ. Simsek Turan, S. Kolemen, E.U. Akkaya, "Chromogenic and Fluorogenic Sensing of Biological Thiols in Aqueous Solutions Using BODIPY-Based Reagents " *Org. Lett.*, vol. 15, no.1, pp. 216-219, 2013.

[109] O. A. Bozdemir, R. Guliyev, O. Buyukcakir, S. Selcuk, S. Kolemen, G. Gulseren, T. Nalbantoglu, H. Boyaci, E.U. Akkaya, "Selective Manipulation of ICT and PET Processes in Styryl-Bodipy Derivatives: Applications in Molecular

Logic and Fluorescence Sensing of Metal Ions" *J*. *Am*. *Chem*. *Soc*., vol. 132, no.23, pp. 8029-8036, 2010.

[110] N. Boens, V. Leen, W. Dehaen, "Fluorescent indicators based on BODIPY" *Chem*. *Soc*. *Rev*., vol. 41, no. 3, pp. 1130, 2012.

[111] (a) Q. Li, Y. Guo, S. Shao, "A BODIPY derivative as a highly selective "Off–On" fluorescent chemosensor for hydrogen sulfate anion "*Analyst*, vol. 137, pp. 4497-4501, 2012. (b) R. Wang, F. Yu, P. Liu, L. Chen, "A turn-on fluorescent probe based on hydroxylamine oxidation for detecting ferric ion selectively in living cells"*Chem*. *Commun*. vol. 48, pp. 5310-5312, 2012. (c) H. Sun, X. Dong, S. Liu, Q. Zhao, X. Mou, H. Ying Yang, W. Huang, "Excellent BODIPY Dye Containing Dimesitylboryl Groups as PeT-Based Fluorescent Probes for Fluoride" *J*. *Phys*. *Chem*. *C*, vol. 115, pp.19947-19954, 2011. (d) O.A. Bozdemir, F. Sozmen, O. Buyukcakir, R. Guliyev, Y. Cakmak, E.U. Akkaya, "Reaction-Based Sensing of Fluoride Ions Using Built-In Triggers for Intramolecular Charge Transfer and Photoinduced Electron Transfer" *Org*. *Lett*. vol. 12, pp.1400-1403, 2010. (e) T. Matsumoto, Y. Urano, T. Shoda, H. Kojima, T. Nagano, "A Thiol-Reactive Fluorescence Probe Based on Donor-Excited Photoinduced Electron Transfer: Key Role of Ortho Substitution" *Org*. *Lett*., vol. 9, pp. 3375-3377, 2007. (f) B. Turfan, E.U. Akkaya, "Modulation of Boradiazaindacene Emission by Cation-Mediated Oxidative PET" *Org*. *Lett*., vol. 4, pp. 2857-2859, 2002. (g) C.N. Saki, E.U. Akkaya, "Boradiazaindacene-Appended Calix[4]arene: Fluorescence Sensing of pH Near Neutrality" *J*. *Org*. *Chem*, vol. 66, pp.1512-1513, 2001.

[112] (a) E. Deniz, G.C. Isbasar, O.A. Bozdemir, L.T. Yildirim, A. Siemiarczuk, E.U. Akkaya, "Bidirectional switching of near IR emitting boradiazaindacene fluorophores" *Org*. *Lett*., vol. 10, pp. 3401-3403, 2008.

[113] (a) L. Y. Niu, Y. S. Guan, Y. Z. Chen, L. Z. Wu, C. H. Tunga, Q. Z. Yang, "A turn-on fluorescent sensor for the discrimination of cystein from homocystein and glutathione" *Chem*. *Commun*. vol. 49, pp. 1294, 2013.

[114] (a) X. Yang, Y. Guo, R. M. Strongin, "Conjugate Addition/Cyclization Sequence Enables Selective and Simultaneous Fluorescence Detection of Cysteine and Homocysteine" *Angew*. *Chem*. *Int*. *Ed*. vol. 50, pp. 10690-10693, 2010.

[115] T. Werner, C. Huber, S. Heinl, M. Kollmannsberger, J. Daub, O. S. Wolfbeis, "Novel optical pH-sensor based on a boradiaza-indacene derivative" *Fresenius' J. Anal*. *Chem* vol. 359, pp. 150-154, 1997.

[116] F. Willeboordse and R. L. Meeker, "Rapid Determination of Primary Hydroxyl Content of Poly(Oxyalkylene) Glycols and Poly(Oxyalkylene) Sorbitols by Pseudo First-Order Differential Reaction Kinetics" *Anal*. *Chem*., vol. 38, no. 7, pp 854-858, 1966.

[117] A. Radzicka and R. Wolfenden, "A proficient enzyme" *Science* vol. 267, no. 5194, pp. 90-93, 1990.

[118] H. R. Horton, L. A. Moran, R. S. Ochs, J. D. Rawn, K. G. Scrimgeour, *Principles of Biochemistry*; Neil Patterson: Englewood Cliffs, NJ, 1993.

[119] L. Whitmore and B. A. Wallace, "Protein Secondary Structure Analyses from Circular Dichroism Spectroscopy: Methods and Reference Databases" *Biopolymers*, vol.89, no.5, pp.392-400, 2008.

[120] L. Whitmore and B. A. Wallace, "DICHROWEB, an online server for protein secondary structure analyses from circular dichroism spectroscopic data" *Nucleic Acids Research* vol. 32, no. W668-673, 2004.

APPENDIX A

SEM IMAGES

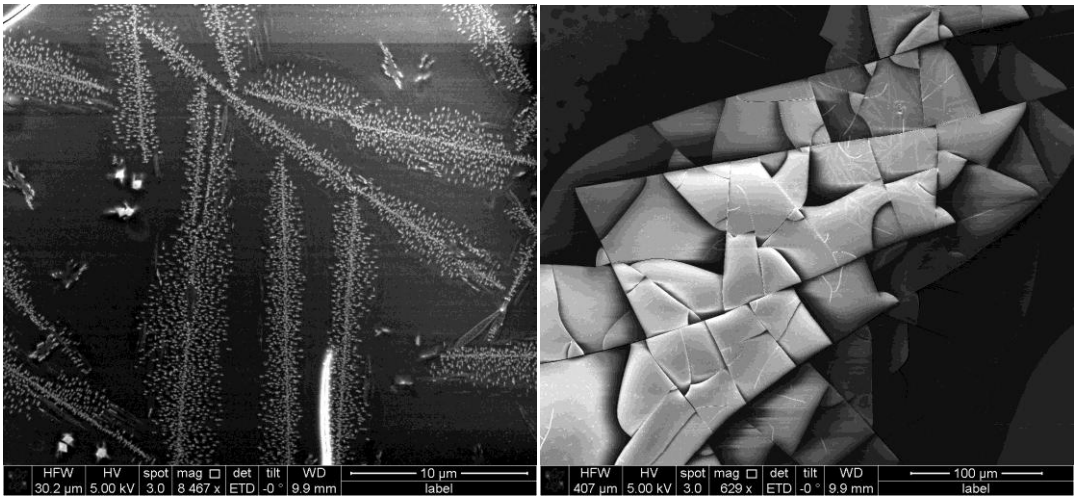

Figure 78. SEM images of peptide Ethanoyl-ADGC-COOH

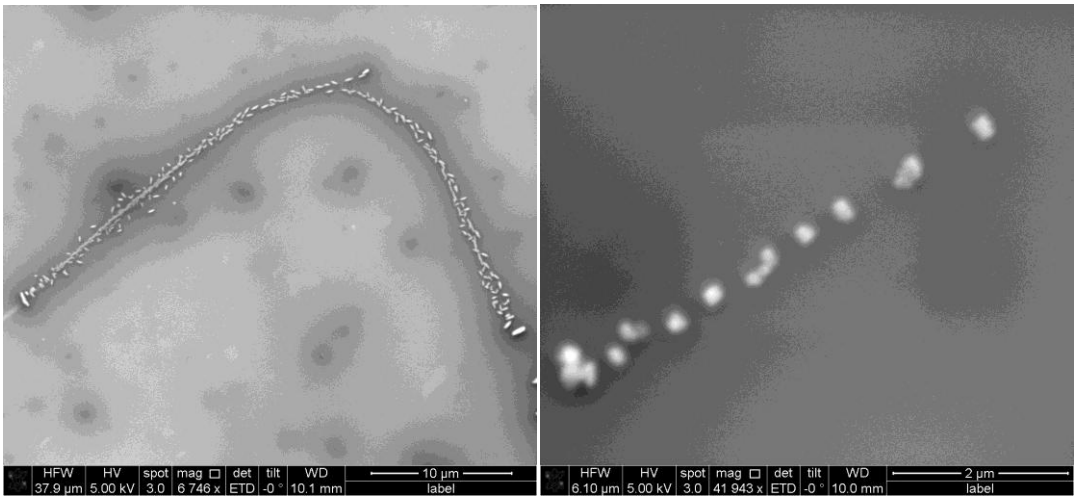

Figure 79. SEM images of peptide Butanoyl-ADGC-COOH

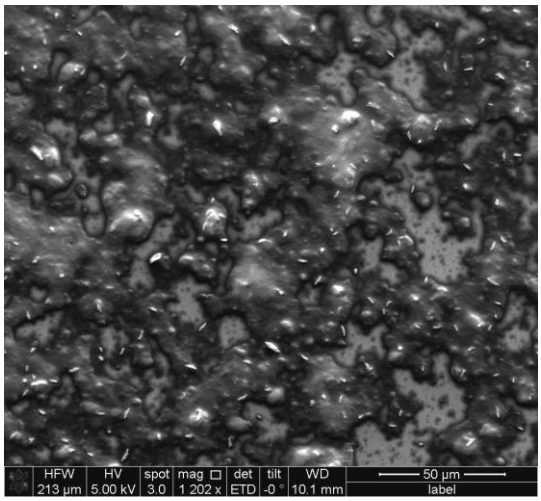

Figure 80. SEM images of peptide Hexanoyl-ADGC-COOH

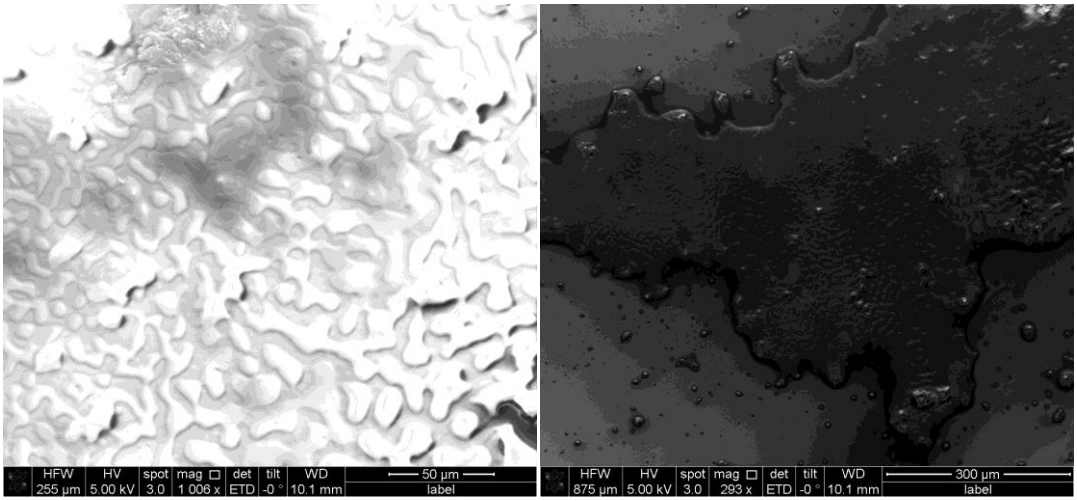

Figure 81. SEM images of peptide Octanoyl-ADGC-COOH

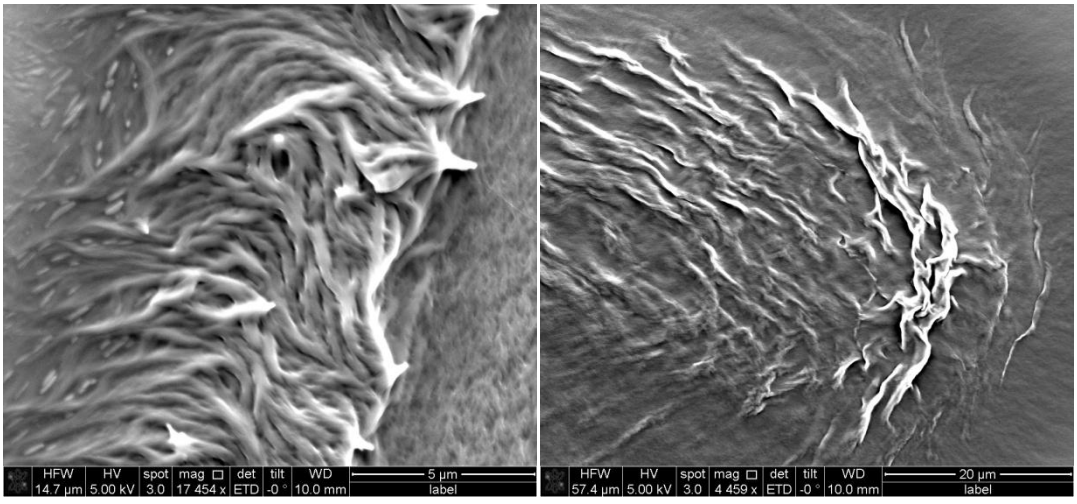

Figure 82. SEM images of peptide Decanoyl-ADGC-COOH

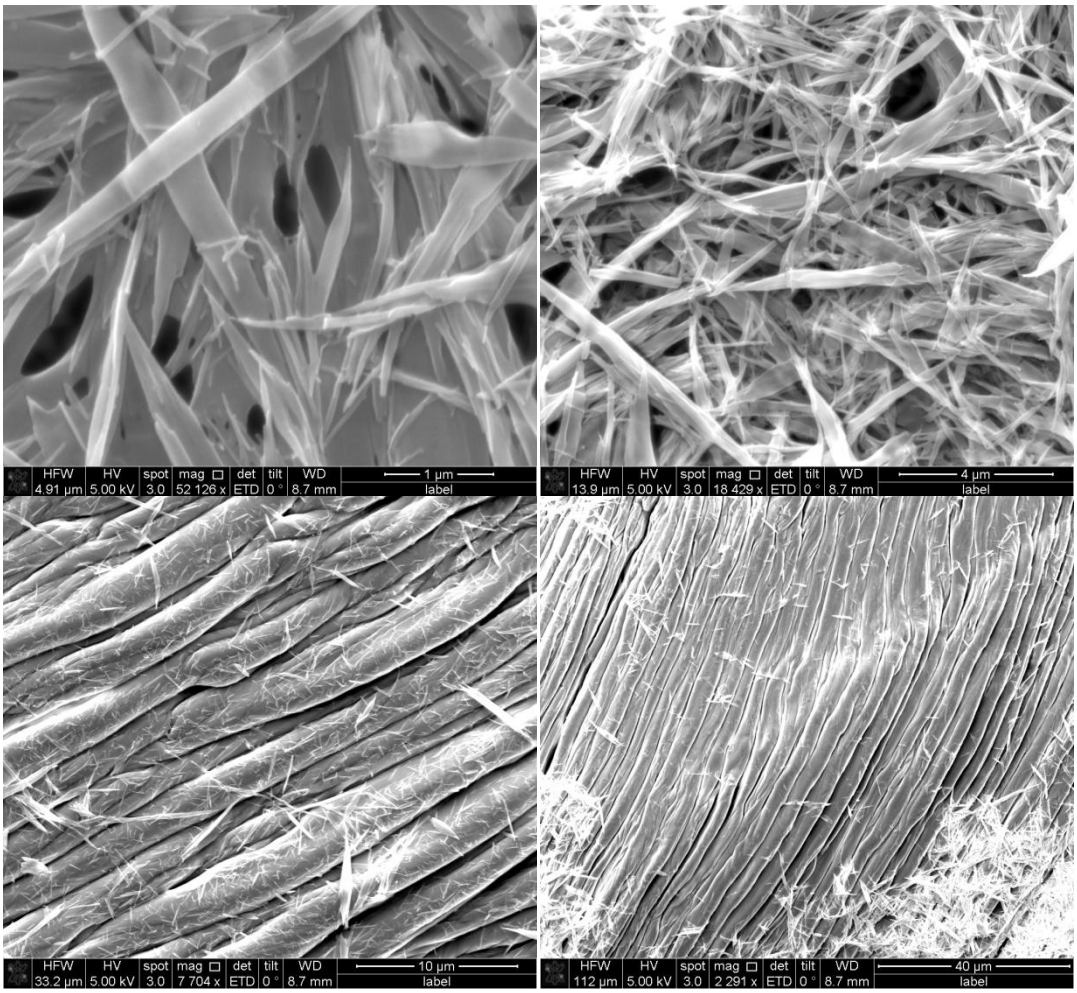

Figure 83. SEM images of peptide Decanoyl-CADG-COOH

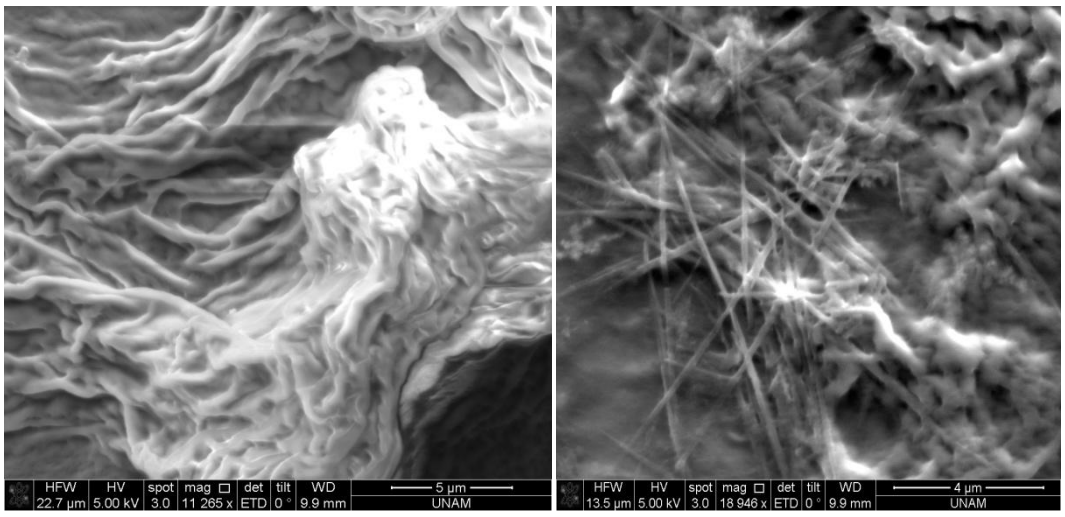

Figure 84. SEM images of peptide Decanoyl-DGAC-COOH

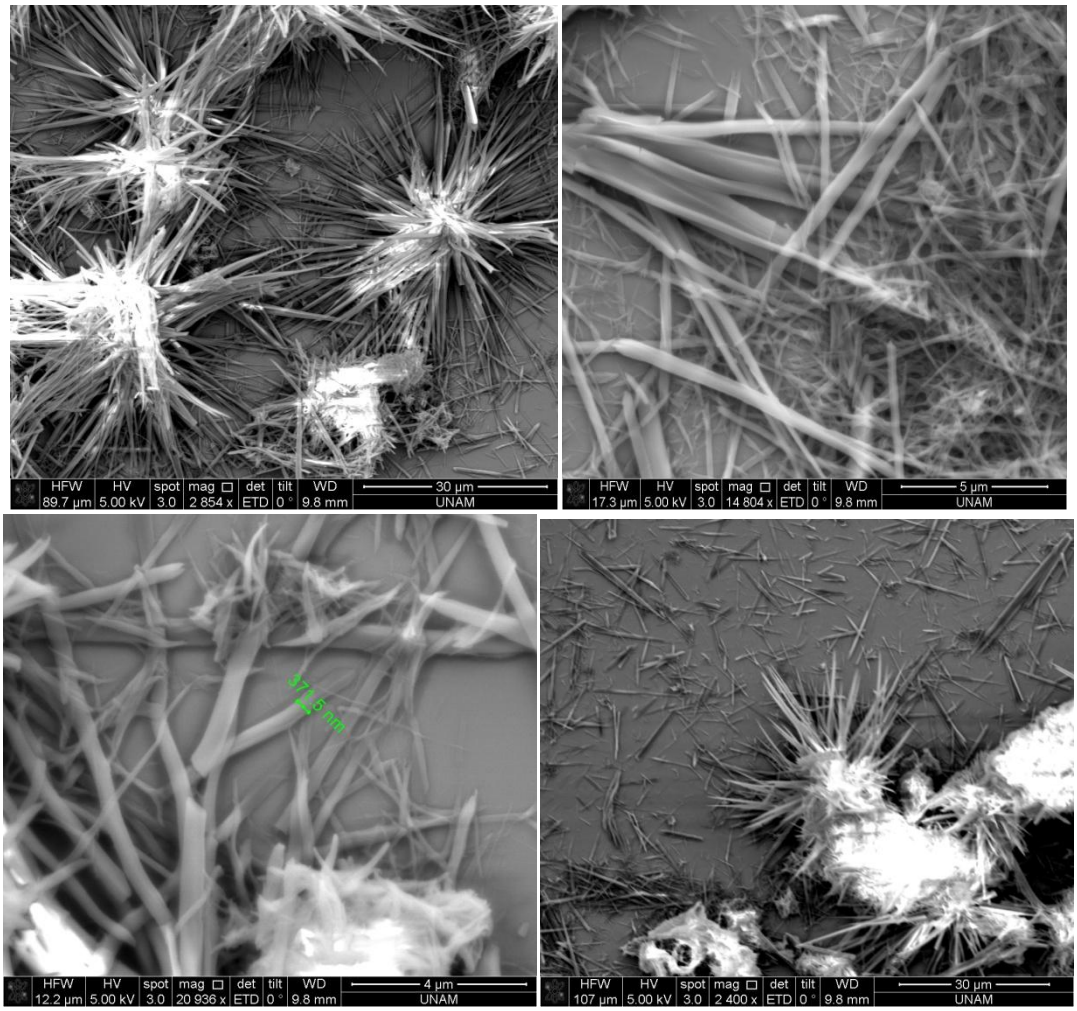

Figure 85. SEM images of peptide Decanoyl-ACGD-COOH

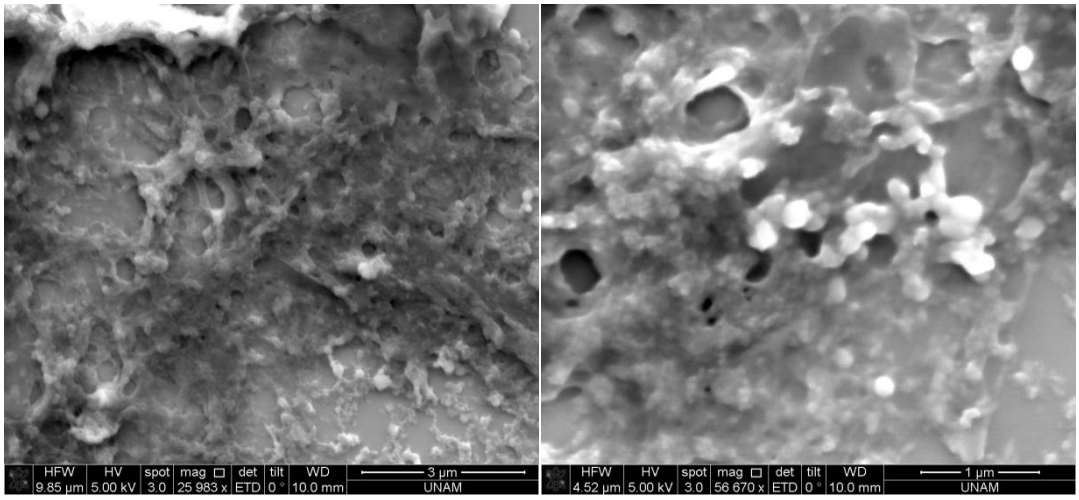

Figure 86. SEM images of peptide Decanoyl-ADCG-COOH

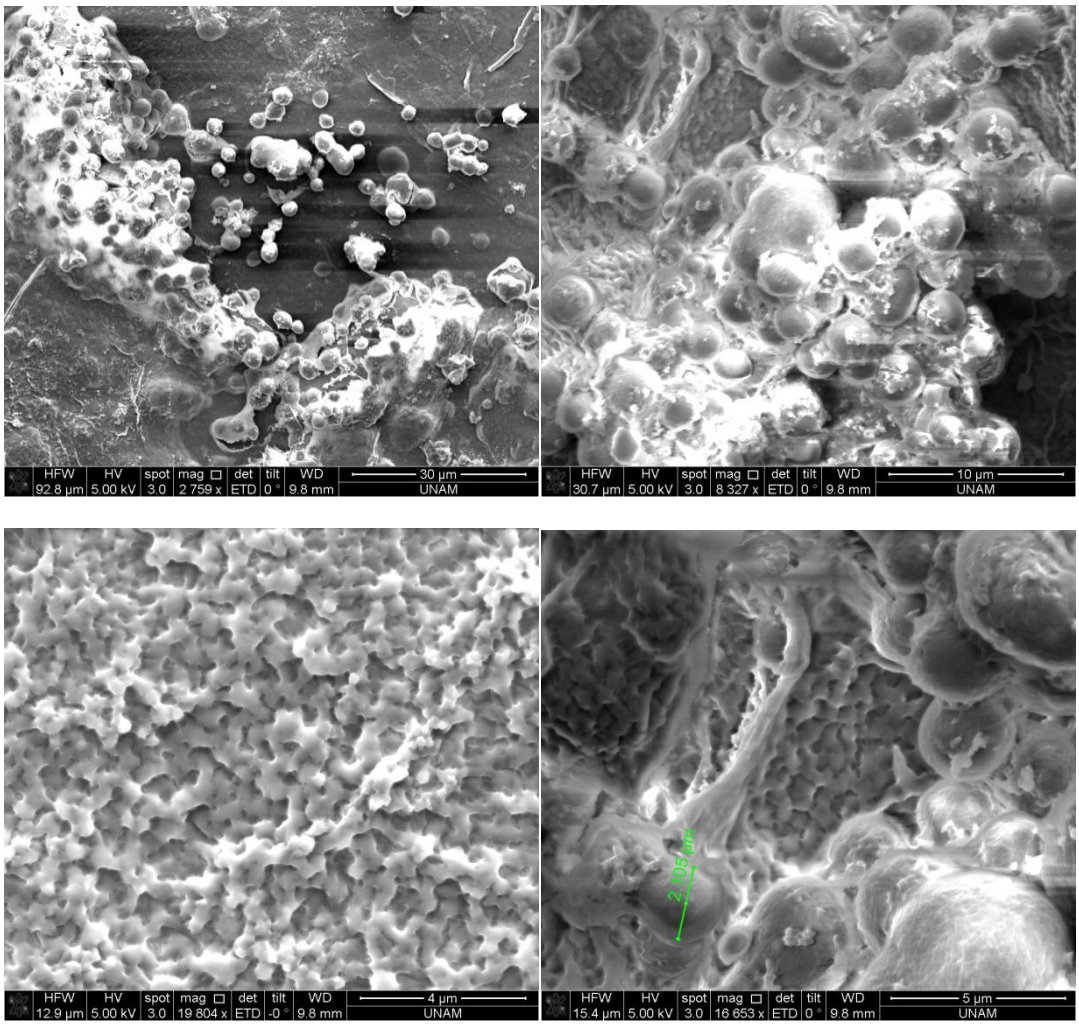

Figure 87. SEM images of peptide Decanoyl-AGCD-COOH

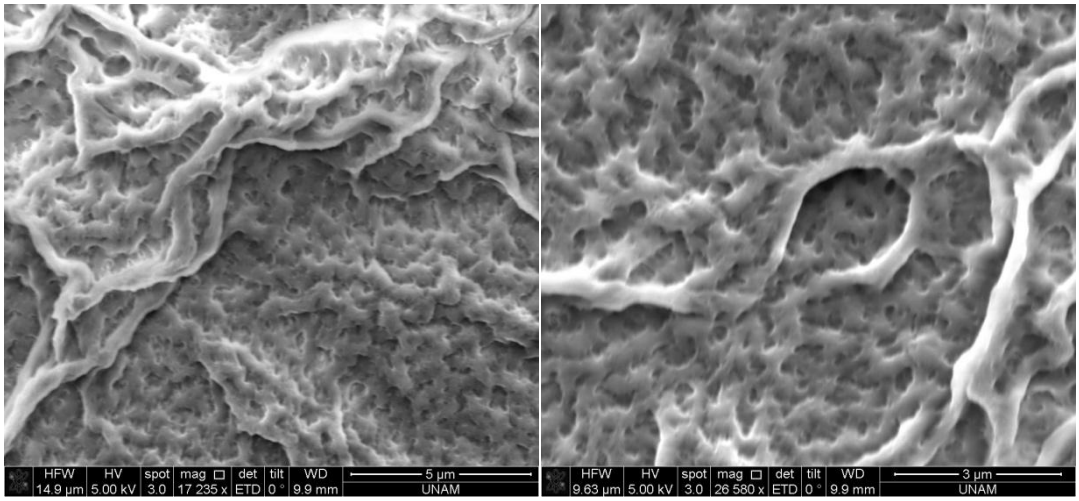

Figure 88. SEM images of peptide Decanoyl-AGDC-COOH

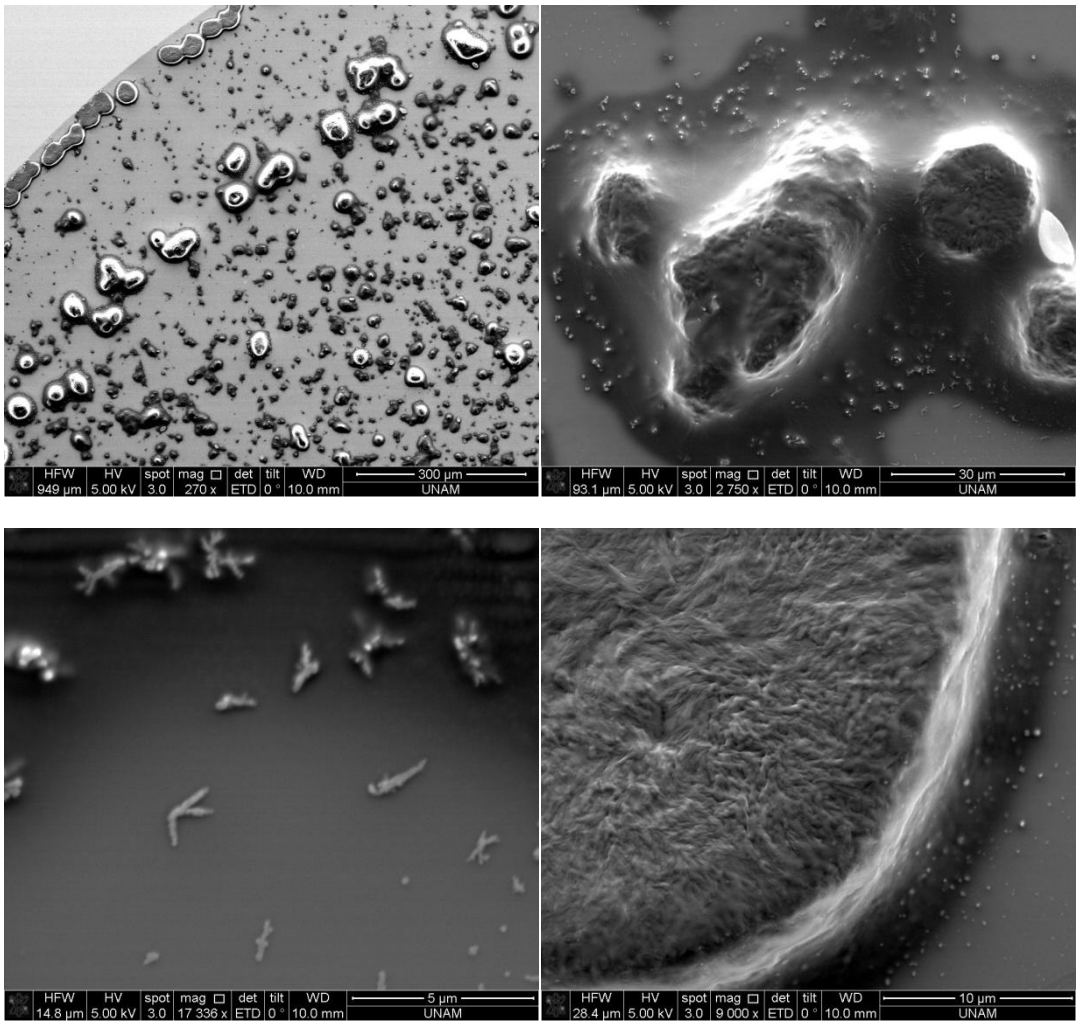

Figure 89. SEM images of peptide Decanoyl-CDAG-COOH

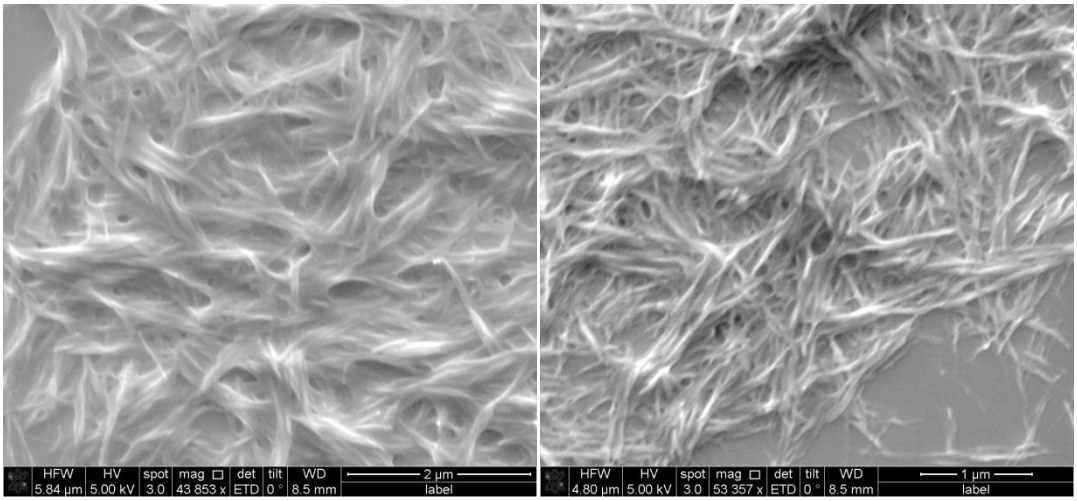

Figure 90. SEM images of peptide Decanoyl-CGDA-COOH

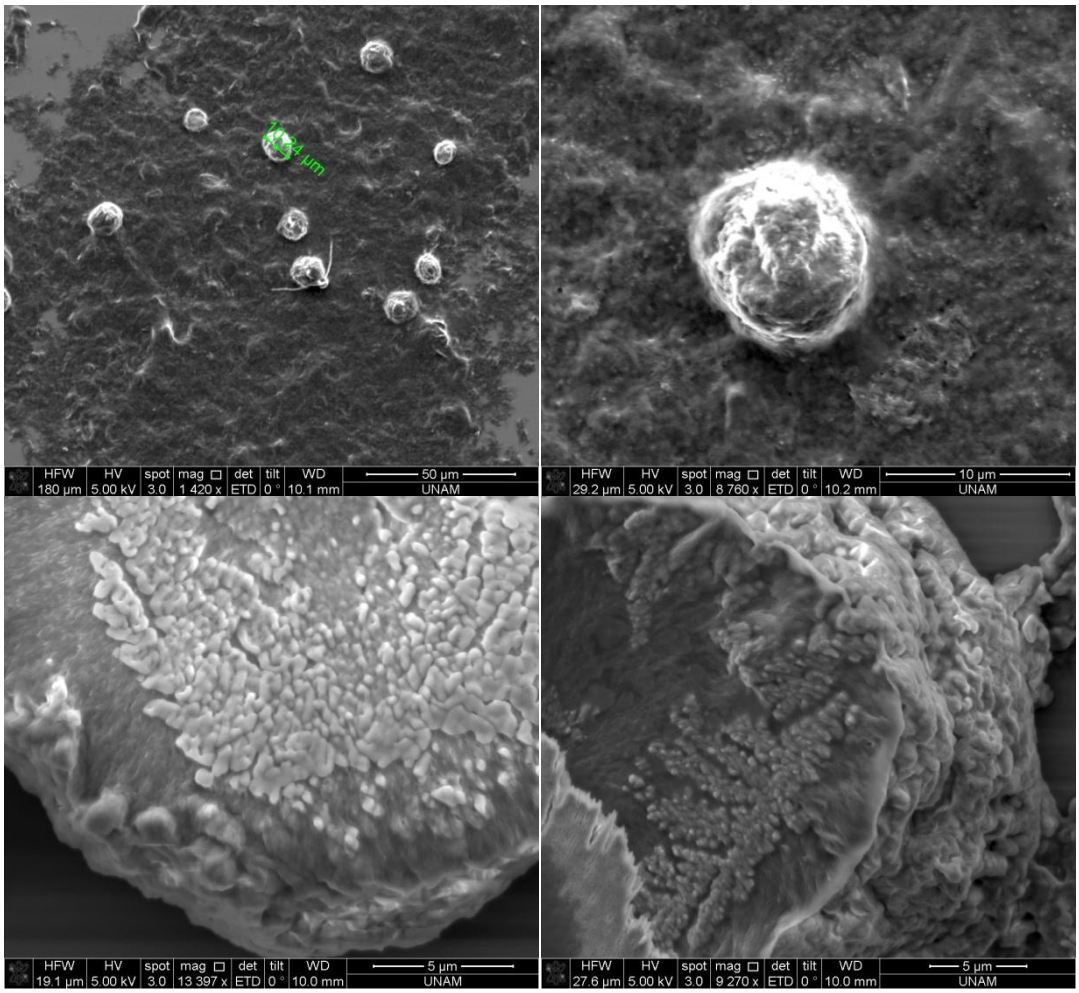

Figure 91. SEM images of peptide Decanoyl-CDGA-COOH

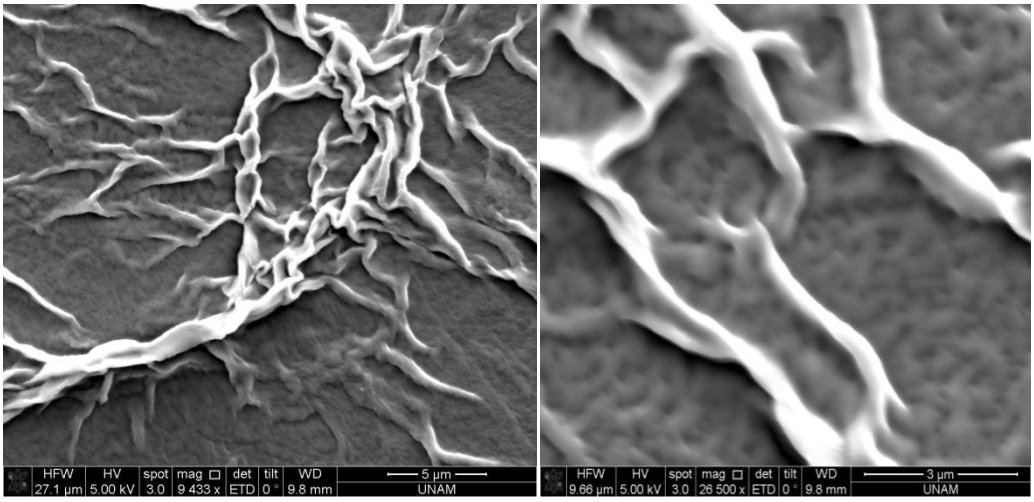

Figure 92. SEM images of peptide Decanoyl-ACDG-COOH.

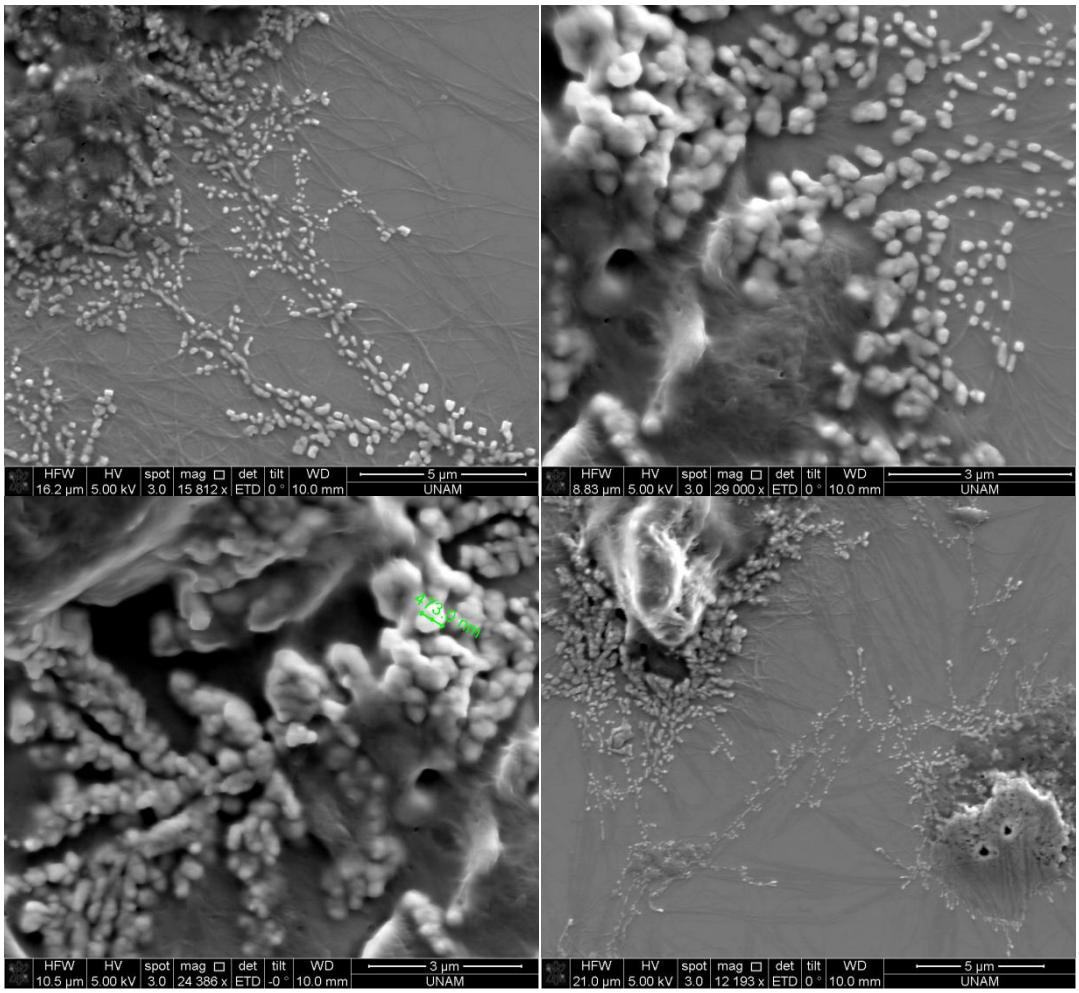

Figure 93. SEM images of peptide Decanoyl-DCGA-COOH

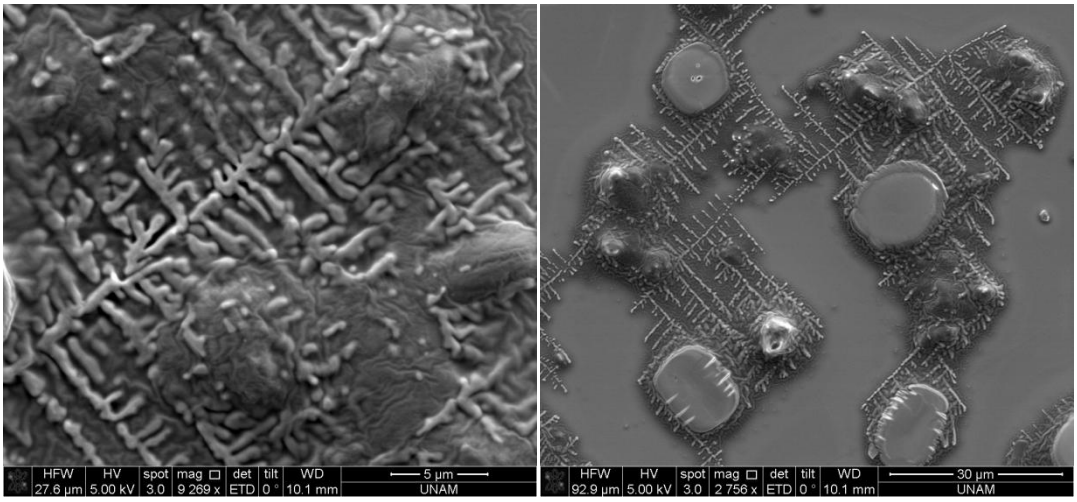

Figure 94. SEM images of peptide Decanoyl-DGCA-COOH

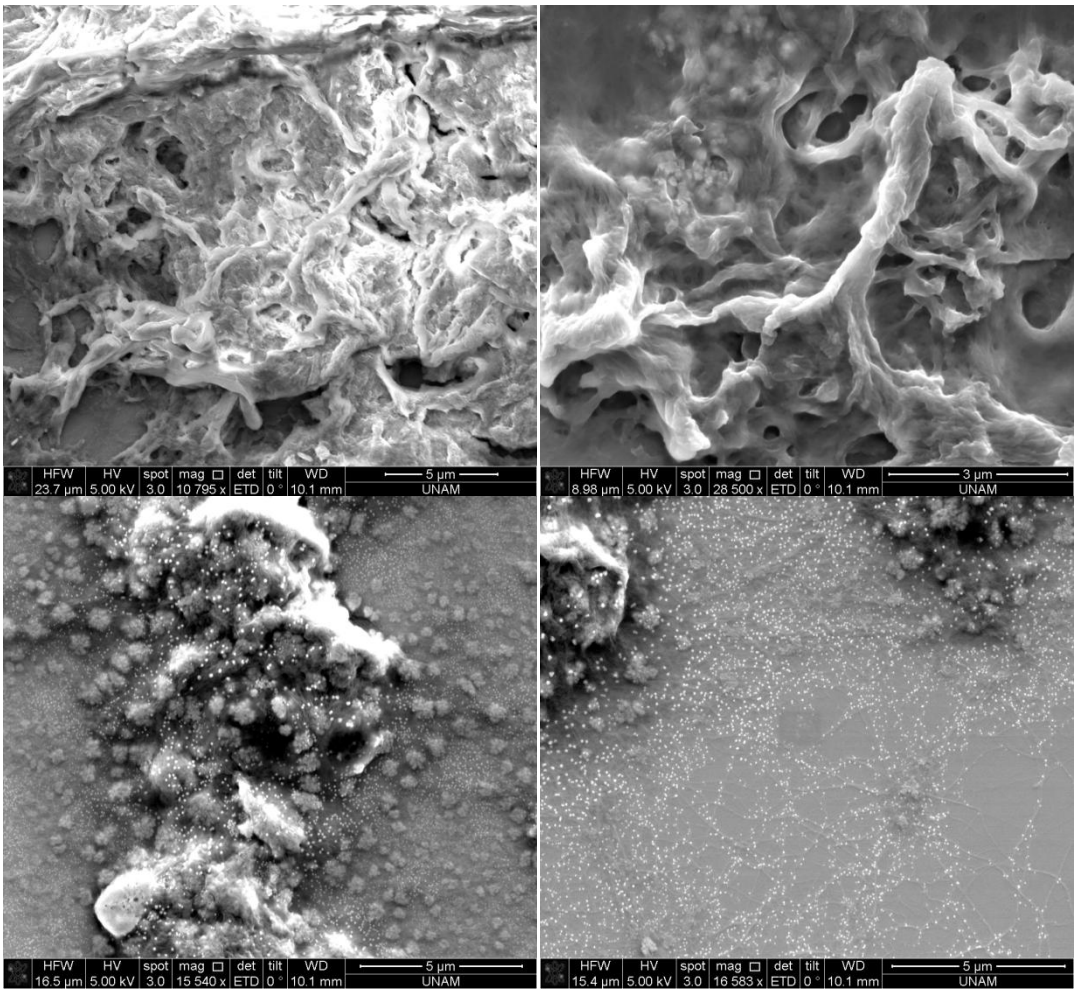

Figure 95. SEM images of peptide Decanoyl-GACD-COOH

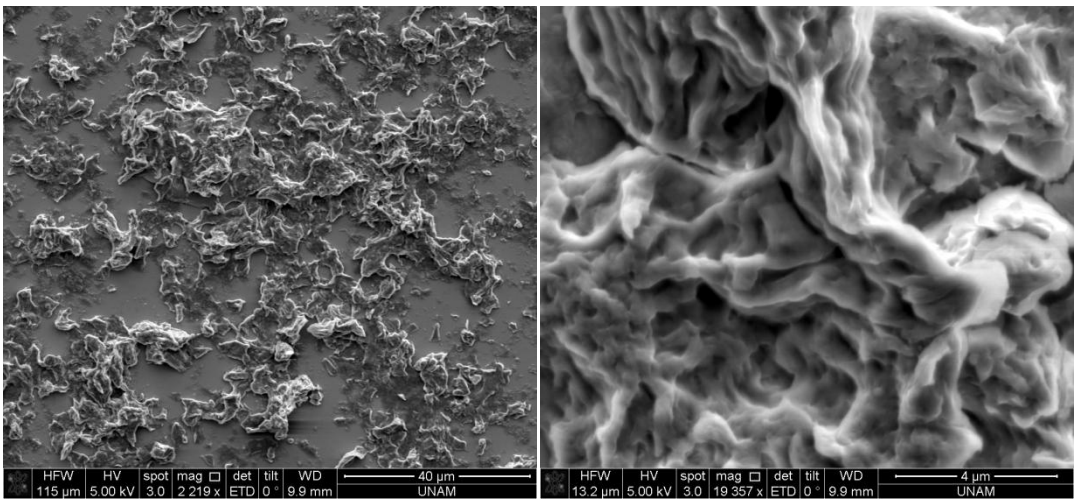

Figure 96. SEM images of peptide Decanoyl-GADC-COOH

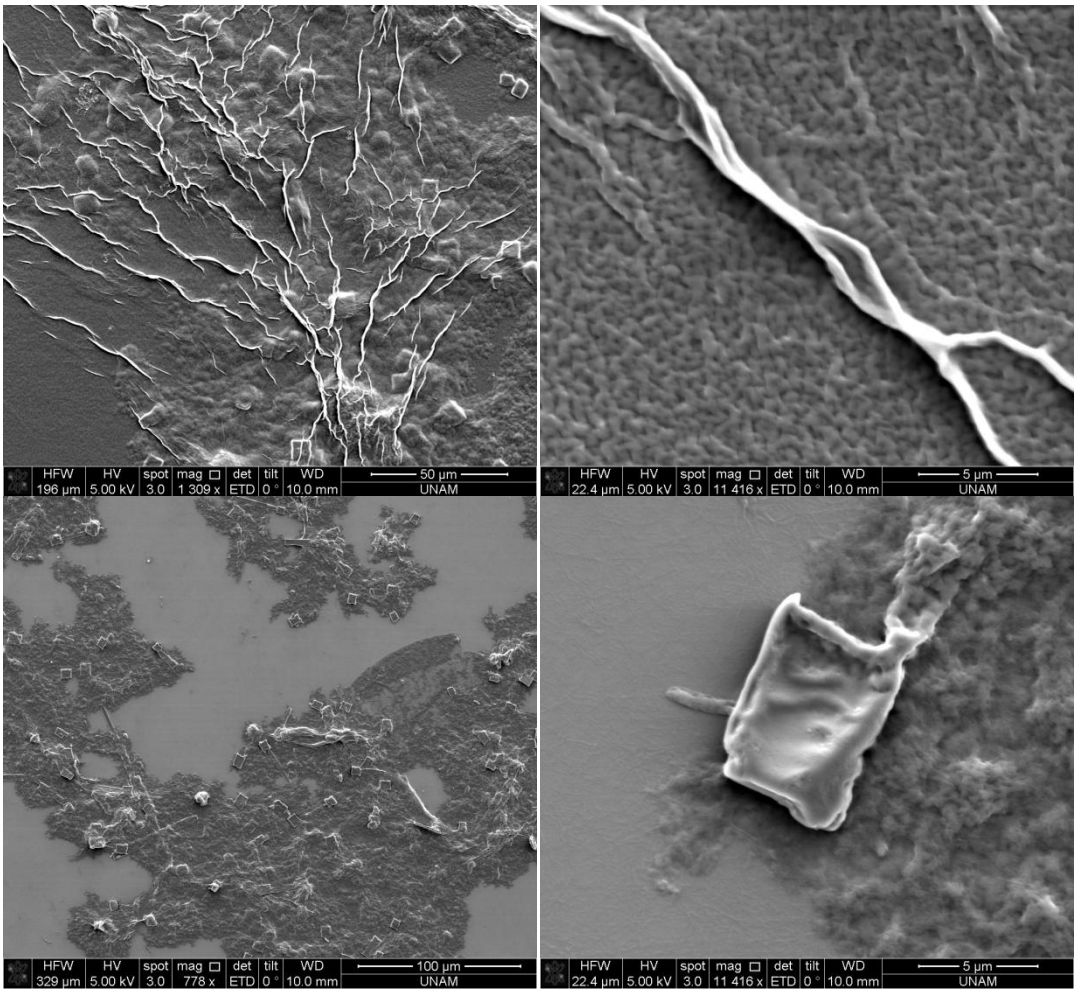

Figure 97. SEM images of peptide Decanoyl-GCDA-COOH

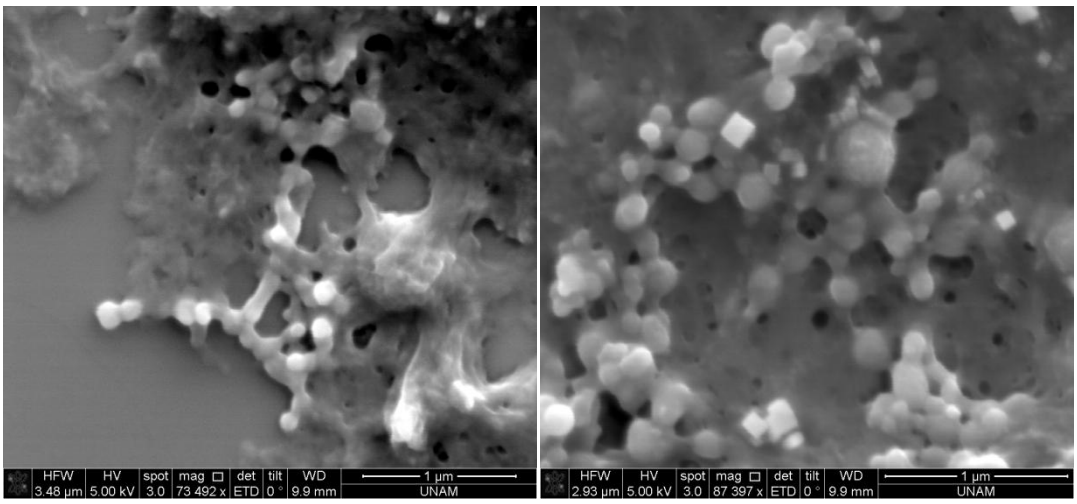

Figure 98. SEM images of peptide Decanoyl-GDCA-COOH

APPENDIX B

Circular Dichroism Spectra

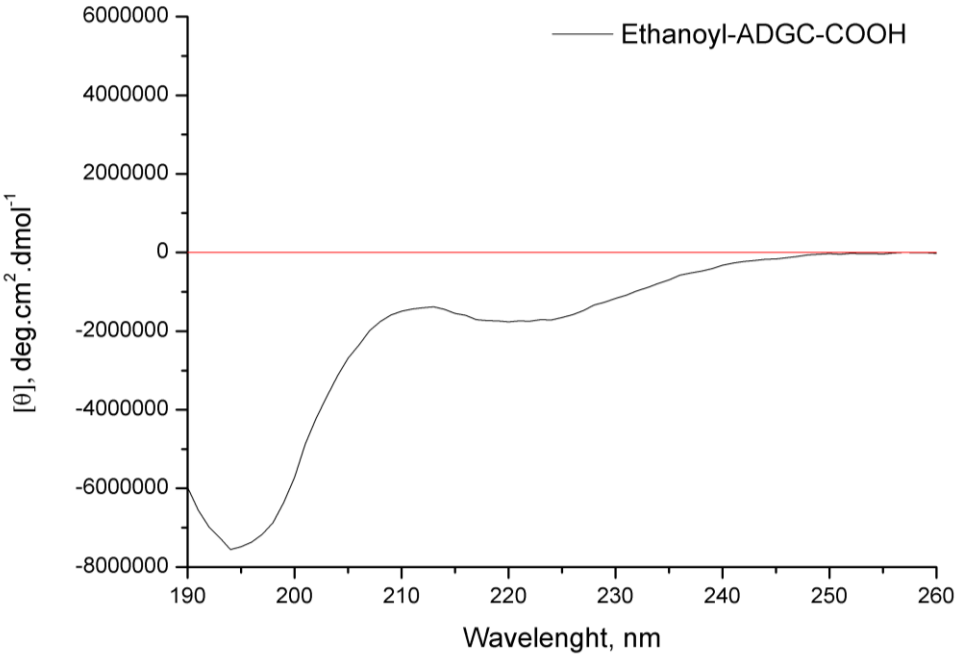

Figure 99. Circular Dichroism spectrum of peptide Ethanoyl-ADGC-COOH

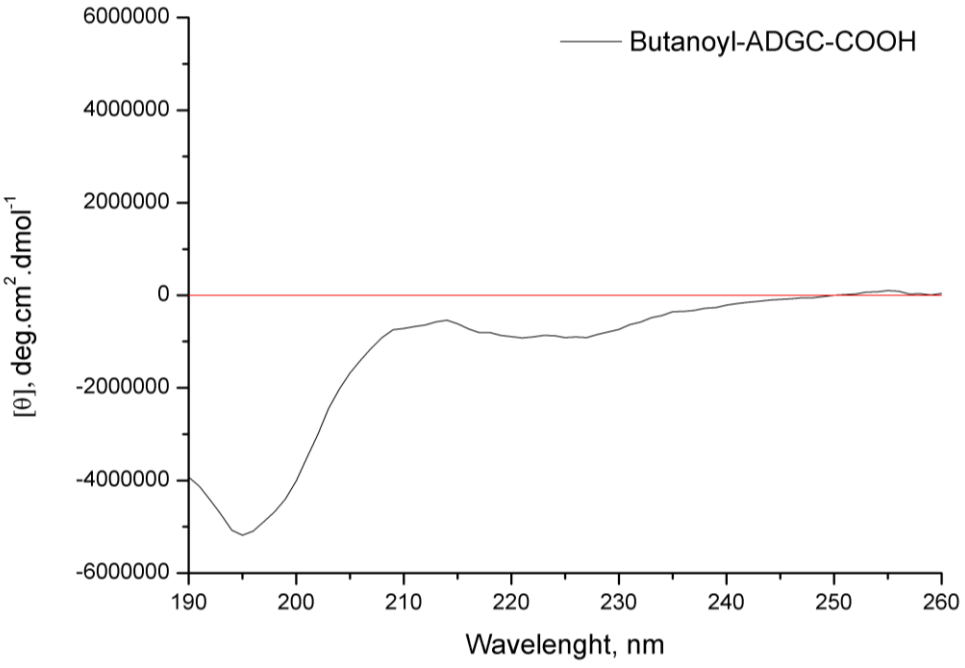

Figure 100. Circular Dichroism spectrum of peptide Butanoyl-ADGC-COOH

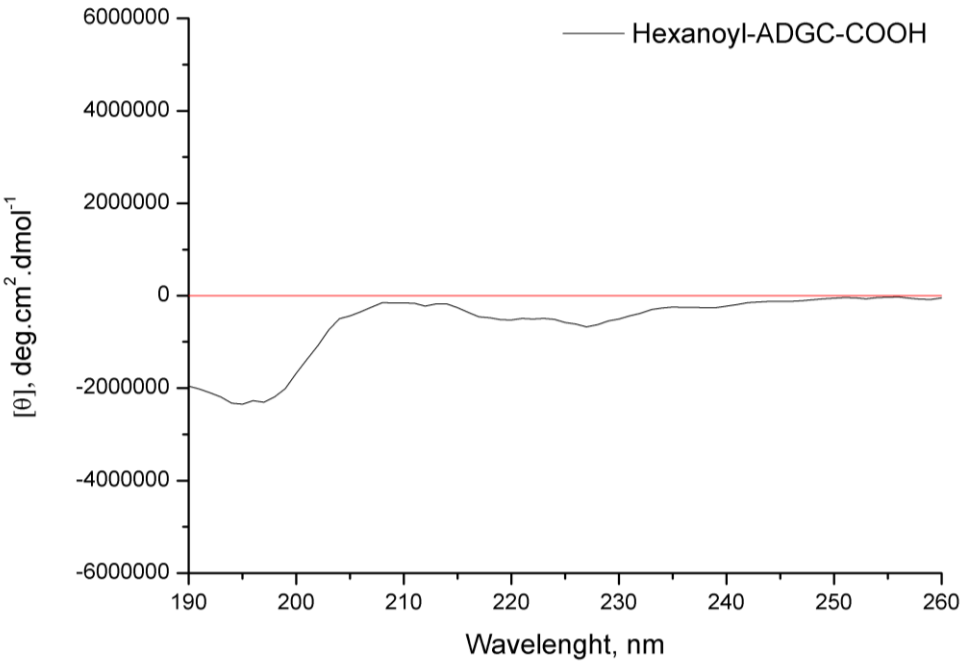

Figure 101. Circular Dichroism spectrum of peptide Hexanoyl-ADGC-COOH

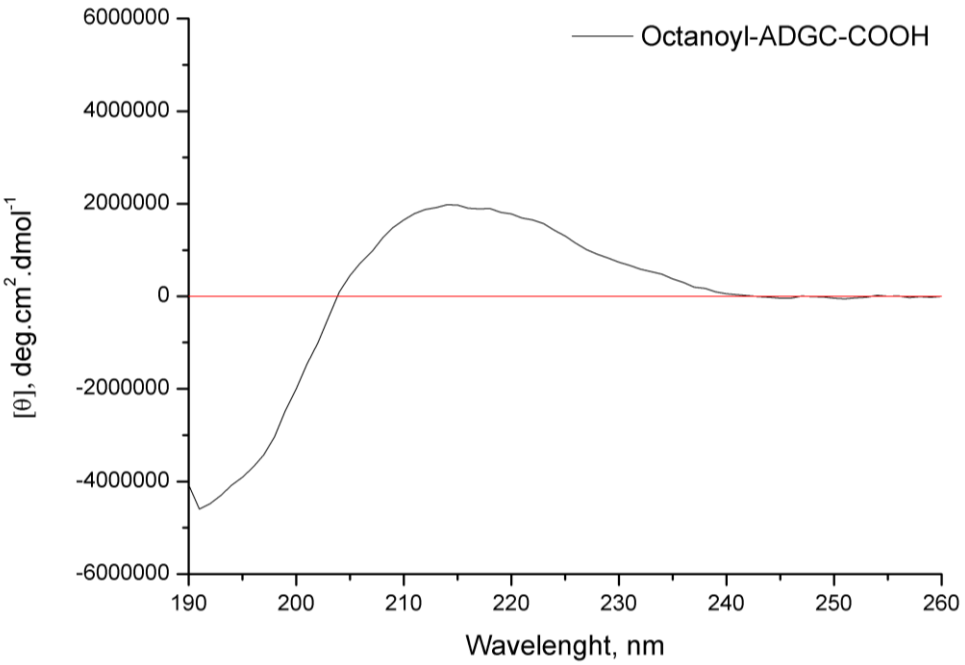

Figure 102. Circular Dichroism spectrum of peptide Octanoyl-ADGC-COOH

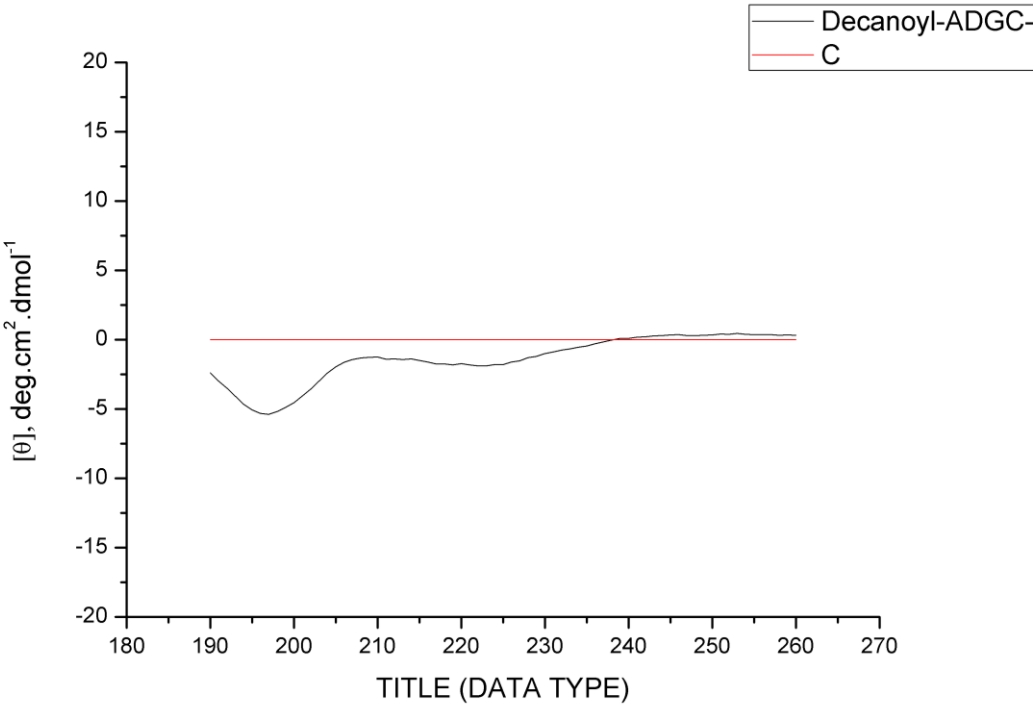

Figure 103. Circular Dichroism spectrum of peptide Decanoyl-ADGC-COOH

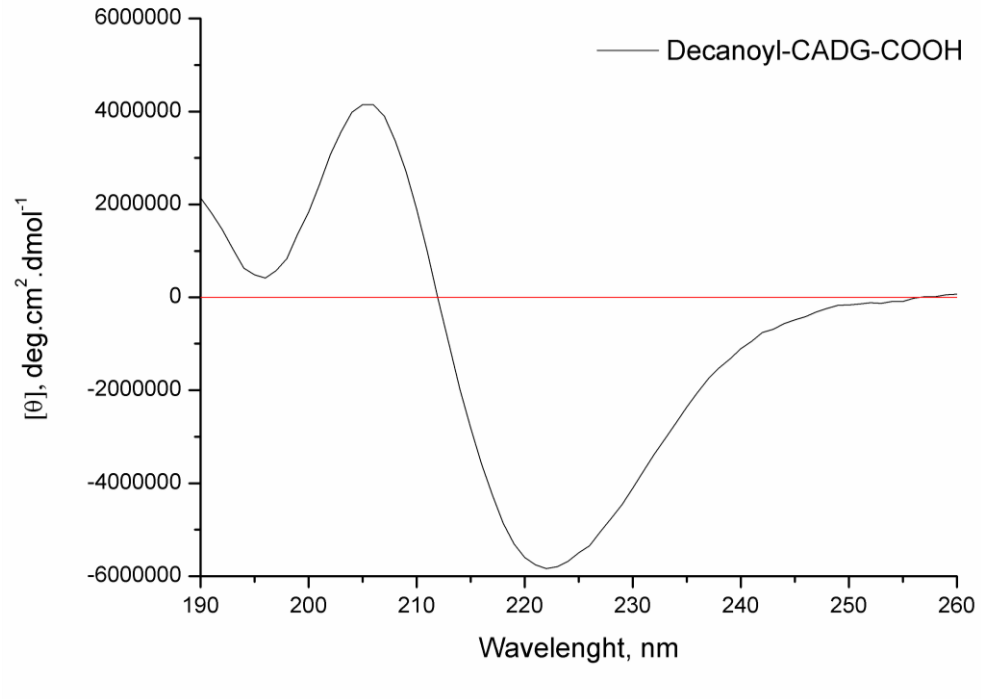

Figure 104. Circular Dichroism spectrum of peptide Decanoyl-CADG-COOH

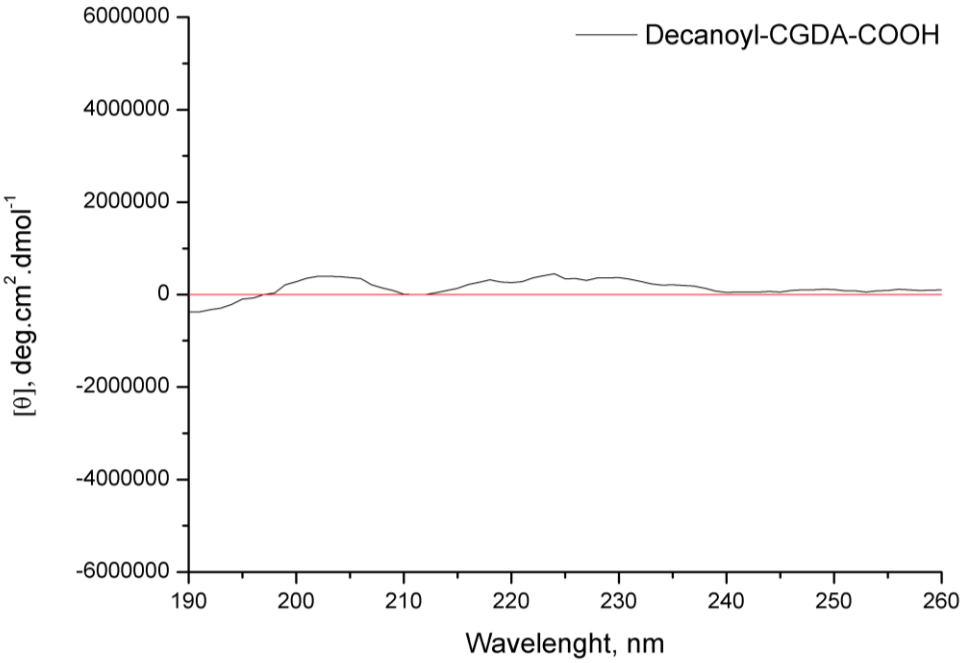

Figure 105. Circular Dichroism spectrum of peptide Decanoyl-CGDA-COOH

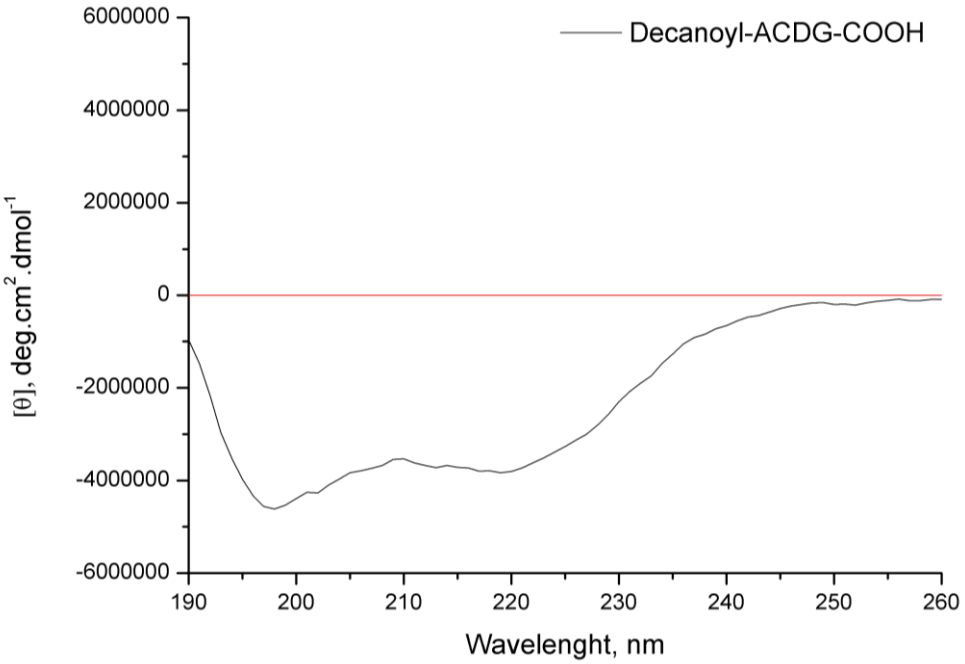

Figure 106. Circular Dichroism spectrum of peptide Decanoyl-ACDG-COOH

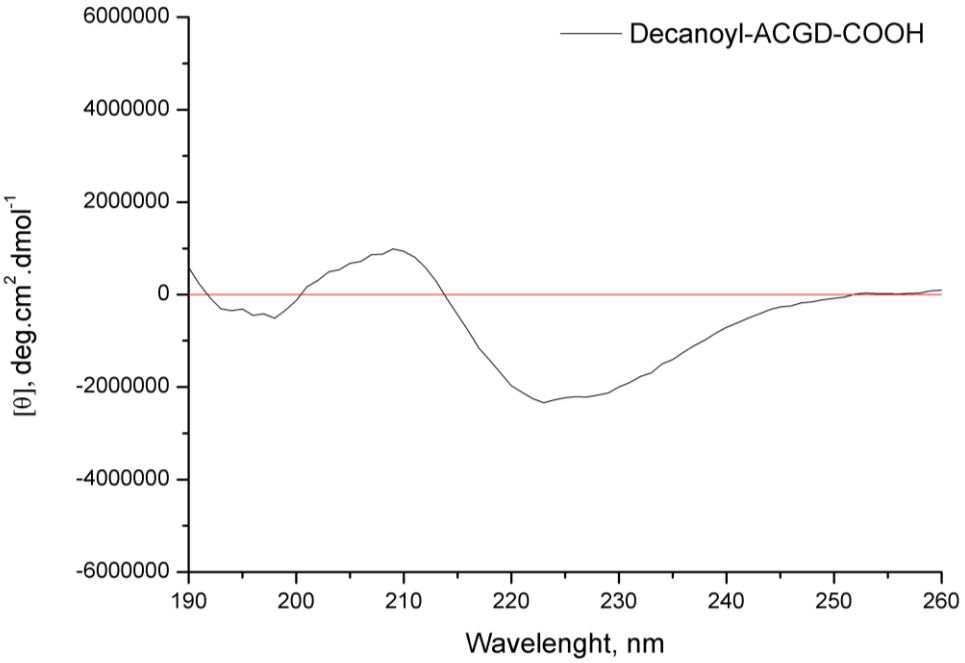

Figure 107. Circular Dichroism spectrum of peptide Decanoyl-ACGD-COOH

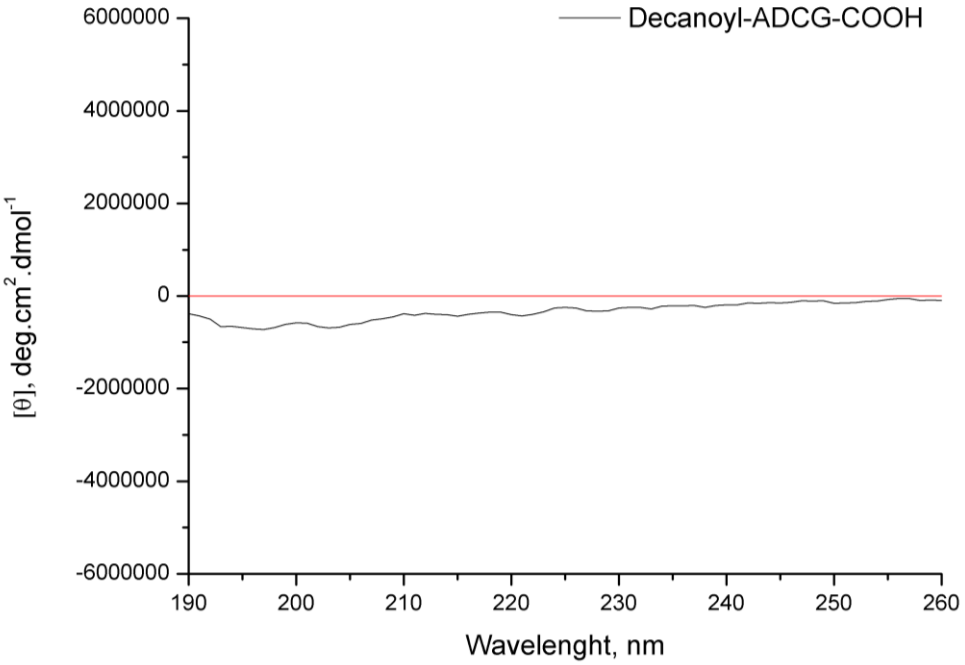

Figure 108. Circular Dichroism spectrum of peptide Decanoyl-ADCG-COOH

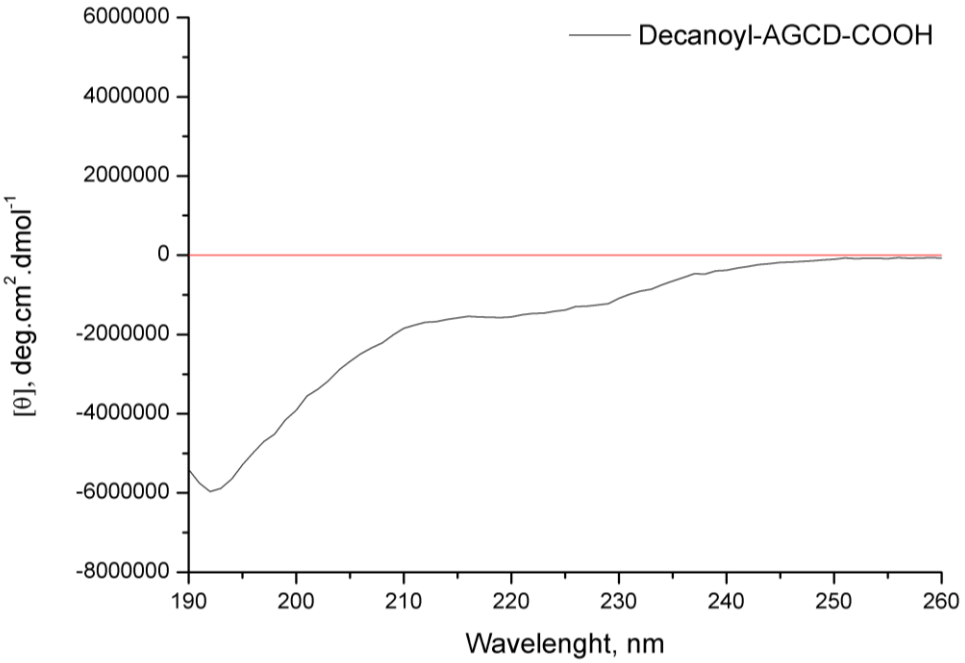

Figure 109. Circular Dichroism spectrum of peptide Decanoyl-AGCD-COOH

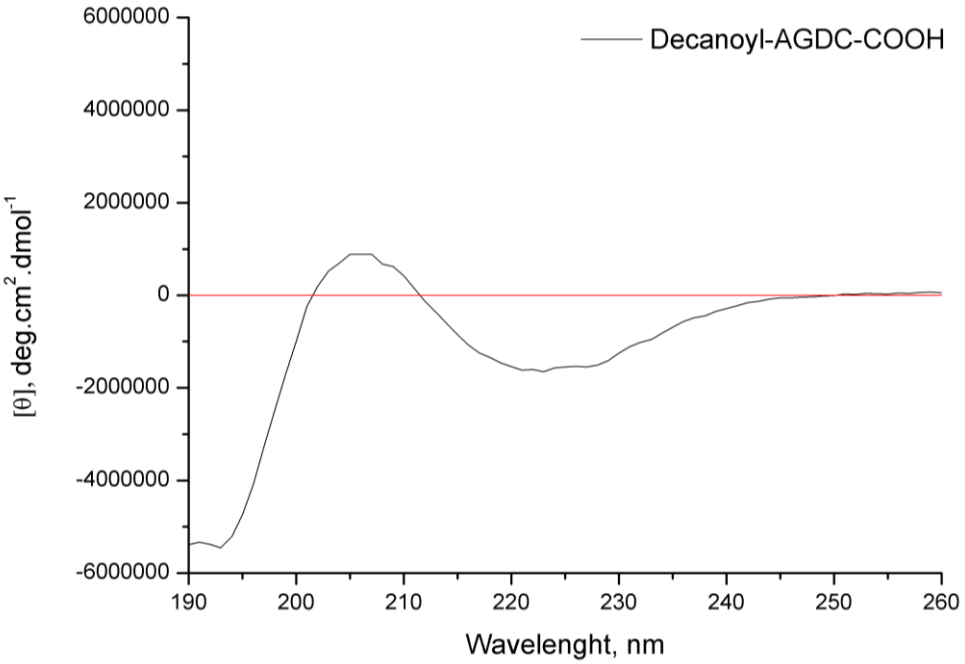

Figure 110. Circular Dichroism spectrum of peptide Decanoyl-AGDC-COOH

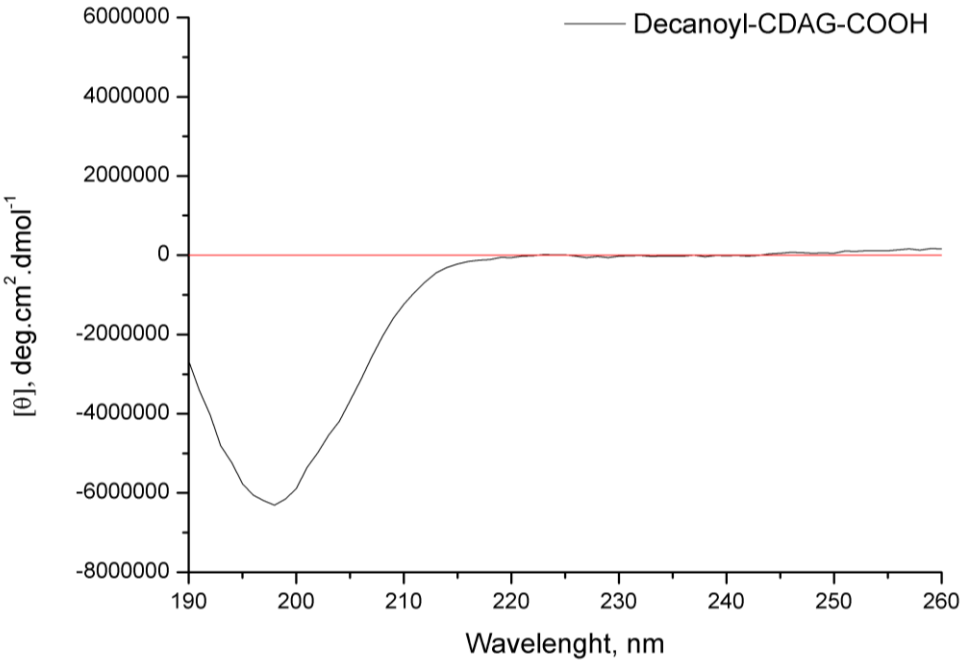

Figure 111. Circular Dichroism spectrum of peptide Decanoyl-CDAG-COOH

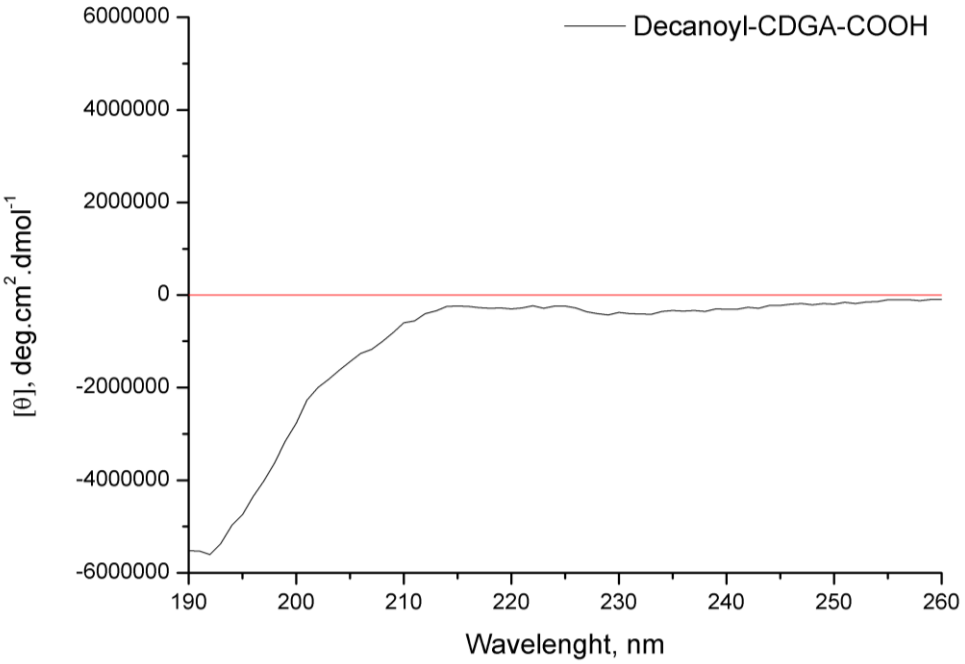

Figure 112. Circular Dichroism spectrum of peptide Decanoyl-CDGA-COOH

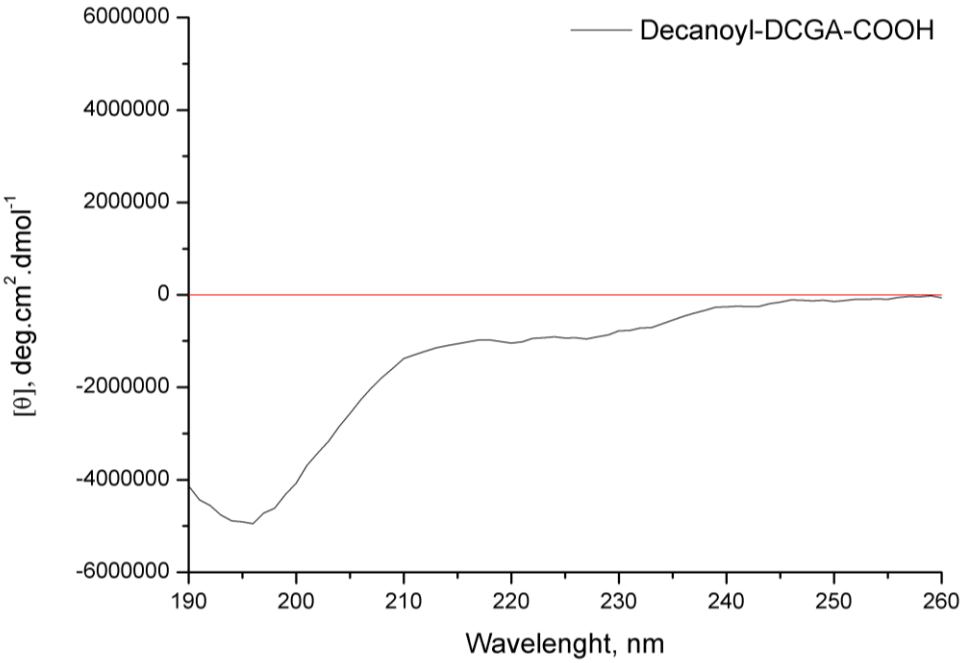

Figure 113. Circular Dichroism spectrum of peptide Decanoyl-DCGA-COOH

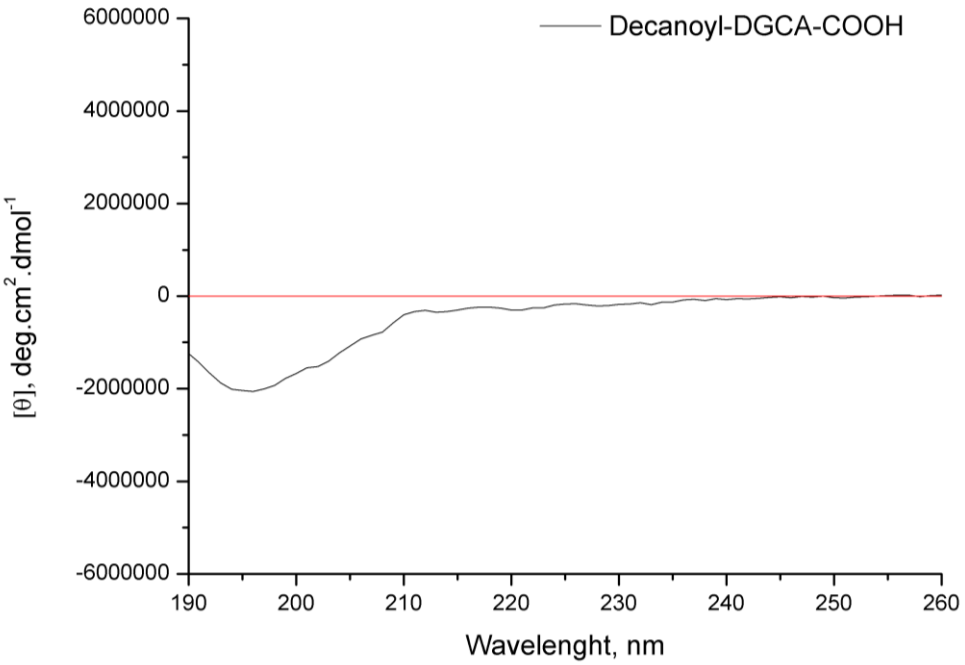

Figure 114. Circular Dichroism spectrum of peptide Decanoyl-DGCA-COOH

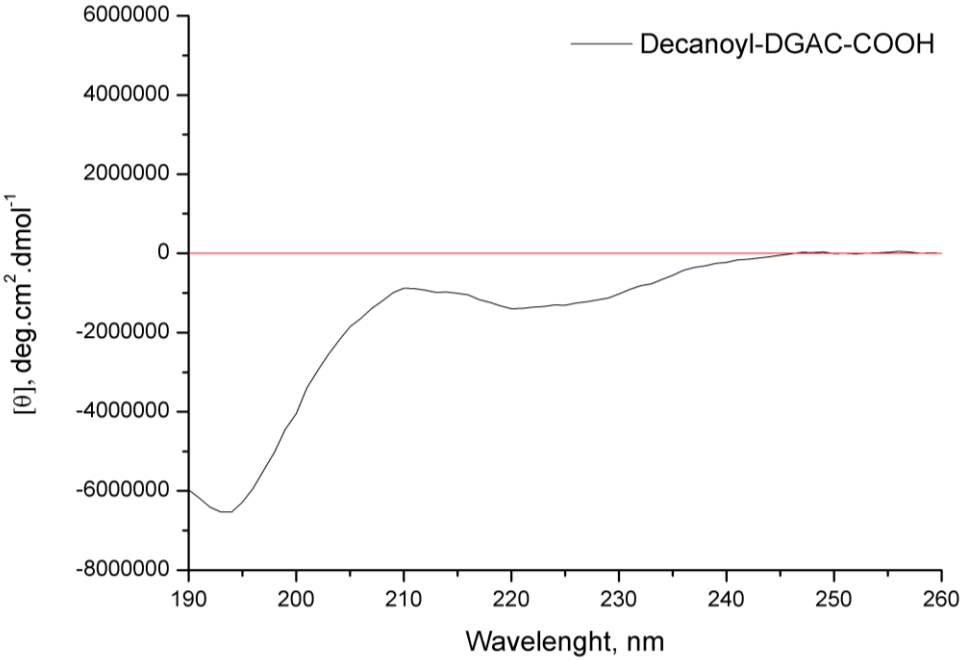

Figure 115. Circular Dichroism spectrum of peptide Decanoyl-DGAC-COOH

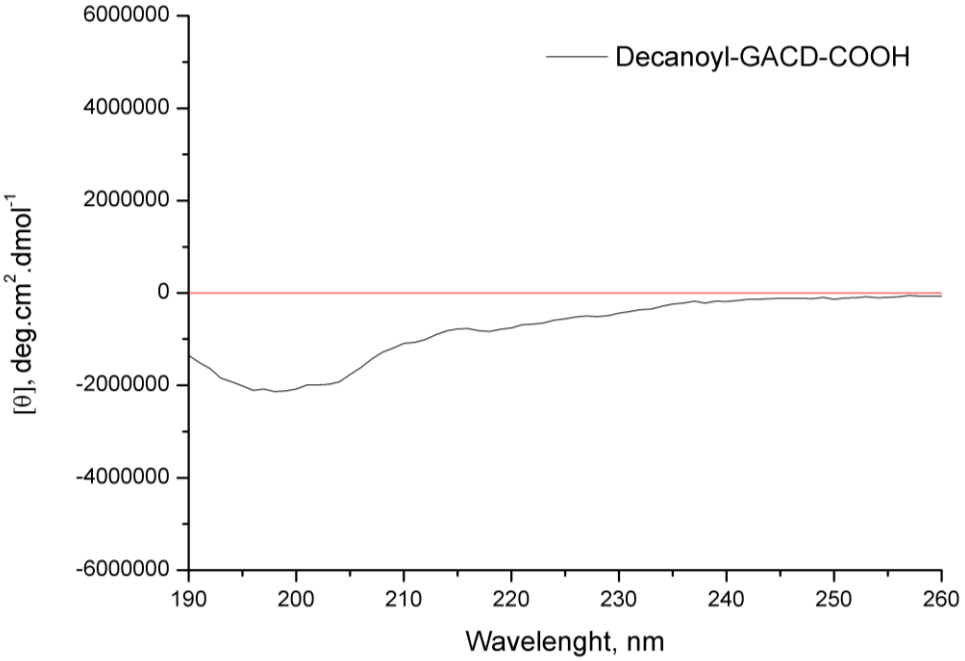

Figure 116. Circular Dichroism spectrum of peptide Decanoyl-GACD-COOH

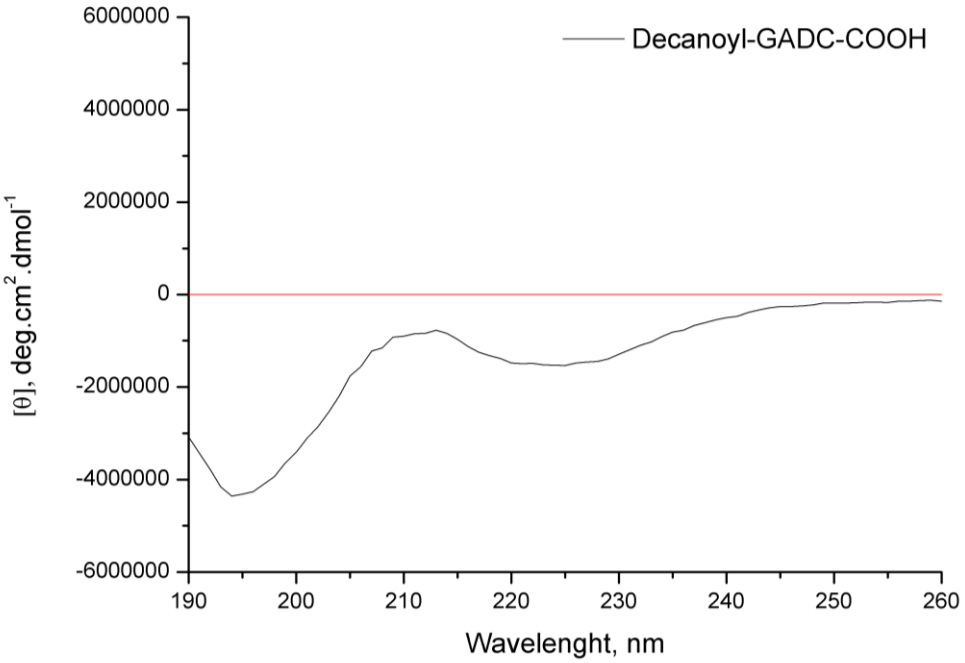

Figure 117. Circular Dichroism spectrum of peptide Decanoyl-GADC-COOH

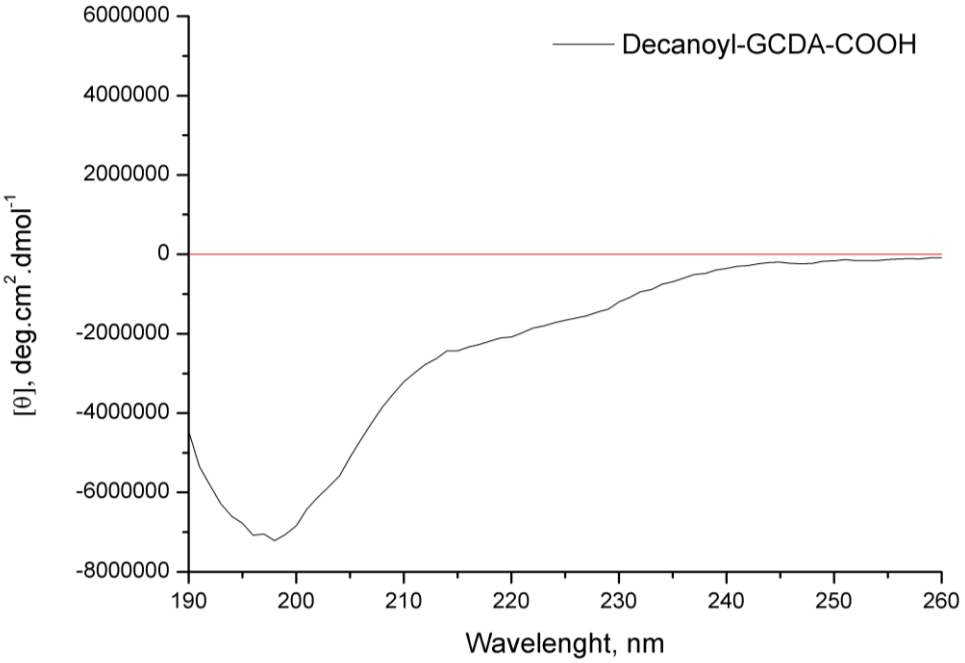

Figure 118. Circular Dichroism spectrum of peptide Decanoyl-GCDA-COOH

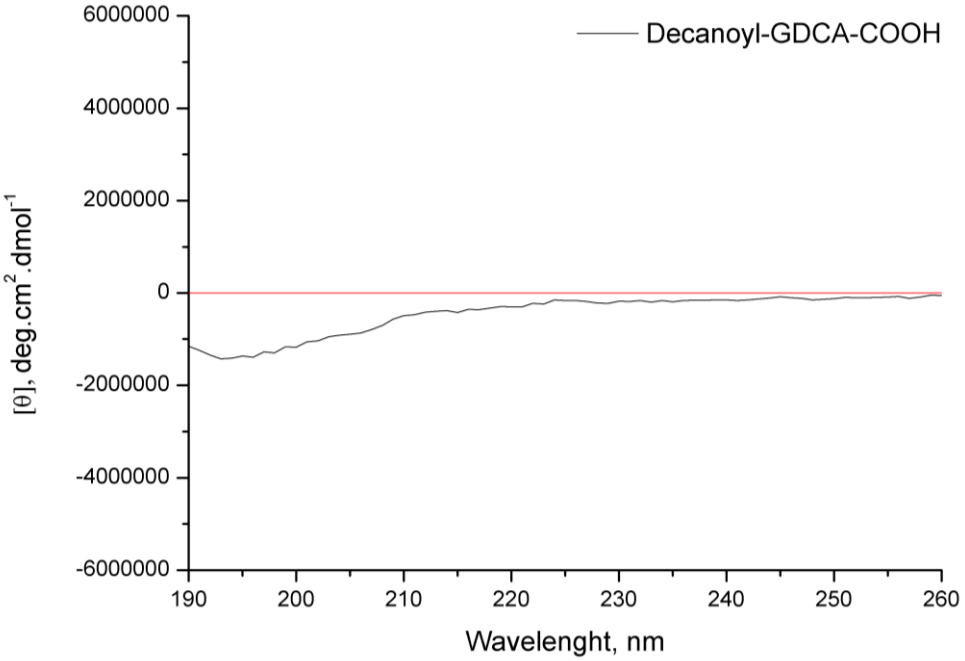

Figure 119. Circular Dichroism spectrum of peptide Decanoyl-GDCA-COOH

APPENDIX C

NMR Spectra

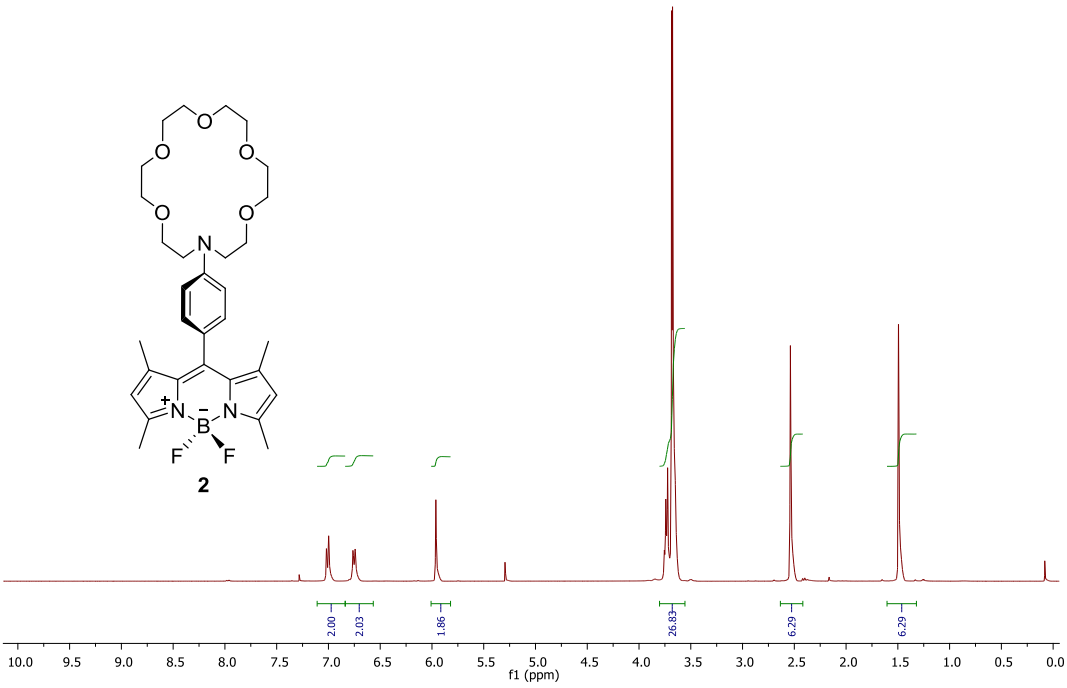

Figure 120. ^{1}H NMR spectrum of Dye 2.

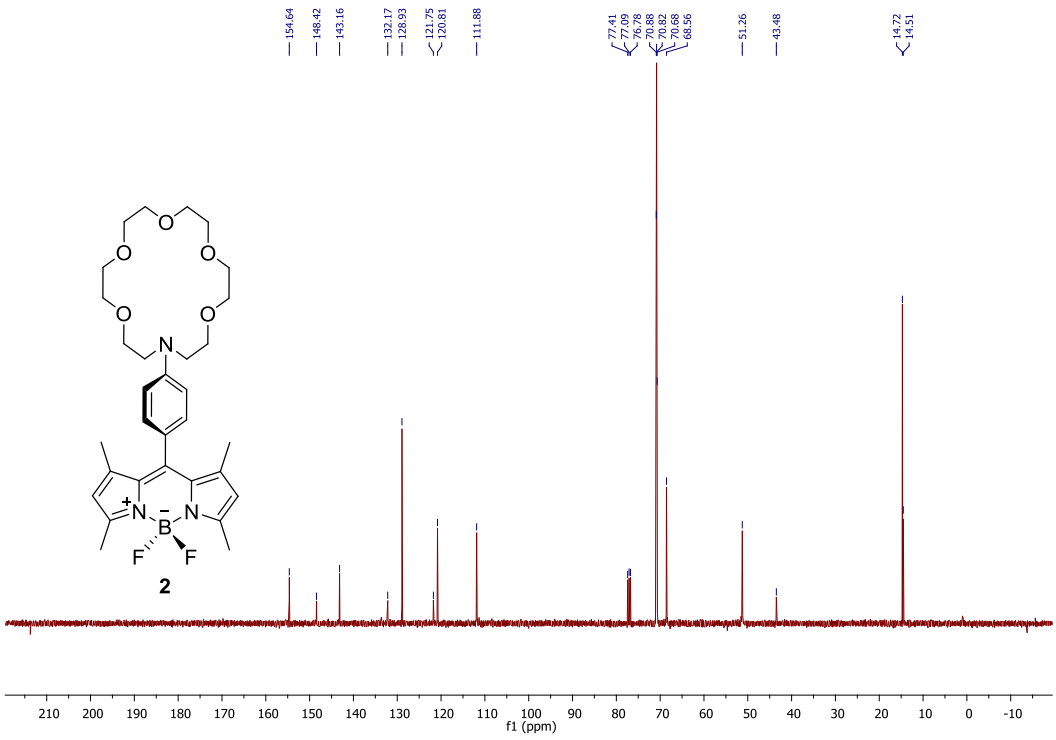

Figure 121. ^{13}C NMR spectrum of Dye 2

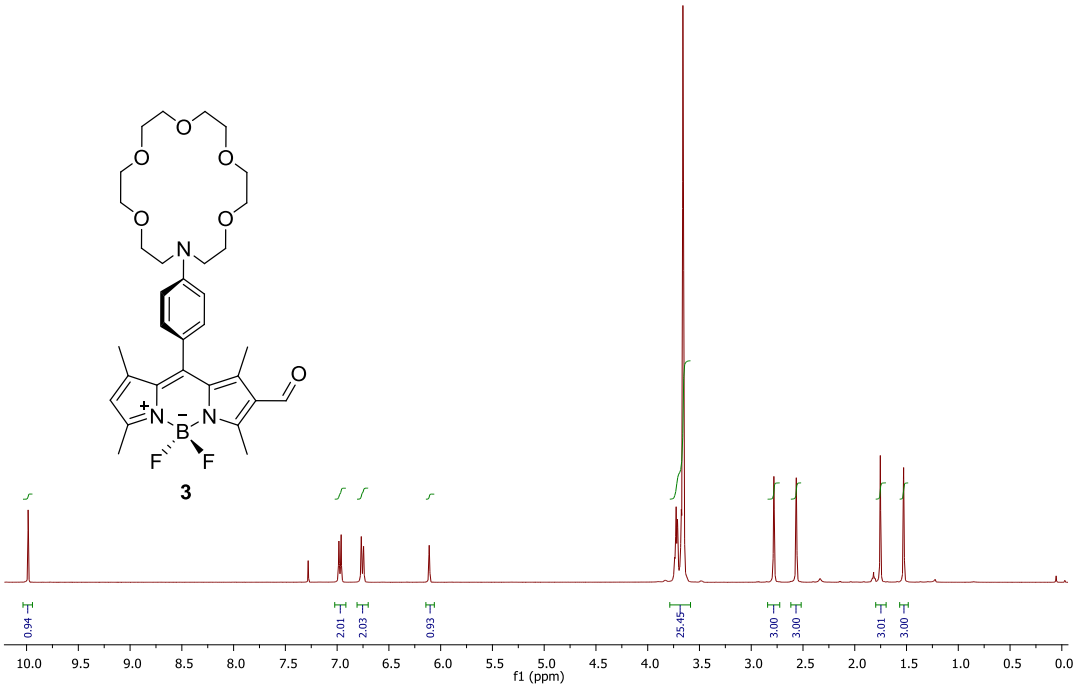

Figure 122. ^{1}H NMR spectrum of compound 3

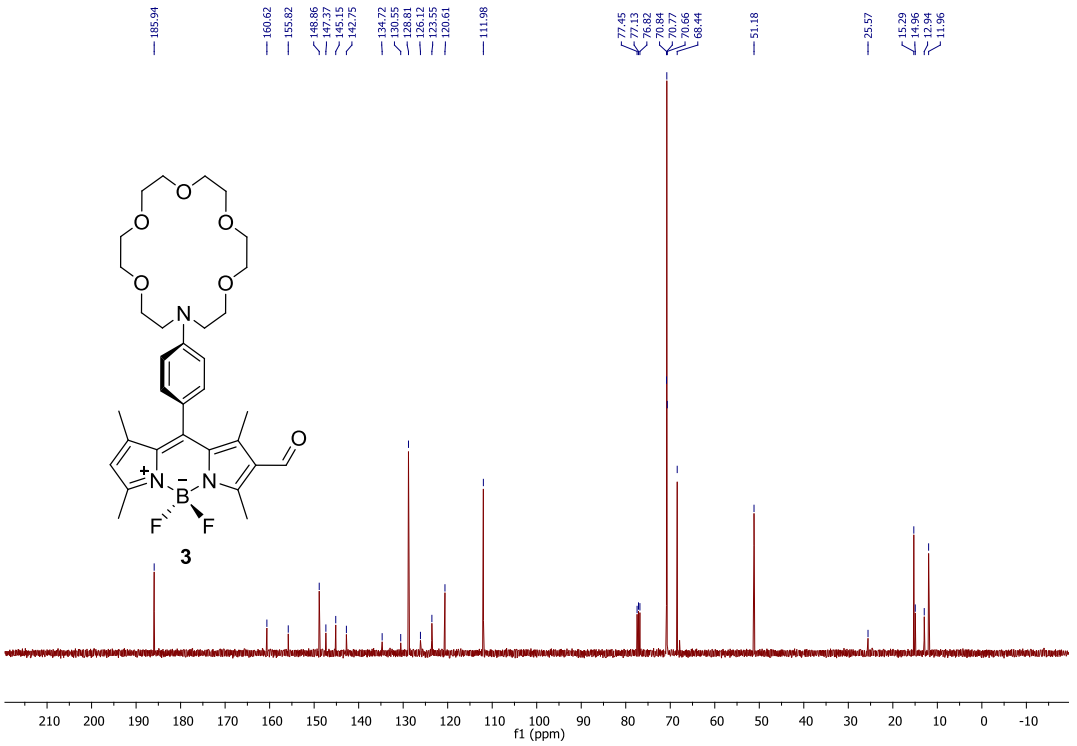

Figure 123. ^{13}C NMR spectrum of compound 3

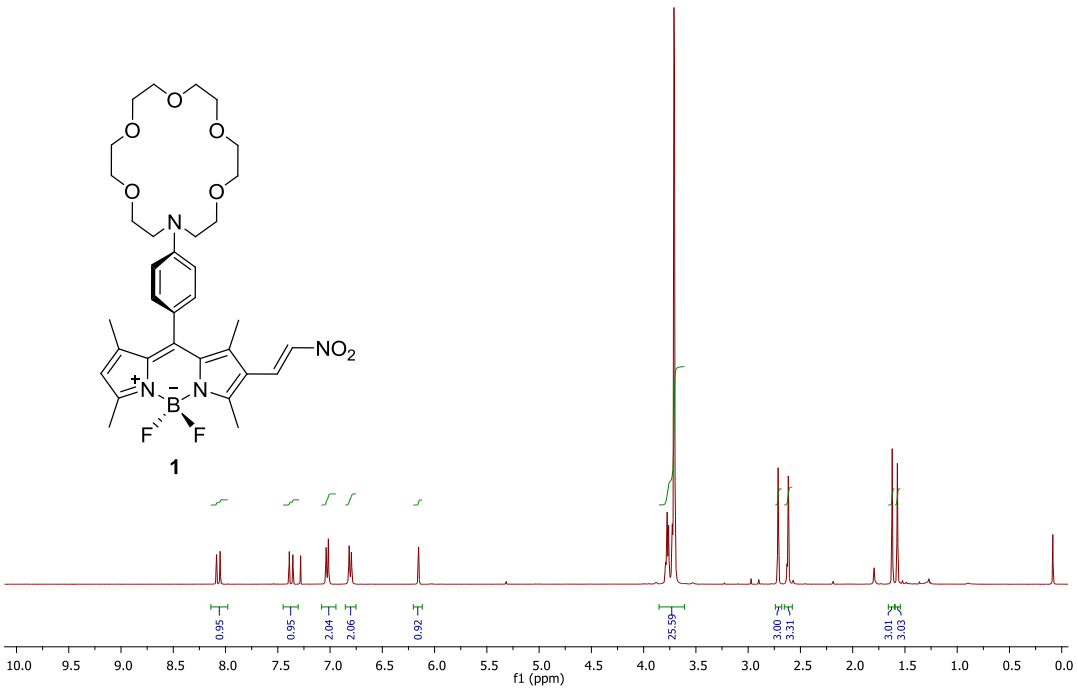

Figure 124. ^{1}H NMR spectrum of Dye 1

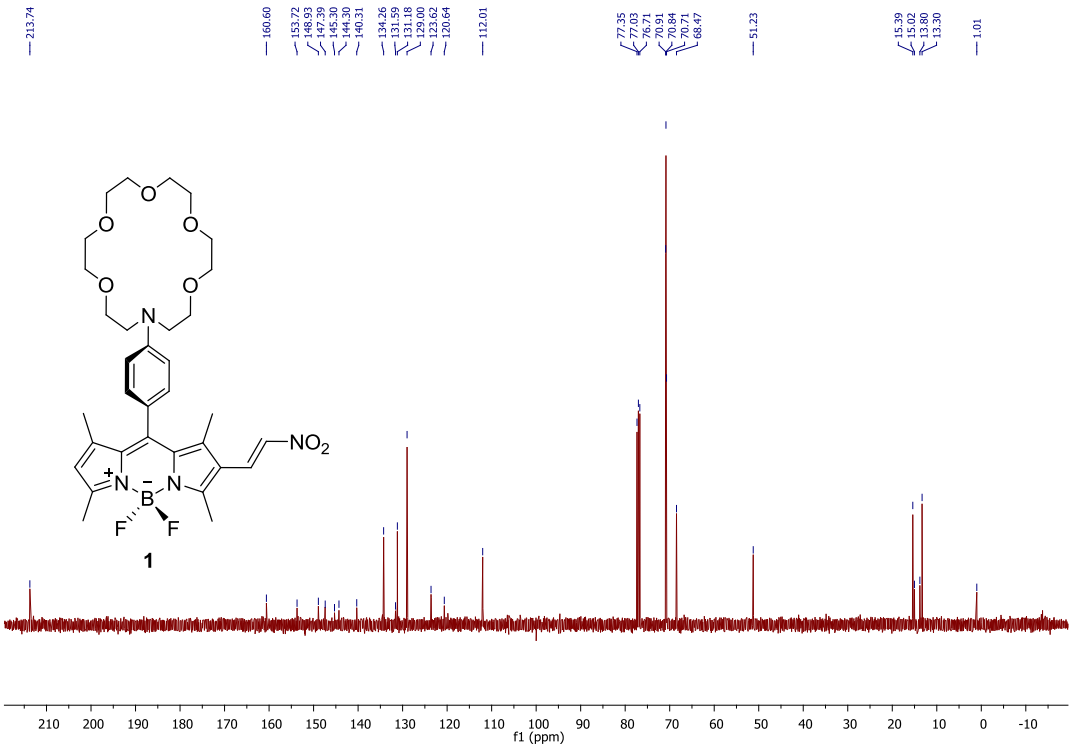

Figure 125. ^{13}C NMR spectrum of Dye 1

APPENDIX D

HRMS Profiles

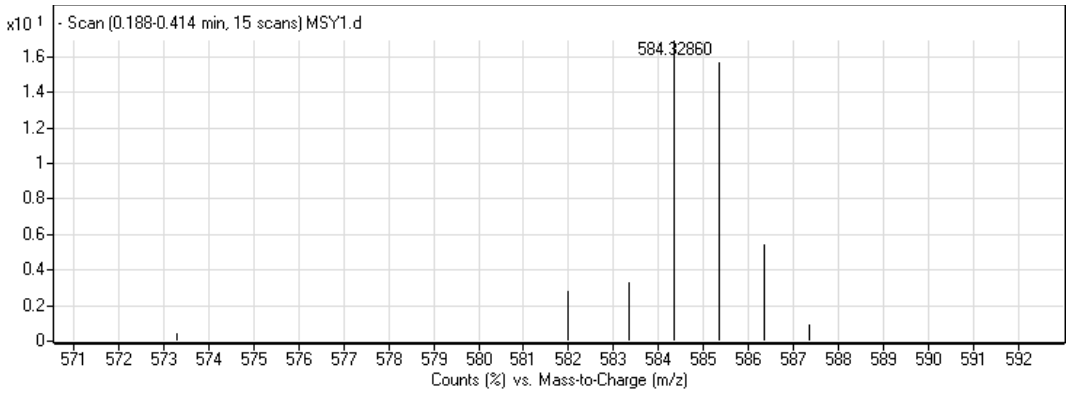

Figure 126. TOF-ESI-MS spectrum of compound 3

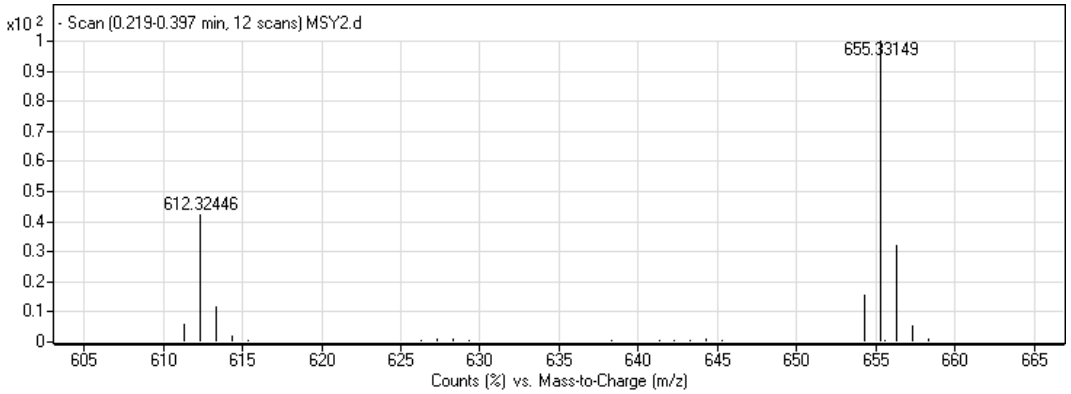

Figure 127. TOF-ESI-MS spectrum of Dye 2

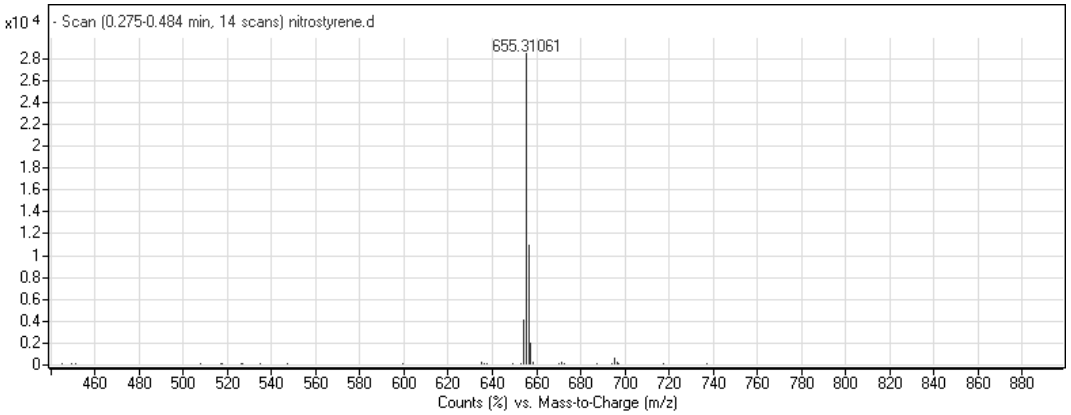

Figure 128. TOF-ESI-MS spectrum of Dye 1

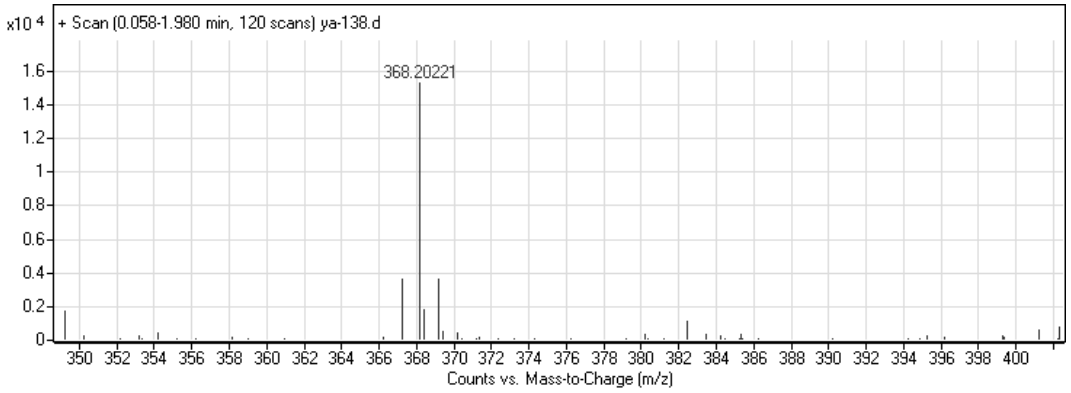

Figure 129. TOF-ESI-MS spectrum of compound 4

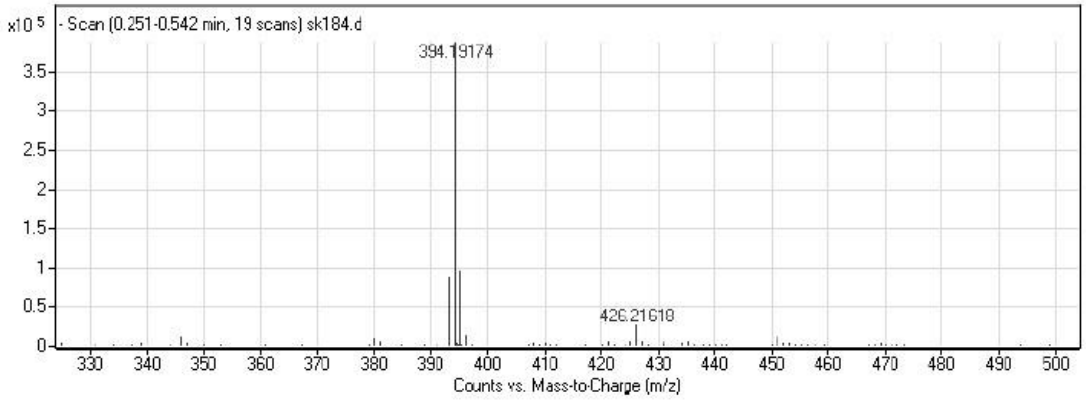

Figure 130. TOF-ESI-MS spectrum of compund 5

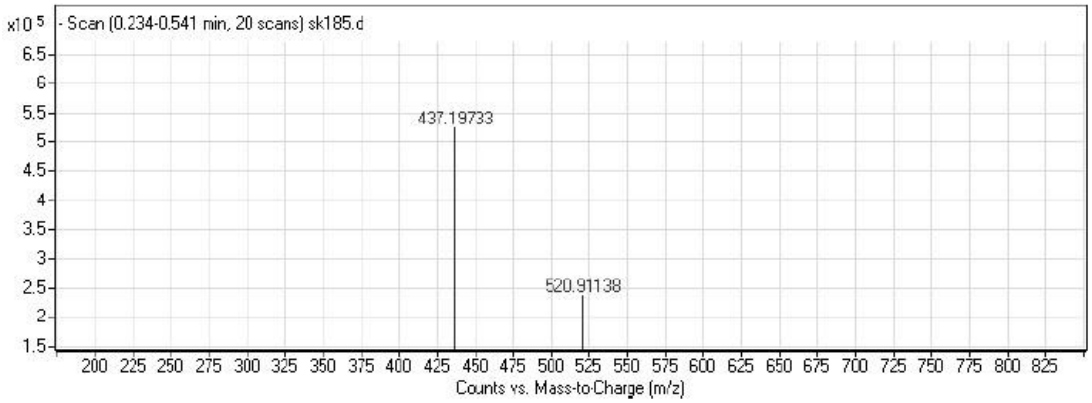

Figure 131. TOF-ESI-MS spectrum of Dye 3

APPENDIX E

Definitions and Characterizations of Life

1855

L. Buchner: "Spontaneous generation exists, and higher forms have gradually and slowly become developed from previously existing lower forms, always determined by the state of the earth, but without immediate influence of a higher power."

1855

R. Virchow: "Life will always remain something apart, even if we should find out that it is mechanically aroused and propagated down to the minutest detail."

1866

E. Haeckel: "Any detailed hypothesis whatever concerning the origin of life must, as yet, be considered worthless, because, up till now, we have not satisfactory information concerning the extremely peculiar conditions which prevailed on the surface of the earth at the time when the first organisms developed."

1868

T.H. Huxley: " The vital forces are molecular forces."

1868

J. von Liebig: " We may only assume that life is just as old and just as eternal as matter itself… Why should not organic life be thought of as present from the very beginning just as much as carbon and its compounds, or as the whole of uncreatable and indestructible matter in general."

1869

J. Browning: "There is no boundary line between organic and inorganic substances… Reasoning and analogy, I believe that we shall before long find it an equally difficult task to draw a distinction between the lowest forms of living matter and dead matter."

1871

L. S. Beale: "Life is a power, force, or property of a special and peculiar kind, temporarily influencing matter and its ordinary force, but entirely different form, and in no way correlated with, any of these."

1872

H. C. Bastian: "Living things are peculiar aggregates of ordinary matter and of ordinary force which in their separate states do not posses the aggregates of qualities known as life."

1878

C. Bernard: "Life is neither a principle nor a resultant. It is not a principle because this principle, in some way dormant or expectant, would be incapable of acting by itself. Life is not a resultant either, because the physicochemical conditions that govern its manifestation can not give it any direction or any definite form… None of these two factors, neither the directing principle of the phenomena nor the ensemble of the material conditions for its manifestation, can alone explain life. Their union is necessary. In consequence, life is to us a conflict.

1878

C. Bernard: "If I had to define life in a single phrase... I should say: Life is creation."

1880

F. Engels: "No physiology is held to be scientific if it does not consider death an essential factor of life... Life means dying."

1884

H. Spencer: "The broadest and most complete definition of life will be 'the continuous adjustment of internal relations to external relations.'"

1897

W. Pfeffer: "Even the best chemical knowledge of the bodies occurring in the protoplasm no more suffices for the explanation and understanding of the vital

processes, than the most complete chemical knowledge of coal and iron suffices for the understanding of a steam engine."

1908

A. B. Macallum: " When we seek to explain the origin of life, we do not require to postulate a highly complex organism... as being the primal parent of all, but rather one which consist of a few molecules only and of such a size that it is beyond the limit of vision with the highest powers of the microscope."

1923

A. Putter: "It is the particular manner of composition of the materials and processes, their spatial and temporal organization which constitute what we call life."

1924

A. I. Oparin (quoted in Bernal, 1967): "Life may be recognized only in bodies which have particular special characteristics. These characteristics are peculiar to living things and are not seen in the world of the dead. What are these characteristics? In the first place there is a definite structure or organization. Then there is the ability of the organism to metabolize, to reproduce other like themselves and also their response to stimulation."

1929

J. H. Woodger: "It does not seem necessary to stop at the word 'life' because this term can be eliminated from scientific vocabulary since it is an indefinable abstraction and we can get along perfectly well with 'living organisms' which is an entity which can be speculatively demonstrated."

1933

L. Bertalanffy: "A living organism is a system organized in hierarchical order ... of a great number of different parts, in which a great number of processes are so disposed that by means of their mutual relations within wide limits with constant change of the materials and energies constituting the system and also in spite of disturbances conditioned by external influences, the system is generated or remains

in the state characteristic of it, or these processes lead to the production of similar systems."

1933

N. Bohr: "The existence of life must be considered as an elementary fact that cannot be explained, but must be taken as a starting point in biology, in a similar way as the quantum of action, which appears as an irrational element from the point of view of classical mechanical physics, taken together with the existence of elementary particles, forms the foundation of atomic physics."

1944

E. Schrödinger: "Life seems to be orderly and lawful behavior of matter, not based exclusively on its tendency to go over from order to disorder, but based partly on existing order that is kept up."

1948

J. Alexander: "The essential criteria of life are twofold: (1) tha ability to direct chemical change by catalysis; (2) the ability to reproduce by autocatalysis. The ability to undergo heritable catalysis changes is general, and is essential where there is competition between different types of living things, as has been the case in the evolution of plants and animals."

1952

J. Perrett: "Life is potentially self-perpetuating open system of linked organic reactions, catalyzed stepwise and almost isothermally by complex and specific organic catalysts which are themselves produced by the system."

1956

R. D. Hotchkiss: "Life is repetitive production of ordered heterogeneity."

1959

N. H. Horowitz: "I suggest that these three properties -mutability, self-duplication and heterocatalysis- comprise a necessary and sufficient definition of living matter."

1965

J. D. Bernal: "All biochemical and biophysical studies lead straight back to the general question of origins. Origin. structure, and function can no longer be seperated."

1967

J. D. Bernal: "Life is a partial, continuous, progressive, multiform and conditionally interactive, self-realization of the potentialities of atomic electron state."

1972

L. Gatlin: "Structural hierarchy of functioning, units that has acquired through evolution the ability to store and process the information necessary for its own reproduction."

1973

P. Fong: "Life is made of three basic elements: matter, energy and information... Any element in life that is not matter and energy can be reduced to information."

1973

J. P. Yockey: "Life... seems to flout the second law of thermodynamics. Biological organisms seem to be something more than chemical systems yet at the same time measurements on these systems reveal that natural laws are obeyed. The fact that information is at the same time a quantity which can be defined mathematically and operationally and yet exists in living matter but not non-living matter may perhaps contribute to a resolution of this paradox."

1975

J. Maynard Smith: "We regard as alive any population of entities which has the properties of multiplication, heredity and variation."

1977

E. Argyle: "Life on earth today is a highly degenerate process in that there are millions of different gene strings (species) that spell the one word 'life'."

1979

C. E. Folsome (Onsager-Morowitz): “Life is that property of matter that results in the coupled cycling of bioelements in aqueous solution, ultimately driven by radiant energy to attain maximum complexity.”

1981

E. H. Mercer: “The sole distinguishing feature, and therefore the defining characteristic, of a living organism is that it is the transient material support of an organization with the property of survival.”

1981

M. Eigen and R. Winkler-Oswatisch: “The most conspicuous attribute of biological organization is its complexity... The physical problem of the origin of life can be reduced to the question: ‘Is there a mechanism of which complexity can be generated in a regular, reproducible way?’”

1982

E. Haukioja: “A living organism is defined as an open system which is able to fulfill the condition: it is able to maintain itself as an automaton... the long-term functioning of automata is possible only if there exists an organization building new automata. An automaton may serve as such an organizaiton.”

1984

P. Schuster: “The uniqueness of life seemingly cannot be traced down to a single feature which is missing in the non-living world. It is the simultaneous presence of all the characteristic properties... and eventually many more, what makes the essence of a biological system.”

1985

V. Csanyi and G. Kampis: “It is suggested that replication - a copying process achieved by a special network of inter-relatedness of components and component-producing processes that produces the same network as that which produces them - characterizes the living organism.”

1986

N. H. Horowitz: "Life is synonymous with the possession of genetic properties. Any system with the capacity to mutate freely and to produce its mutation must almost inevitably evolve in directions that will ensure its preservation. Given sufficient time, the system will acquire the complexity, variety and purposefulness that we recognize as 'alive'."

1986

M. J. Katz: "Lie is characterized by maximally-complex determinate patterns, patterns requiring maximal determinate for their assembly... Biological templets are determinant templets, and the uniquely biological templets have stability, coherence, and permanence... Stable templets-reproducibility was the great leap, for life is matter that learned to recreate faithfully what are in all other respects random patterns."

1986

R. Sattler: "Living system = an open system that is self-replicating, self-regulating, and feeds on energy from environment."

1987

S. Lifson: "Just as wave-particle duality signifies microscopic systems, irreversibility and trend toward equilibrium is characteristic of thermodynamic systems, space-symmetry groups are typical for crystals, so do organization and telemony signify animate matter. Animate, and only animate matter can be said to be organized, meaning that it is a system made of elements, each one having a function to fulfill as a necessary contribution to the functioning of the system as a whole."

1993

S. A. Kauffman: "Life is an expected, collectively self-organized property of catalytic polymers."

1993

A. de Loof: "Life as the ability to communicate."

1994

NASA's definition: "Life is a self-sustained chemical system capable of undergoing Darwinian evolution." (Joyce, 1994, p. xi)

1994

Varela et al.: "An autopoietic system is organized (defined as unity) as a network of processes of production (synthesis and destruction) of components such that: i) continuously regenerate and realize the network that produces them, and ii) constitute the system as a distinguishable unity in the domain in which they exist."

1997

F. Hucho and K. Buchner: "Signal transudction is as fundamental a feature of life as metabolism and self-replication."

1997

H. Baltscheffsky: "Life may well be described as 'a flow of energy, matter and information."

1997

R. S. Root-Bernstein and P. F. Dillon: "We propose that living organisms are systems characterized by being highly integrated through the process of organization driven by molecular (and higher levels of) complementarity."